

Electronic Thesis and Dissertation Repository

---

8-18-2017 10:30 AM

## Turn Detection and Analysis of Turn Parameters for Driver Characterization

Jennifer Emily Knull, *The University of Western Ontario*

Supervisor: Michael Bauer, *The University of Western Ontario*

A thesis submitted in partial fulfillment of the requirements for the Master of Science degree in Computer Science

© Jennifer Emily Knull 2017

Follow this and additional works at: <https://ir.lib.uwo.ca/etd>

---

### Recommended Citation

Knull, Jennifer Emily, "Turn Detection and Analysis of Turn Parameters for Driver Characterization" (2017). *Electronic Thesis and Dissertation Repository*. 4818.  
<https://ir.lib.uwo.ca/etd/4818>

This Dissertation/Thesis is brought to you for free and open access by Scholarship@Western. It has been accepted for inclusion in Electronic Thesis and Dissertation Repository by an authorized administrator of Scholarship@Western. For more information, please contact [wlsadmin@uwo.ca](mailto:wlsadmin@uwo.ca).

## Abstract

Advanced Driver Assistance Systems, or ADAS, which can notify the driver of potential dangers or even perform emergency maneuvers in dangerous situations, have been shown to play a crucial role in accident prevention and driver feedback. An Intelligent ADAS, or i-ADAS, relies on information about the state of the driver, their behavior or condition, the vehicle and the environment. Understanding the behavior requires the development of *driver models*, which can help predict how a person may react in certain situations or help determine if the individual is not performing at their usual level of ability. A key element in building such models is the ability to detect and analyze common driving maneuvers, such as making turns, on an individual-by-individual basis. Thus algorithms are needed which can detect and characterize individual driving maneuvers. In this research, we present a position-based turn detection algorithm for detecting turns from vehicle data and GPS coordinates. Based on a dataset of sixteen drivers involving 278 turns, the algorithm achieves an accuracy of 97.84%. The turn parameters detected by the algorithm are then averaged for each driver and clustered using K-Means. Turn parameters  $t - 5$  seconds are also clustered prior to each detected turn and  $t + 5$  seconds are clustered after each turn. The cluster centroids at each point in time determine particular driving behaviours which are summarized in four categories, and the cluster assignments are examined over time to categorize drivers into these behaviour categories. This analysis reveals two optimal times for analyzing driver behaviour. Our overall aim is to be able to build automated methods that can use this research to eventually determine characteristics of individual drivers during turns in order to build models of drivers for use with i-ADAS.

**Keywords:** Time series analysis, turn detection, data mining, driver characterization

# Contents

<b>Abstract</b>	<b>i</b>
<b>List of Figures</b>	<b>iv</b>
<b>List of Tables</b>	<b>vi</b>
<b>List of Algorithms</b>	<b>viii</b>
<b>List of Appendices</b>	<b>ix</b>
<b>1 Introduction</b>	<b>1</b>
<b>2 Related Work</b>	<b>3</b>
<b>3 RoadLab Data</b>	<b>7</b>
3.1 RoadLab . . . . .	7
3.2 Structure of the Data . . . . .	9
3.3 Relevant Data . . . . .	11
3.4 Data Constraints . . . . .	11
3.5 Related Work in RoadLab . . . . .	12
<b>4 Position-Based Turn Detection</b>	<b>14</b>
4.1 Concept . . . . .	14
4.2 Implementation . . . . .	18
4.2.1 <i>main()</i> . . . . .	19
4.2.2 <i>detectTurns()</i> and <i>detectTurnsRotated()</i> . . . . .	19
4.2.3 <i>mergeTurns()</i> . . . . .	23
4.2.4 <i>removeDuplicates()</i> . . . . .	23
4.3 Results and Discussion . . . . .	25
<b>5 Cluster Analysis</b>	<b>38</b>
5.1 Preprocessing . . . . .	39
5.2 K-Means Clustering . . . . .	42
5.3 Results and Cluster Descriptions . . . . .	47
5.4 Driver Characterization . . . . .	54
5.5 Optimal Time for Analysis . . . . .	57
5.6 Key Observations . . . . .	59

<b>6 Conclusion and Future Work</b>	<b>60</b>
<b>Bibliography</b>	<b>63</b>
<b>A Preprocessed Files for Analysis</b>	<b>66</b>
<b>B Cluster Assignments of Drivers</b>	<b>77</b>
<b>Curriculum Vitae</b>	<b>89</b>

# List of Figures

3.1	The RoadLab in-vehicle laboratory: <b>a) (left):</b> on-board computer and LCD screen, <b>b) (center):</b> dual stereo front visual sensors, <b>c) (right):</b> side stereo visual sensors [4]. . . . .	7
3.2	A map view of the closed route . . . . .	9
4.1	Projection of the Earth overlaid with geographic latitude and longitude . . . . .	14
4.2	Example of vectors $\vec{u}$ and $\vec{v}$ where $m_1$ and $m_2$ are in adjacent quadrants . . . . .	15
4.3	Example of vectors $\vec{u}$ and $\vec{v}$ where $m_1$ and $m_2$ are in the same quadrant . . . . .	16
4.4	Example of an undetected turn . . . . .	17
4.5	Block diagram of the position-based turn detection program . . . . .	19
4.6	Turns that occur in a parking lot . . . . .	25
4.7	Plotted route of driver 1 . . . . .	26
4.8	Plotted route of driver 2 . . . . .	26
4.9	Plotted route of driver 3 with 2 FP . . . . .	27
4.10	Map view of driver 3 where the first false turn was detected . . . . .	28
4.11	Map view of driver 3 where the second false turn was detected . . . . .	28
4.12	Plotted route of driver 4 . . . . .	28
4.13	Plotted route of driver 5 . . . . .	29
4.14	Plotted route of driver 6 . . . . .	29
4.15	Plotted route of driver 7 . . . . .	30
4.16	Plotted route of driver 8 . . . . .	30
4.17	Plotted route of driver 9 . . . . .	31
4.18	Plotted route of driver 10 with 1 FN . . . . .	31
4.19	Plotted route of driver 11 . . . . .	32
4.20	Plotted route of driver 12 . . . . .	32
4.21	Plotted route of driver 13 with 1 FP and 2 FN . . . . .	33
4.22	Map view of driver 13 where a false turn was detected . . . . .	33
4.23	Plotted route of driver 14 . . . . .	34
4.24	Plotted route of driver 15 . . . . .	35
4.25	Plotted route of driver 16 . . . . .	35
5.1	Result of the elbow method for all drivers 5 seconds prior to all turns . . . . .	43
5.2	Result of the elbow method for all drivers 4 seconds prior to all turns . . . . .	43
5.3	Result of the elbow method for all drivers 3 seconds prior to all turns . . . . .	44
5.4	Result of the elbow method for all drivers 2 seconds prior to all turns . . . . .	44
5.5	Result of the elbow method for all drivers 1 second prior to all turns . . . . .	44
5.6	Result of the elbow method for all drivers during turns . . . . .	44

5.7	Result of the elbow method for all drivers 1 second after all turns . . . . .	45
5.8	Result of the elbow method for all drivers 2 seconds after all turns . . . . .	45
5.9	Result of the elbow method for all drivers 3 seconds after all turns . . . . .	45
5.10	Result of the elbow method for all drivers 4 seconds after all turns . . . . .	45
5.11	Result of the elbow method for all drivers 5 seconds after all turns . . . . .	45

# List of Tables

3.1	Summary of participant information and driving conditions . . . . .	8
3.2	The closed route used for the RoadLab data collection . . . . .	9
3.3	Example of raw data frame information . . . . .	9
3.4	Data extracted for this research . . . . .	11
3.5	Example of noisy geographical data and missing data . . . . .	12
4.1	Results from Figures 4.2, 4.3 and 4.4 for $m_1 * m_2$ . . . . .	17
4.2	Results from Figures 4.2, 4.3 and 4.4 when the coordinates are rotated by 45 degrees . . . . .	18
4.3	Raw data of driver 3 where the first false turn was detected . . . . .	27
4.4	Raw data of driver 3 where the second false turn was detected . . . . .	28
4.5	Raw data of driver 10 where a turn should have been detected . . . . .	31
4.6	Raw data of driver 13 where a false turn was detected . . . . .	32
4.7	Raw data of driver 13 where the first FN should have been detected . . . . .	33
4.8	Raw data of driver 13 where the second FN should have been detected . . . . .	34
4.9	Results of the Position-Based Turn Detection algorithm . . . . .	35
4.10	Results of the Position-Based Turn Detection algorithm with missed turns (due to missing data) included as actual turns . . . . .	36
5.1	Zero values of steering wheel position and acceleration during turns . . . . .	39
5.2	Summary of how the final set of descriptors are to be interpreted . . . . .	40
5.3	Translation of 1-second intervals to number of frames . . . . .	41
5.4	Silhouette scores of all analysis files for 1 to 6 clusters . . . . .	46
5.5	The chosen $K$ -value(s) for each file . . . . .	46
5.6	Cluster centroids for cluster0 ( $v$ ), cluster1 ( $w$ ) and cluster2 ( $z$ ) at 5 seconds pre-turns . . . . .	47
5.7	Angle between the 3 clusters 5 seconds pre-turns . . . . .	48
5.8	Cluster centroids for cluster0 ( $v$ ) and cluster1 ( $w$ ) . . . . .	48
5.9	Angle between the 2 clusters at each point in time . . . . .	49
5.10	Cluster assignments of drivers pre-turns of 5 seconds with 3 clusters and 5 seconds with 2 clusters . . . . .	50
5.11	Cluster assignments of drivers pre-turns of 4 and 3 seconds with 2 clusters . . . . .	50
5.12	Cluster assignments of drivers pre-turns of 2 and 1 seconds with 2 clusters . . . . .	51
5.13	Cluster assignments of drivers during turns and post-turns of 1 second with 2 clusters . . . . .	51
5.14	Cluster assignments of drivers post-turns of 2 and 3 seconds with 2 clusters . . . . .	52
5.15	Cluster assignments of drivers post-turns of 4 and 5 seconds with 2 clusters . . . . .	52

5.16	Observations about cluster0 and cluster1 at each point in time . . . . .	53
5.17	Cluster assignments over time . . . . .	55
5.18	The 4 categories of driving behaviour . . . . .	55
5.19	Driver classification . . . . .	57
5.20	Number of times each driver occurs in cluster0 and cluster1 . . . . .	58
5.21	Cluster assignment based on count . . . . .	58
5.22	Cluster assignments at 4 and 3 seconds pre-turns and 1 second post-turns compared to their categorization . . . . .	59
A.1	Average driver descriptors 5 seconds pre-turns . . . . .	66
A.2	Average driver descriptors 4 seconds pre-turns . . . . .	67
A.3	Average driver descriptors 3 seconds pre-turns . . . . .	68
A.4	Average driver descriptors 2 seconds pre-turns . . . . .	69
A.5	Average driver descriptors 1 second pre-turns . . . . .	70
A.6	Average driver descriptors during turns . . . . .	71
A.7	Average driver descriptors 1 second post-turns . . . . .	72
A.8	Average driver descriptors 2 seconds post-turns . . . . .	73
A.9	Average driver descriptors 3 seconds post-turns . . . . .	74
A.10	Average driver descriptors 4 seconds post-turns . . . . .	75
A.11	Average driver descriptors 5 seconds post-turns . . . . .	76
B.1	Cluster assignments of drivers pre-turns of 5 seconds with 3 clusters . . . . .	77
B.2	Cluster assignments of drivers pre-turns of 5 seconds with 2 clusters . . . . .	78
B.3	Cluster assignments of drivers pre-turns of 4 seconds with 2 clusters . . . . .	79
B.4	Cluster assignments of drivers pre-turns of 3 seconds with 2 clusters . . . . .	80
B.5	Cluster assignments of drivers pre-turns of 2 seconds with 2 clusters . . . . .	81
B.6	Cluster assignments of drivers pre-turns of 1 second with 2 clusters . . . . .	82
B.7	Cluster assignments of drivers during turns with 2 clusters . . . . .	83
B.8	Cluster assignments of drivers post-turns of 1 second with 2 clusters . . . . .	84
B.9	Cluster assignments of drivers post-turns of 2 seconds with 2 clusters . . . . .	85
B.10	Cluster assignments of drivers post-turns of 3 seconds with 2 clusters . . . . .	86
B.11	Cluster assignments of drivers post-turns of 4 seconds with 2 clusters . . . . .	87
B.12	Cluster assignments of drivers post-turns of 5 seconds with 2 clusters . . . . .	88



# List of Algorithms

1	<i>main(dData)</i> . . . . .	19
2	<i>detectTurns(fSeq)</i> . . . . .	21
3	<i>detectTurnsRotated(fSeq)</i> . . . . .	22
4	<i>mergeTurns(S<sub>1</sub>, S<sub>2</sub>)</i> . . . . .	23
5	<i>removeDuplicates(S)</i> . . . . .	24
6	<i>pre(t)</i> . . . . .	41
7	<i>post(t)</i> . . . . .	42

# List of Appendices

Appendix A Preprocessed Files for Analysis . . . . .	66
Appendix B Cluster Assignments of Drivers . . . . .	77

# Chapter 1

## Introduction

Driving is a risky activity that continues to be part of the everyday lives of people, whether they are a driver, passenger or pedestrian. According to the National Highway Traffic and Safety Administration (NHTSA), there were 6,296,000 police-reported motor vehicle accidents in the United States alone in 2015, with an estimated 96 fatalities per day. The cause of almost all these accidents is persistently due to driver error.

Efforts have been made by automobile manufacturers and researchers to enhance the driving experience to improve safety while driving. There are two technologies at the forefront of this revolution - autonomous vehicles and augmented vehicles. Autonomous vehicles take full control of the vehicle at all times and is, essentially, a self-driving vehicle. Here, the driver takes the role of a passenger as the vehicle drives itself. Augmented vehicles, or Advanced Driver Assistance Systems (ADAS), aid the driver as they operate the vehicle themselves, and take full control of the vehicle and decision-making when there is impending risk. ADAS can help reduce the burden of driving on humans and can improve safety by notifying the driver of potential dangers and may even perform emergency maneuvers in dangerous situations. ADASs have been shown to play a crucial role in accident prevention and driver feedback.

Intelligent ADAS, or i-ADAS, relies on information about the state of the driver, his or her behaviour or condition, the vehicle and the environment. Understanding the state of a driver or their behaviour requires the development of *driver models*, which can predict driver behaviour in certain situations based on their performance. These driver models must be built dynamically and adhere to specific individual behaviours and characteristics, as each driver can react differently given similar situations.

A key element in building such models is the ability to detect and analyze common driving maneuvers, such as making turns from one road to another, on an individual-by-individual basis. Analyzing these driving maneuvers then become the building blocks to creating dynamic driver models to characterize drivers. The challenge to analyzing driver behaviour is to consider the driving environment at all times; any triggers or outside influences that can explain the behaviour. Driver behaviour can greatly vary leading up to a turn and coming out of a turn, but it is believed that the environment and driving conditions are more consistently similar during a turn. This is why turns will be the driving maneuver analyzed for this research to help

understand driving behaviour, with a strict focus on vehicle data that is not computationally expensive.

For any driving maneuver, algorithms are needed to detect and characterize these maneuvers on individual drivers. In this paper, a position-based turn detection (PBTD) algorithm will be employed to detect turns from vehicle data. This algorithm is used for post processing of turn data before, during, and after a turn maneuver. The overall aim is provide the capability of building automated methods that will use the PBTD algorithm to determine characteristics of individual drivers throughout turns. These methods are intended to help build models of drivers.

This thesis is organized as follows. Chapter 2 provides a literature overview of related work on modelling driver behaviour for driving maneuvers. Chapter 3 provides an overview of the dataset used for this research. Chapter 4 describes the position-based turn detection algorithm in more detail and summarizes the results of the algorithm and its accuracy. Chapter 5 introduces the clustering method performed on the turn data and analyzes the cluster assignments. Finally, Chapter 6 concludes this research and provides other avenues for future work.

# Chapter 2

## Related Work

Driver modeling, as the name suggests, tries to model driver behaviour in various driving situations. Driver modeling is very broad and there has been a variety of research over the past many years. Central to the discussion of driving models is the notion of a driving maneuver. A specific move or series of moves in driving is termed a *maneuver*. Driving maneuvers can be defined based on traffic and road infrastructure. Driving maneuvers can include “following”, “turning at intersection”, “changing lanes”, “reacting to an obstacle”, etc. These maneuvers can be differentiated by situational factors, such as the type of road, speed limit, number of lanes and the existence of other vehicles, pedestrians, traffic signs or traffic lights ahead of the vehicle.

Plochl and Edelmann [23] provide an overview of different driving models. They divide the models into four categories:

- Focus on the vehicle. The vehicle is the main goal of the model. In this case, the driver model usually serves as part of the closed loop testing of vehicle performance under various driving conditions.
- Focus on the driver. In this case the driver is the target. This includes efforts to model aspects such as driving style or psychological states while driving, such as stress or distraction.
- Focus on the vehicle/driver combination. This is really a combination of the two previous areas where the focus is on the interaction between the driver and the vehicle.
- Focus on the environment/traffic. These models simulate traffic conditions and focus on broader traffic/driving issues.

In this work, we concentrate on those works that focus on the driver or on a driver and vehicle combination.

Following Plochl and Edelmann [23], the research in this area falls into two broad subareas: a) understanding the driver and (the individual) driver behaviour (our particular focus) and b) path and speed planning, and optimized driver/driving behaviour. The first is related to modeling

how a person drives a vehicle, i.e. how they execute maneuvers - this is the focus of our work and we shall restrict our review of related work to this area.

In turn, driver behaviour models can be grouped into two categories [2]: cognitive driver models and behaviourist driver models. Cognitive driver models are based on human psychological behaviours and pay attention to, for example, mental and attentional features that a driver shows in performing different maneuvers. Behaviourist models utilize the information about the environment surrounding the driver, including vehicles, pedestrians and other objects in the road. Most of the proposed methods in this area are based on one of these two categories, but ultimately a combination of information in both categories can be more helpful and practical in understanding driver behaviour and predicting the most probable next maneuver.

We first consider work that falls into the behaviourist class (though in many cases this separation is not exact). Behaviourist driver models try to model how the driver interacts with the surrounding environment including the other vehicles and also his vehicle parts, such as brake and accelerator pedals, turn signals, steering wheel and other sensors/actuators within vehicles. Modern vehicles, for example, are already equipped with some cameras and sensors to measure the internal vehicular information. Radar systems for detecting distance, lidar systems [18] for obstacle detection, visual systems [31] for detecting road objects [1] and vehicle navigation systems, such as GPS [17], have been used in advanced driving assistance systems.

Driver behaviour can be predicted by knowing how a driver acts in certain driving tasks, such as turning, lane changing and overtaking a vehicle. Chandler, et al. [7] implemented a vehicle-following model and used data from experiments with real vehicles to set the model's parameters. Ioannou [21] implemented an Automatic Cruise Control (ACC) system and compared it to three different human driver models. The results were that the ACC system was able to provide safer driving. A hybrid, three-layered ACC system based on fuzzy logic and neural networks has also been implemented by Dermann et al. [9].

Other maneuvers have been also studied: emergency braking [30, 29], lane change [14, 20], and turning at intersections [6, 8]. Predicting the driver's intention could provide valuable information in the context of ADAS.

A number of methods have also been implemented for assessing the driver's sleepiness. Most of them utilize some features in the driver's face through video cameras and use eye and eyelid movements [5, 11, 22, 28] or head movements [5, 11, 12] or some combination of both to infer sleepiness. A few indirect algorithms, usually using steering behaviour in the context of lane keeping [28, 27] have also been developed.

Other researchers have focused specifically on cognitive driver models which are based on human psychological behaviours. These models pay attention to, for example, mental and attentional features that a driver shows in performing different maneuvers. These models typically consider human information processing, such as memory and visual information. The psychological factors that can be incorporated into cognitive driver behaviour modeling include distraction, reaction time, body strength (stamina, strength of muscles, etc.), vision, impairment

(stress, fatigue, alcohol, etc.) and so on [10]. Metari et al. [21] analyzed the cephalo-ocular behaviour of drivers in vehicle/road events, such as overtaking and crossing an intersection. This work was specifically concerned with finding the relationship between vision behaviour of older drivers and their actions in road events. They posited that the cephalo-ocular information can be related to the driving maneuvers a driver decides to make. Some other researchers have also tested the impact of eye movements on control of actions in everyday events, such as driving [15, 16].

Analysis of driver behaviour within the context of a cognitive architecture can be important in determining the motivation behind making a specific decision in a driving event [25]. For example, when a driver decides to make a left or right turn, visual information can show that they look at the mirrors, blind spot, traffic and so on. Baumann et al. [3] model the situation awareness of a driver in a cognitive architecture with the aim of assisting an i-ADAS to assist the driver during driving and to augment safety. Despite the fact that visual information, such as gaze tracking, is important in predicting driver behaviour, little research has been done in this domain. The main reason that these models have not received much attention are the challenges in measuring cognitive behaviour in such complex systems.

It is clear that details of driving maneuvers have been considered essential in the development of driver models. Much of this work, however, has relied on the researcher to first identify such maneuvers, often manually, which are then used in subsequent analyses. To be able to infer models of individual drivers, driving maneuvers must first be determined in situ and then used to build the model. A first step is to be able to identify such maneuvers from the data available from the vehicle, which is covered in this thesis.

Another area that has received attention by researchers is the detection of driving maneuvers. Kasper et al. [13] provide a novel approach for detecting lane-change maneuvers in structured highway scenarios using object-oriented Bayesian Networks (OOBNs) with a vehicle-lane relation. Mandalia et al. [19] proposes a technique for observing driver intent to change lanes using a support vector machine (SVM). Alternatively, Weiss et al. [32] detect lane changes of an observed target vehicle with a motion model that detects significant variability in lateral direction. A second motion model also determines if the target vehicle is staying within the lane by looking for high variability in longitudinal direction. Salvucci et al. [26] introduces a robust, real-time system for detecting lane changes. In this work, a model-tracing system simulates driver intention and consequent behaviour based on a simplified, previously validated computational model of driver behaviour. The system compares the model's simulated behaviour with actual observed driver behaviour, and constantly infer the driver's unobservable intentions from their observable actions.

The work of Rodemerk et al. [24] attempts to predict the driver's turn intentions at urban intersections with the use of context-based indicators before changes occur in the vehicle's trajectory. Context-based indicators include the driver's motion within the vehicle, such as head pose and gaze direction, the state of the vehicle, such as steering wheel and speed indicators, and the environment around the vehicle, such as the existence of another lane beside the vehicle.

There has been considerable research in the identification of different driving maneuvers and, discussed earlier, the modelling of driver behaviour in the context of these driving maneuvers. This research has a focus on the detection of turn maneuvers and the analysis of driving behaviours in the context of turns. This will work towards modelling driver behaviour for turn maneuvers.



# Chapter 3

## RoadLab Data

### 3.1 RoadLab

RoadLab is an initiative that provides data for the development of i-ADAS. The aim is to support research for i-ADAS cognizant of driver behaviour, intent, surrounding traffic and general driving conditions to help alleviate injuries caused by vehicle accidents. The initial dataset provides a resource for researchers to analyze driver data with the hope of reducing the social and economic costs caused by human errors made while driving.

RoadLab data is collected by an in-vehicle laboratory instrumented with an on-board diagnostic system (OBD-II) using the CANbus protocol as described in [4] (see Figure 3.1). The instrumentation was able to retrieve video sequences of the driving environment in front of the vehicle, ocular behaviour of the driver such as driver gaze, geographic position of the vehicle using GPS units, and data describing the state of all the vehicle parameters such as brake pedal position, steering wheel position, etc. This research has its primary focus on the vehicular data for turn detection.



Figure 3.1: The RoadLab in-vehicle laboratory: **a) (left):** on-board computer and LCD screen, **b) (center):** dual stereo front visual sensors, **c) (right):** side stereo visual sensors [4].

The data comes from a study that was conducted on 16 individuals between the ages of 20 and 47 from London, Ontario; a summary of the participants and driving conditions is provided in

Table 3.1. Each participant used the RoadLab vehicle to drive along a predetermined route, shown in Figure 3.2 and Table 3.2, and were accompanied by two observants. One observant was present to monitor the equipment and ensure its proper performance. The second observant helped navigate the participants along the chosen route.

<i>Participant</i>	<i>Date</i>	<i>Time</i>	<i>Weather Conditions</i>	<i>Age</i>	<i>Gender</i>
1	2012-08-24	13:15	29C, Sunny	37	M
2	2012-08-24	15:30	31C, Sunny	37	M
3	2012-08-30	12:15	23C, Sunny	41	F
4	2012-08-31	11:00	24C, Sunny	41	M
5	2012-09-05	12:05	27C, Partially Cloudy	37	F
6	2012-09-10	13:00	21C, Partially Cloudy	22	F
7	2012-09-12	11:30	21C, Sunny	31	F
8	2012-09-12	14:45	27C, Sunny	21	M
9	2012-09-17	13:00	24C, Partially Cloudy	21	F
10	2012-09-19	09:30	8C, Sunny	20	M
11	2012-09-19	14:45	12C, Sunny	22	F
12	2012-09-21	11:45	18C, Partially Sunny	24	F
13	2012-09-21	14:45	19C, Partially Sunny	23	M
14	2012-09-24	11:00	7C, Sunny	47	F
15	2012-09-24	14:00	13C, Partially Sunny	44	F
16	2012-09-28	10:00	14C, Partially Sunny	25	M

Table 3.1: Summary of participant information and driving conditions



Figure 3.2: A map view of the closed route

<i>Turn Type</i>	<i>Start Road</i>	<i>End Road</i>
Right	Perth Dr	Windermere Rd
Left	Windermere Rd	Richmond St
Right	Richmond St	Sunningdale Rd E
Right	Sunningdale Rd E	Highbury Ave N
Right	Highbury Ave N	Dundas St
Left	Dundas St	Ridout St N
Left	Ridout St N	York St
Left	York St	Talbot St
Right	Talbot St	King St
Left	King St	Richmond St
Right	Richmond St	Dufferin Ave
Left	Dufferin Ave	Waterloo St
Left	Waterloo St	Central Ave
Right	Central Ave	Richmond St
Left	Richmond St	Oxford St E
Right	Oxford St E	Wharncliffe Rd N
Right	Western Rd	Windermere Rd
Right	Windermere Rd	Perth Dr

Table 3.2: The closed route used for the Road-Lab data collection

### 3.2 Structure of the Data

The data from RoadLab has been collected in real-time as each participant, or driver, navigated along the route. There is a total of approximately 60 minutes of driving data for each participant, which varies based on how long it took for each driver to complete the route. The time-series data was collected at a sampling rate of 15Hz, which were captured into data frames. Each data frame represents approximately  $\frac{1}{15}$  seconds of data, and contains current contextual information about the vehicle and its geographical position.

<i>Frame Number</i>	<i>Timestamp</i>	<i>Latitude</i>	<i>Longitude</i>	<i>GPS Speed</i>	<i>Speed</i>
1	588534044	43.0103	-81.2711	0	0
2	588580132	43.0103	-81.2711	0	0
3	588617063	43.0103	-81.2711	0	0

<i>Brake Pressure</i>	<i>Gas Pressure</i>	<i>Steering Wheel Position</i>	<i>Left Turn Signal</i>	<i>Right Turn Signal</i>
156	0	-567	0	0
155	0	-567	0	0
155	0	-567	0	0

Table 3.3: Example of raw data frame information

Table 3.3 contains three sample data frames found in the RoadLab data. Every data frame contains a:

- **Frame Number:** an index that indicates the current frame.
- **Timestamp:** this represents the time of occurrence of the information within the frame.
- **Latitude:** geographic latitude value in signed degrees format with four decimal precision.
- **Longitude:** geographic longitude value in signed degrees format with four decimal precision.
- **GPS Speed:** the speed of the vehicle in km/hr, measured by satellite.
- **Speed:** the speed of the vehicle in km/hr, measured by vehicle sensors.
- **Brake Pressure:** amount of pressure on the brake pedal, ranging from 0 (no pressure) to 156 (maximum pressure).
- **Gas Pressure:** amount of pressure on the gas pedal, ranging from 0 (no pressure) to 187 (maximum pressure).
- **Steering Wheel Position:** represents the angle of the steering wheel, ranging from -567 to 579. A negative angle indicates the steering wheel is left of the centre, or rest, position, and a positive angle indicates the right.
- **Left Turn Signal:** this value is either 0 if the left turn signal is off, or 1 if the left turn signal is on.
- **Right Turn Signal:** this value is either 0 if the right turn signal is off, or 1 if the right turn signal is on.

The values of brake pressure, gas pressure and steering wheel position were generated from CANbus signals and have no specific units.

In the sample data, some assumptions can be made about the state of the vehicle based on specific values of the vehicle parameters. Three data frames represent approximately 1/5th of a second of time, so that is the duration of this particular example. In the first frame, the brake pressure is at its maximum value. In the same frame, speed and gas pressure are 0. With the brake all the way down, and no pressure on the gas pedal, it can be assumed that the vehicle is not moving. Additionally, the steering wheel is turned all the way to the left. This could indicate multiple scenarios. The vehicle could be in the middle of an intersection waiting to turn left, it could be in parked position, or some outlying case that can't be speculated. The left turn signal could indicate that the vehicle is turning left, however this signal is dependent on the driver and can be unreliable. Finally, the last two frames have similar values, except there is slightly less brake pressure. This could indicate that the vehicle is getting ready to move. The gas pressure is still 0, so it appears as if the driver is slowly releasing the brake pedal. Since there are only three frames in this example, it is difficult to assume that this is the case.

### 3.3 Relevant Data

This research specially uses latitude, longitude and steering wheel position to detect all turns along the route taken by the RoadLab vehicle. The following parameters are used as descriptors for all the detected turns: speed, brake pressure, gas pressure and steering wheel position. These are the same parameters that were used in the previous example. These descriptors also provide a basis for deriving more data such as acceleration, duration, and average, standard deviation, skewness and kurtosis.

<i>Frame Number</i>	<i>Timestamp</i>	<i>Latitude</i>	<i>Longitude</i>	<i>GPS Speed</i>	<i>Speed</i>
1	588534044	43.0103	-81.2711	0	0
2	588580132	43.0103	-81.2711	0	0
3	588617063	43.0103	-81.2711	0	0
<i>Brake Pressure</i>	<i>Gas Pressure</i>	<i>Steering Wheel Position</i>	<i>Left Turn Signal</i>	<i>Right Turn Signal</i>	
156	0	-567	0	0	
155	0	-567	0	0	
155	0	-567	0	0	

Table 3.4: Data extracted for this research

A decision has been made to exclude GPS speed from the analysis. It has been found that this parameter is subject to noise since it is measured by satellite. It is more accurate to use sensors on the vehicle to measure speed, so this measurement of speed will be used. Left and right turn signals are also excluded. The left and right turn signals can be unreliable since they are triggered by the driver. Steering wheel position will act as a substitute for these flags, and a threshold will indicate a left turn or a right turn.

Table 3.4 highlights the set of parameters that will be used for this research. Frame number was not selected for analysis, but will be used in the algorithms for turn detection.

### 3.4 Data Constraints

There are several constraints that need to be considered. The RoadLab dataset excels with depth, but lacks in breadth. There is approximately 54,000 frames of data across all 16 drivers, and this provides ample information to conduct analysis. However, the sample size of the study contains only 16 drivers, which can make it difficult for the results to provide conclusions and concrete assumptions for driver characterization.

The turn detection software, described later in this thesis, relies solely on the vehicular data received from OBD-II and there are the occasional missing sensor readings from the different vehicle components. Missing values are encoded as zero (not simply missing), and, hence, remain undetected as actual values can also be zero. For this research, the turn detection software treats each value equally, despite the possibility of missing values.

<i>Frame Number</i>	<i>Timestamp</i>	<i>Latitude</i>	<i>Longitude</i>	<i>GPS Speed</i>	<i>Speed</i>
23448	1606770659	43.0433	-81.2270	44	47
23449	1632795784	43.0403	-81.2255	44	44
<i>Brake Pressure</i>	<i>Gas Pressure</i>	<i>Steering Wheel Position</i>	<i>Left Turn Signal</i>	<i>Right Turn Signal</i>	
1	57	0	0	0	
1	35	-12	0	0	

Table 3.5: Example of noisy geographical data and missing data

Geographical data is retrieved by satellite using the GPS. GPS is vulnerable to signal interference for different reasons, which causes sporadic jumps in latitude and longitude readings. The turn detection software eliminates risk of this affecting the results by enforcing a threshold. Missing data can also occur when the in-vehicle laboratory goes offline due to a technical issue. Any turns executed during this state cannot be detected and will be missing from the analysis. Table 3.5 provides an example from the raw data. There should be an incremental increase or decrease (or no difference at all) between latitude and longitude values going from one frame to the next. In this example, there is a 0.003 difference in latitude values and a 0.0015 difference in longitude values. This much of a difference entirely displaces the vehicle approximately 350 metres in 1/15th of a second, which is most likely not the case. Because the turn detection algorithm uses a position-based approach, this difference is considered to be noisy. From an analysis perspective, there is a gap between these two data frames, so there is also missing data.

Lastly, the study was conducted under supervision, which may have caused the participants to behave differently and drive less naturally, in contrast to being unsupervised. This issue cannot be avoided since without the instrumentation, there would be no data. The RoadLab instrumentation cannot be legally installed on an individual's vehicle without their consent. Each participant was also guided along the route by one observant. There are instances where the participants deviated slightly away from the route due to erroneous commands. Because of this, the routes for some participants are slightly different from the predetermined route they were meant to follow. All detected turns that do not belong in the route will also be included in the analysis, as this research aims to characterize drivers, not turns.

### 3.5 Related Work in RoadLab

There has been considerable research produced using RoadLab that is similar to the research of this thesis. M. Zardosht [34] provided an analysis of pre-turn maneuvers of drivers from the RoadLab dataset. That work made use of the turns detected by the research in this thesis in order to analyze driver behaviour 5, 10 and 15 seconds before turns. That work explored alternative ways of analyzing the pre-turn driving data. Our work is an extension to the work in [34] and is more encompassing by providing an analysis of driver behaviour up to 5 seconds before turns and 5 seconds after turns, as well as during turns themselves.

S.M. Zabihi [33] developed a turn prediction model using an Input-Output Hidden Markov Model (IO-HMM) on the RoadLab data, which included vehicle dynamics and gaze information. This model calculated the probability of a left turn, right turn and straight driving at 3.8 seconds before the maneuver occurred with an accuracy of over 80% in real-time. The focus of this thesis is not turn prediction, but turn detection and the analysis of turn parameters for each individual driver.

# Chapter 4

## Position-Based Turn Detection

### 4.1 Concept

As a vehicle travels along the Earth, its position can be uniquely represented as a latitude and longitude coordinate using GPS. This coordinate maps to only one location, making the position of any vehicle identifiable and traceable. The idea behind the position-based approach is to use latitude,  $\varphi$ , and longitude values,  $\lambda$ , to identify a change from one road to another. Since GPS can pinpoint any location, it is assumed that we can analyze the coordinates that represent these locations to detect turns.

The RoadLAB dataset provides  $\varphi$  and  $\lambda$  in signed degrees format of up to (and including) four decimal places. This degree of precision can identify individual streets and land parcels according to the qualitative scale, which, shown later in this work, provides enough accuracy for turn identification.

Geographic latitude and longitude can be mapped to a Cartesian coordinate system (see Figure 4.1), in which  $\varphi$  represents a numerical value along the y-axis and  $\lambda$  represents a value along the x-axis. Turns will be detected, using the coordinate system, by specific fluctuations in  $\Delta\varphi$  and  $\Delta\lambda$ .

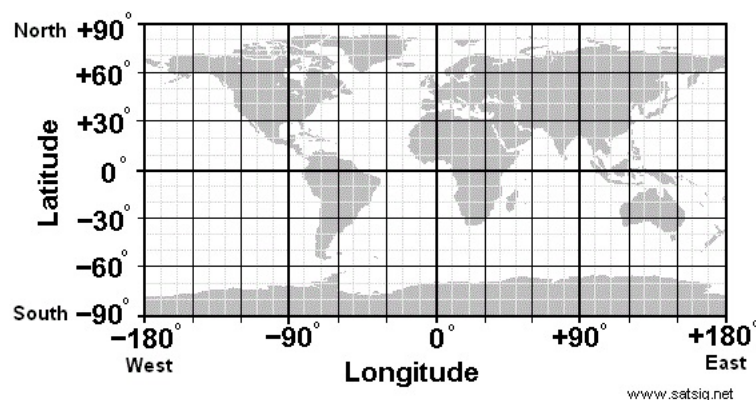


Figure 4.1: Projection of the Earth overlaid with geographic latitude and longitude



As a vehicle travels along a path, its position vector can be calculated. This vector signifies the direction of travel using two  $(\lambda, \varphi)$  endpoints. The position-based algorithm takes two position vectors,  $\vec{u}$  and  $\vec{v}$ , when there is a change in endpoints, and if the angle between  $\vec{u}$  and  $\vec{v}$  is greater or equal to 90 degrees then there is evidence of a turn.

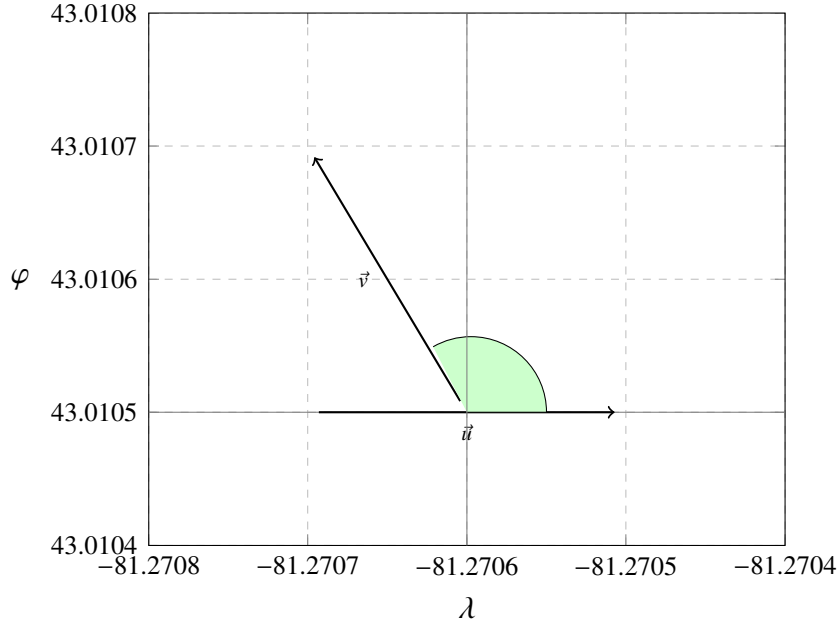


Figure 4.2: Example of vectors  $\vec{u}$  and  $\vec{v}$  where  $m_1$  and  $m_2$  are in adjacent quadrants

Two slopes,  $m_1$  and  $m_2$ , are used to describe how much of a change there is in direction between one position vector and the other. Instead of calculating the angle between  $\vec{u}$  and  $\vec{v}$ , we can determine if there is a shift between quadrants in the coordinate system (see Figures 4.2 and 4.3). Each quadrant is separated by 90 degrees, so if  $m_1$  and  $m_2$  define two adjacent quadrants, then a turn has occurred.

The values  $m_1$  and  $m_2$  are defined as the change in latitude values,  $\Delta\varphi$ , over the change in longitude values,  $\Delta\lambda$ :

$$m_1 = \frac{\varphi_2 - \varphi_1}{\lambda_2 - \lambda_1} \quad (4.1)$$

and

$$m_2 = \frac{\varphi_3 - \varphi_2}{\lambda_3 - \lambda_2}. \quad (4.2)$$

The issue with using the formula in this form is that there is a possibility of a division by zero. For example, there may be a change in latitude values while longitude remains the same, i.e.  $\Delta\lambda = 0$ . The purpose of analyzing  $m_1$  and  $m_2$  is to determine if they occur in adjacent quadrants. There are four cases between  $m_1$  and  $m_2$  when it comes to determining quadrants:

1.  $m_1$  and  $m_2$  are both positive.
2.  $m_1$  and  $m_2$  are both negative.
3.  $m_1$  is positive and  $m_2$  is negative.
4.  $m_1$  is negative and  $m_2$  is positive.

Cases 1 and 2 suggest that the slopes are not in adjacent quadrants. This is because there would be an opposition in sign if they were. Cases 3 and 4 suggest that the slopes are adjacent, in which cases a turn is detected.

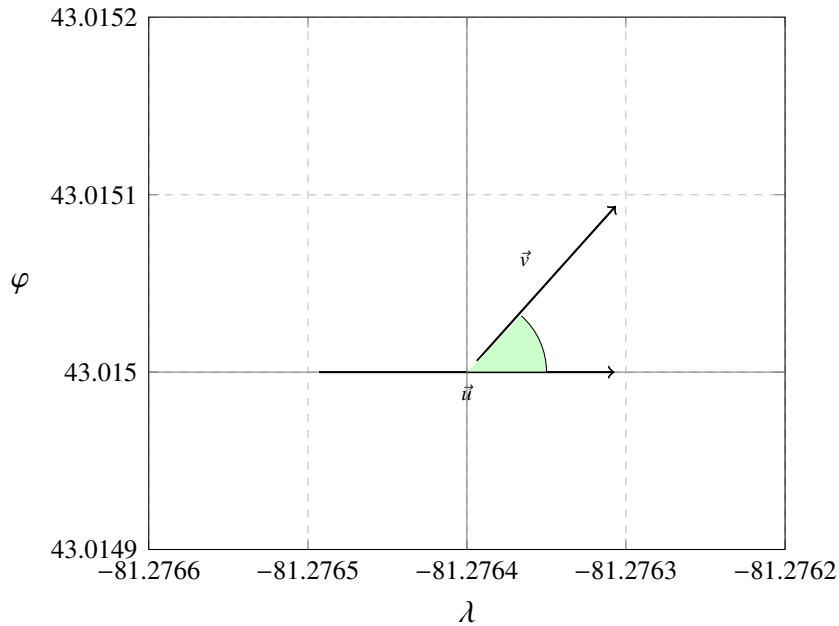


Figure 4.3: Example of vectors  $\vec{u}$  and  $\vec{v}$  where  $m_1$  and  $m_2$  are in the same quadrant

Since only the signs are being considered, the formulas for  $m_1$  and  $m_2$  can be rewritten as:

$$m_1 = (\varphi_2 - \varphi_1)(\lambda_2 - \lambda_1) \quad (4.3)$$

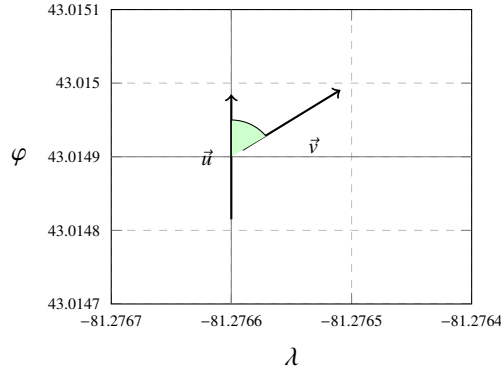
and

$$m_2 = (\varphi_3 - \varphi_2)(\lambda_3 - \lambda_2), \quad (4.4)$$

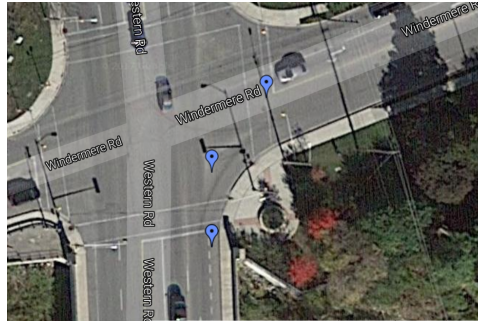
which solves the division by zero problem. This narrows the classification to two cases:

1.  $m_1 * m_2$  is negative, and
2.  $m_1 * m_2$  is positive.

Here, Case 1 identifies a turn maneuver and Case 2 indicates otherwise.



(a)  $\vec{u}$  and  $\vec{v}$  where  $m_1$  and  $m_2$  are in the same quadrant



(b) Western Rd. to Windermere Rd.

Figure 4.4: Example of an undetected turn

Figure	$\varphi_1$	$\varphi_2$	$\varphi_3$	$\lambda_1$	$\lambda_2$	$\lambda_3$	$m_1 * m_2$
4.2	43.0105	43.0105	43.0107	-81.2707	-81.2706	-81.2707	negative
4.3	43.015	43.015	43.0151	-81.2765	-81.2764	-81.2763	positive
4.4	43.0148	43.0149	43.0150	-81.2766	-81.2766	-81.2765	positive

Table 4.1: Results from Figures 4.2, 4.3 and 4.4 for  $m_1 * m_2$

It is assumed that turn maneuvers take place at 90 degrees or more, but it's possible for them to occur at  $< 90$  degrees and remain in the same quadrant (see Figure 4.4). A quick fix would be to rotate  $(\lambda_1, \varphi_1)$ ,  $(\lambda_2, \varphi_2)$  and  $(\lambda_3, \varphi_3)$  by 45 degrees using this formula:

$$\begin{bmatrix} \cos 45 & -\sin 45 \\ \sin 45 & \cos 45 \end{bmatrix} \begin{bmatrix} \Delta\lambda \\ \Delta\varphi \end{bmatrix} \tag{4.5}$$

yielding

$$\Delta\lambda' = 0.707\Delta\lambda - 0.707\Delta\varphi \tag{4.6}$$

and

$$\Delta\varphi' = 0.707\Delta\lambda + 0.707\Delta\varphi. \quad (4.7)$$

Then  $m_1$  and  $m_2$  can be calculated to determine a turn:

$$m_1 * m_2 = \Delta\varphi'_2\Delta\varphi'_1\Delta\lambda'_2\Delta\lambda'_1. \quad (4.8)$$

<i>Figure</i>	$\varphi_1$	$\varphi_2$	$\varphi_3$	$\lambda_1$	$\lambda_2$	$\lambda_3$	$m_1 * m_2$
4.2	43.0105	43.0105	43.0107	-81.2707	-81.2706	-81.2707	positive
4.3	43.015	43.015	43.0151	-81.2765	-81.2764	-81.2763	positive
4.4	43.0148	43.0149	43.0150	-81.2766	-81.2766	-81.2765	negative

Table 4.2: Results from Figures 4.2, 4.3 and 4.4 when the coordinates are rotated by 45 degrees

The results from Table 4.2 show that the turn from Western Rd. to Windermere Rd. is now detected. However the results from Figure 4.2 have changed. By rotating all the coordinates by 45 degrees, the classification has changed from a turn to no turn at all. This is why, described further in the next section, the set of results from the original calculation,  $S_1$ , and the set of results from rotating the coordinates,  $S_2$ , will constitute all turns detected by the algorithm:

$$S_1 \cup S_2. \quad (4.9)$$

By taking the union, a turn is detected from Figure 4.2 and Figure 4.4, and Figure 4.3 does not count as a turn. This is the correct turn identification for these three examples.

## 4.2 Implementation

The turn detection algorithm consists of three stages, with the amalgamation of these stages producing the final set of turns for each driver. The three stages are:

1. Turn Detection
  - (a) Without rotation.
  - (b) With rotation.
2. Merge Turns
3. Remove Duplicates

Each stage is programmed in its own method, which are called in order by a main program; the block diagram of the processing is presented in Figure 4.5.

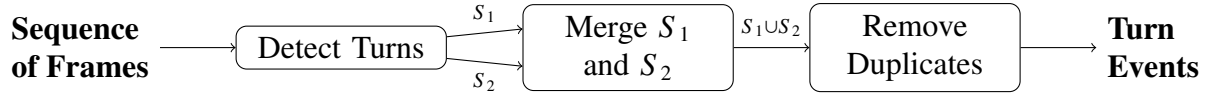


Figure 4.5: Block diagram of the position-based turn detection program

### 4.2.1 *main()*

The main program loops through the raw data for all 16 drivers and generates a file containing the detected turns with comma-separated values. The sequence of frames for each driver is supplied to the main program, which is then passed to the detection methods, *detectTurns()* and *detectTurnsRotated()*. These two methods use the sequence of frames to detect turns. *detectTurns()* and *detectTurnsRotated()* will produce different results, which is why *mergeTurns()* takes these results and combines them. There will also be turns detected by both methods, as seen at the end of the previous section, so the *removeDuplicates()* method is called to ensure that each turn in the set is unique. Lastly, the final set is saved to a file.

---

#### Algorithm 1: *main(dData)*

---

```

1 Input: dData % this contains raw data about each driver, shown in Table 3.1
2 Output: 16 files of turn events % where each file contains turn events of the driver
3 for driver in dData do
4    $S_1 \leftarrow \text{detectTurns}(\text{driver.fSeq}())$ 
5    $S_2 \leftarrow \text{detectTurnsRotated}(\text{driver.fSeq}())$ 
6    $S \leftarrow \text{mergeTurns}(S_1, S_2)$ 
7    $S' \leftarrow \text{removeDuplicates}(S)$ 
8    $S'.\text{write}()$ 

```

---

### 4.2.2 *detectTurns()* and *detectTurnsRotated()*

Algorithm 2 and Algorithm 3 are implementations of the concepts discussed in the previous section. Both methods read *FSeq* frame by frame, and keep track of the latitude and longitude values of the current frame and the previous frame:  $\lambda_1, \varphi_1, \lambda_2$  and  $\varphi_2$ . The algorithm looks for a change in latitude values,  $\Delta\varphi \neq 0$ , and a change in longitude values,  $\Delta\lambda \neq 0$ , between the previous frame and the current frame. This change indicates that the vehicle has moved to a different geographical location, and this must be checked to see if a turn could have occurred. The change in latitude and longitude is compared against a *NOISY\_THRESHOLD* which has been set to 0.0002. This threshold is used to avoid any false positives that may cause a turn to be detected when there is missing data. The latitude and longitude values were examined and they do not increase or decrease by more than 0.0001. *NOISY\_THRESHOLD* is thus set to 0.0002 to ensure that the vehicle is travelling incrementally when a change is detected.

The flag *change* is used to determine if a change has been detected before (*change = True*) or if this is the first change the program has seen (*change = False*). Once the program confirms

that a difference has occurred in Line 13 and this difference is valid, the flag is checked to determine if this could be a) the start of a turn, or b) the end of a turn. A start of a turn means that  $change = False$  since a difference has not yet been detected, and an end of a turn means that  $change = True$  since the program has already detected a difference in geographical location and this could mean the end of a turn.

When the start of a turn is identified, the program saves the value of  $m_1$  at Line 18, which is used later when the program detects a second change in latitude and longitude. When a possible end of a turn is identified, this could mean either a) a turn is detected, or b) a turn is not detected and the vehicle is simply travelling along a straight path. In both cases,  $m_2$  is calculated and the program checks  $m_1 * m_2$ . If  $m_1 * m_2 \leq 0$  then the program detects a turn. Before this turn is added to  $S_1$  ( $S_2$  for Algorithm 3), the absolute average steering wheel position between  $f_{start}$  to  $f_{end}$  needs to be checked against a  $BEND\_THRESHOLD$ .  $BEND\_THRESHOLD$  is needed to differentiate actual turns from bends in the road. Without this threshold some bends may be detected as turns if given the proper  $\lambda_1, \varphi_1, \lambda_2$  and  $\varphi_2$ . An example of a detected bend is the one north of Oxford Street along Western Road. The value of  $BEND\_THRESHOLD$  was chosen by trial and error. The threshold is set to 40 for Algorithm 2 and 100 for Algorithm 3 as they proved most successful in identifying turns and excluding bends. If  $m_1 * m_2 \leq 0$  and the absolute value of the average steering wheel position is less than  $BEND\_THRESHOLD$ , then the turn event is added to  $S_1$  ( $S_2$  for Algorithm 3). The method  $wheelDirection()$  calculates the average steering wheel position from  $f_{start}$  to  $f_{end}$ . If the average is negative, then the steering wheel position was, on average, to the left of the center position which signifies a left turn. If the average was positive, then  $wheelDirection()$  would indicate that, on average, the steering wheel was to the right of the center and label a right turn.

If  $m_1 * m_2 > 0$  then the program does not detect a turn. In this case, the vehicle is continuing along a straight path. However, this could also indicate the start of a new turn. The program does not ignore the possibility of a new turn, so it sets  $m_1$  to  $m_2$  and  $change$  remains to be  $True$ .

Based on the turn detection program, the start of an identified turn is defined as the first change in latitude or longitude values. The end of the turn is defined as the second change in latitude or longitude values. The frame number of  $f_{start}$  and  $f_{end}$  are converted to a time, in seconds, using this formula:

$$t_1 = \frac{f_{start}}{15} \quad (4.10)$$

and

$$t_2 = \frac{f_{end}}{15}, \quad (4.11)$$

and their difference constitutes the duration of the turn in seconds:

$$d = t_2 - t_1. \quad (4.12)$$

**Algorithm 2:** *detectTurns(fSeq)*


---

```

1 Input: fSeq % sequence of frames
2 Output:  $S_1$  % set of turns containing start and end frames, start and end latitude and
   longitude
3  $S_1 \leftarrow \phi$ 
4  $f_1 \leftarrow fSeq[1]$  % first frame
5  $\varphi_1 = latitude(f_1)$ 
6  $\lambda_1 = longitude(f_1)$ 
7 change  $\leftarrow False$  % True if possible turn detected
8 for f in fSeq do
9    $\varphi_2 = latitude(f)$ 
10   $\lambda_2 = longitude(f)$ 
11   $\Delta\varphi = \varphi_2 - \varphi_1$ 
12   $\Delta\lambda = \lambda_2 - \lambda_1$ 
13  if ( $\Delta\varphi \neq 0$  or  $\Delta\lambda \neq 0$ ) and  $\Delta\varphi < NOISY\_THRESHOLD$  and
      $\Delta\lambda < NOISY\_THRESHOLD$  then
14    % change in latitude or longitude is detected
15    if change == False then
16      % possible start of a turn
17      change  $\leftarrow True$ 
18       $m_1 \leftarrow \Delta\varphi\Delta\lambda$ 
19       $f_{start} \leftarrow f$ 
20       $\varphi_1 = \varphi_2$ 
21       $\lambda_1 = \lambda_2$ 
22    else
23      % possible end of a turn
24       $f_{end} \leftarrow f$ 
25       $m_2 \leftarrow \Delta\varphi\Delta\lambda$ 
26      if  $m_1 * m_2 \leq 0$  and averageWheel( $f_{start}, f_{end}$ ) < BEND\_THRESHOLD then
27        % turn detected
28        turn_type  $\leftarrow wheelDirection(f_{start}, f_{end})$ 
29        turn  $\leftarrow (f_{start}, f_{end}, turn\_type)$ 
30         $S_1.append(turn)$ 
31        change  $\leftarrow False$ 
32      else
33        % turn not detected, possible start of a turn
34         $f_{start} \leftarrow f_{end}$ 
35         $m_1 = m_2$ 
36         $\varphi_1 = \varphi_2$ 
37         $\lambda_1 = \lambda_2$ 
38    else
39       $\varphi_1 = \varphi_2$ 
40       $\lambda_1 = \lambda_2$ 

```

---

**Algorithm 3:** *detectTurnsRotated(fSeq)*


---

```

1 Input: fSeq % sequence of frames
2 Output:  $S_2$  % set of turns containing start and end frames, start and end latitude and
   longitude
3  $S_2 \leftarrow \phi$ 
4  $f_1 \leftarrow fSeq[1]$  % first frame
5  $\varphi_1 = \text{latitude}(f_1)$ 
6  $\lambda_1 = \text{longitude}(f_1)$ 
7 change  $\leftarrow$  False % True if possible turn detected
8 for f in fSeq do
9    $\varphi_2 = \text{latitude}(f)$ 
10   $\lambda_2 = \text{longitude}(f)$ 
11   $\Delta\varphi = \varphi_2 - \varphi_1$ 
12   $\Delta\lambda = \lambda_2 - \lambda_1$ 
13  if ( $\Delta\varphi \neq 0$  or  $\Delta\lambda \neq 0$ ) and  $\Delta\varphi < \text{NOISY\_THRESHOLD}$  and
      $\Delta\lambda < \text{NOISY\_THRESHOLD}$  then
14    % change in latitude or longitude is detected
15    if change == False then
16      % possible start of a turn
17      change  $\leftarrow$  True
18       $\Delta\lambda' \leftarrow 0.707\Delta\lambda - 0.707\Delta\varphi$ 
19       $\Delta\varphi' \leftarrow 0.707\Delta\lambda + 0.707\Delta\varphi$ 
20       $m_1 \leftarrow \Delta\varphi'\Delta\lambda'$ 
21       $f_{start} \leftarrow f$ 
22       $\varphi_1 = \varphi_2$ 
23       $\lambda_1 = \lambda_2$ 
24    else
25      % possible end of a turn
26       $f_{end} \leftarrow f$ 
27       $\Delta\lambda' \leftarrow 0.707\Delta\lambda - 0.707\Delta\varphi$ 
28       $\Delta\varphi' \leftarrow 0.707\Delta\lambda + 0.707\Delta\varphi$ 
29       $m_2 \leftarrow \Delta\varphi'\Delta\lambda'$ 
30      if  $m_1 * m_2 \leq 0$  and  $\text{averageWheel}(f_{start}, f_{end}) < \text{BEND\_THRESHOLD}$  then
31        % turn detected
32        turn_type  $\leftarrow$  wheelDirection( $f_{start}, f_{end}$ )
33        turn  $\leftarrow$  ( $f_{start}, f_{end}, \text{turn\_type}$ )
34         $S_2.append(\text{turn})$ 
35        change  $\leftarrow$  False
36      else
37        % turn not detected, possible start of a turn
38         $f_{start} \leftarrow f_{end}$ 
39         $m_1 = m_2$ 
40         $\varphi_1 = \varphi_2$ 
41         $\lambda_1 = \lambda_2$ 
42    else
43       $\varphi_1 = \varphi_2$ 
44       $\lambda_1 = \lambda_2$ 

```

---



Algorithm 2 detects turns directly from the sequence of frames for each driver. Algorithm 3 does the same, except the coordinates are rotated by 45 degrees. This is so wide turns, such as the turn from Western Road to Windermere Road, can be detected even though the angle between  $\vec{u}$  and  $\vec{v}$  is less than 90 degrees and remain in the same quadrant. Lines 18 and 19, and 27 and 28 in Algorithm 3 rotate the latitude and longitude coordinates before calculating  $m_1 * m_2$ .

### 4.2.3 *mergeTurns()*

The previous section observed that the results of Algorithm 2 and Algorithm 3 are different, and, thus, need to be combined using a merging algorithm.

The merging algorithm reads all turn events from  $S_1$  and  $S_2$  and stores them in a dictionary, ordered by the starting frame of the turn (see Lines 6 and 8). They are stored by starting frame so that the dictionary can be sorted at Line 9. The starting frame of a turn indicates the time at which the turn started (see Equation 4.10). The method produces a list of turns, ordered by occurrence, that were detected by both Algorithm 2 and Algorithm 3.

---

#### **Algorithm 4:** *mergeTurns*( $S_1, S_2$ )

---

```

1 Input:  $S_1$  and  $S_2$  % two sets of turn events
2 Output:  $S$  % the combined set of turn events
3  $S \leftarrow \phi$ 
4  $turnDict \leftarrow \phi$  % dictionary of turns stored by start frame
5 for  $turn$  in  $S_1$  do
6    $turnDict[turn.startFrame()] \leftarrow turn$ 
7 for  $turn$  in  $S_2$  do
8    $turnDict[turn.startFrame()] \leftarrow turn$ 
9  $S \leftarrow sort(turnDict)$ 

```

---

### 4.2.4 *removeDuplicates()*

Algorithm 2 and Algorithm 3 produce different sets of turns, however, there are also similarities between  $S_1$  and  $S_2$ , i.e. they can both detect turns that represent the same turn event. This results in a set of duplicate turns when the merge method unifies the sets.

The *removeDuplicates()* method extracts distinct turn events from the combined set of turns. This will represent the final the set of turns to write to the file. It reads the first two turns from  $S$  and tests whether the two turns are the same turn or two separate turns. The start frame and end frame of both turns are evaluated to determine the closeness between the turns. A *FRAME\_THRESHOLD* measures this closeness. If the difference between start frames and end frames is less than this threshold, then both turns occur within a certain amount of time such that they are the same turn. If the difference between start frames and end frames is more than the threshold, the turns occur far apart and define two separate turn events.

*FRAME\_THRESHOLD* was tested on values between a 15 and 225 frame difference, which is equivalent to 1 to 15 seconds. It was assumed that turns could not occur back-to-back in less than 1 second. The testing proved that 170 was the most optimal value for *FRAME\_THRESHOLD*. It was found that if it was more than 170 the method would start merging turns that were actually different. This proved that turns were separated by at least 11.3 seconds. If *FRAME\_THRESHOLD* was set to a value less than 170, the method would separate turns that were the same, thus leaving duplicate turns in the final set.

If the first two turn events represent different turns, then both turn events were added to  $S'$ . If they are duplicates of the same turn, then the second turn was added to  $S'$  (see Line 10). There is no advantage to taking one turn over the other, so *turn2* was chosen by default. The method proceeds to read the rest of the turn events from  $S$ , one turn at a time. It updates *turn1* and *turn2* by setting *turn1* to *turn2* and *turn2* to the new turn being read. Since the turns in  $S$  are sorted by occurrence, it is suitable to read and compare turns in sequential pairs. If there are duplicate turns, then they will be listed one after the other in  $S$ .

If *turn1* and *turn2* are separate turn events, then only *turn2* will be added to  $S'$ . If they are the same event, none of them are added to  $S'$ . In the loop, the second turn is the only one copied to  $S'$ , so if the turns are the same, they are essentially skipped so that there is no duplicate of *turn2* in  $S'$ . Remember, *turn2* is reset to *turn1* at the start of the loop.

---

**Algorithm 5:** *removeDuplicates(S)*

---

```

1 Input:  $S$  % set of turn events
2 Output:  $S'$  % set of distinct turn events
3  $S' \leftarrow \phi$ 
4  $turn1 \leftarrow S.readTurn()$ 
5  $turn2 \leftarrow S.readTurn()$ 
6 if  $!(abs(turn1.startFrame() - turn2.startFrame()) < FRAME\_TRHESHOLD$  or
    $abs(turn1.endFrame() - turn2.endFrame()) < FRAME\_THRESHOLD)$  then
7    $S'.append(turn1)$ 
8    $S'.append(turn2)$ 
9 else
10   $S'.append(turn2)$ 
11 for  $turn$  in  $S$  do
12    $turn1 \leftarrow turn2$ 
13    $turn2 \leftarrow turn$ 
14   if  $!(abs(turn1.startFrame() - turn2.startFrame()) < FRAME\_TRHESHOLD$  or
      $abs(turn1.endFrame() - turn2.endFrame()) < FRAME\_THRESHOLD)$  then
15      $S'.append(turn2)$ 

```

---

### 4.3 Results and Discussion

After executing *main()*, which executes *detectTurns()*, *detectTurnsRotated()*, *mergeTurns()* and *removeDuplicates()*, 16 files of turn events were generated where each file contains the turn events of its respective driver. Figures 4.7 to 4.25 show the plotted route based on the GPS data. Overlying these routes are red and green points. A red point represents a left turn that was detected by the PBT method and a green point represents a right turn. These turns were taken from the driver's turn events file provided by *main()*.

Any turns that were detected going in and out of parking lots were excluded, along with turns occurring in a parking lot. This was to prevent these turns from skewing the results of the analysis. The points circled in Figure 4.6 were excluded since they represent turns in the Middlesex parking lot. There are a few special cases where parking lot turns occur elsewhere along the route for drivers 6, 7 and 8. These turns were specially omitted for these drivers.



Figure 4.6: Turns that occur in a parking lot

Figure 4.7 shows a plotted view of all the latitude and longitude coordinates found in the data for driver 1. In Chapter 3, a map view of the route was provided in Figure 3.2. Table 3.2 describes this map view with the start road, end road and turn type for each turn. There is an exact match between Figure 4.7, Figure 3.2 and Table 3.2. In total, 18 turns were detected for driver 1 out of 18 true turns shown by Figure 4.7.

The following accuracy formula will be employed to gauge the effectiveness of the PBT method algorithm for a specific driver:

$$A_i = \frac{n - FP - FN}{n}, \quad (4.13)$$



Figure 4.7: Plotted route of driver 1



Figure 4.8: Plotted route of driver 2

where  $n$  is the number of true turns for driver  $i$ ,  $FP$  is the number of false positives detected for driver  $i$ , and  $FN$  is the number of false negatives not detected for driver  $i$ .

The accuracy of the PBTB method will thus be the sum of the accuracy of each driver divided by the number of drivers:

$$A = \frac{\sum_{i=1}^{16} A_i}{16} \quad (4.14)$$

or

$$A = \frac{n_T - FP_T - FN_T}{n_T}, \quad (4.15)$$

where  $n_T$  is the number of true turns across all drivers,  $FP$  is the total number of false positives, and  $FN$  is the total number of false negatives.

Figure 4.8 for driver 2 shows the same set of results as Figure 4.7 for driver 1. The PBTB algorithm detected two false positives for driver 3, shown in Figure 4.9. Note that there are two turns in the yellow circle in Figure 4.9 that occur close together.

Table 4.3 shows the raw data frames where the first false positive was detected. This false positive was detected by Algorithm 3, so if the coordinates were rotated by  $90^\circ$  then there would be a change in direction. The wheel position also appears to be fluctuating enough that it exceeds the *BEND\_THRESHOLD*. Figure 4.10 shows the coordinates on a map. Based on the map and the average steering wheel position, it appears to be that the algorithm was correct to detect a turn here, however a turn did not actually occur.

Table 4.4 shows the raw data frames where the second false positive was detected, which was shortly after the first FP. Again, the steering wheel position is large, this time to the right, and there is a change in direction as detected by Algorithm 2. Figure 4.11 also shows a map view of this FP and, again, it looks like a turn occurred.



Figure 4.9: Plotted route of driver 3 with 2 FP

<i>Frame Number</i>	<i>Latitude</i>	<i>Longitude</i>	<i>Speed</i>	<i>Brake Pressure</i>	<i>Gas Pressure</i>	<i>Steering Wheel Position</i>
37977	42.9947	-81.2116	7	1	0	60
37978	42.9947	-81.2117	7	1	0	54
...						
38067	42.9947	-81.2117	12	1	0	-234
38068	42.9947	-81.2118	13	1	0	-237

Table 4.3: Raw data of driver 3 where the first false turn was detected

Driver 4 has correct results like drivers 1 and 2, except driver 4 turned from Waterloo Street to Pall Mall Street and Pall Mall Street to Richmond Street instead of Waterloo Street to Central Avenue and Central Avenue to Richmond Street (refer to Figure 4.12). This is the first instance of the driver deviating from the predetermined route. Turns detected for these deviations will be included in the analysis, as long as they do not occur in parking lots.

This is also the first instance of missing data. There are two occurrences along Highbury Avenue where there is no GPS data. They did not affect the results for driver 4, however it will be shown later that missing data will not detect turns that occur during that time frame. This is one of the limitations of the PBTD algorithm.

The RoadLab vehicle experienced slight distortions from the GPS signals for driver 5, shown in Figure 4.13, as well as missing data in the northern area of the route. Even with these

Frame Number	Latitude	Longitude	Speed	Brake Pressure	Gas Pressure	Steering Wheel Position
38247	42.9947	-81.2119	5	39	0	524
38248	42.9947	-81.212	5	38	0	524
...						
38386	42.9947	-81.212	1	1	1	276
38387	42.9946	-81.2118	17	1	65	56

Table 4.4: Raw data of driver 3 where the second false turn was detected

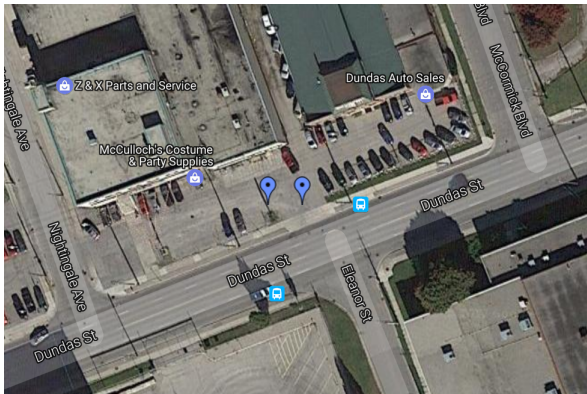


Figure 4.10: Map view of driver 3 where the first false turn was detected

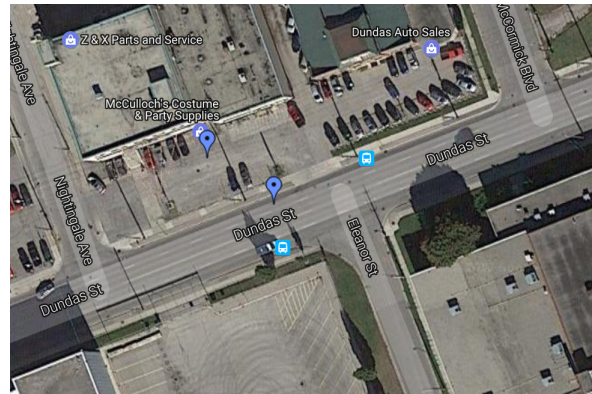


Figure 4.11: Map view of driver 3 where the second false turn was detected

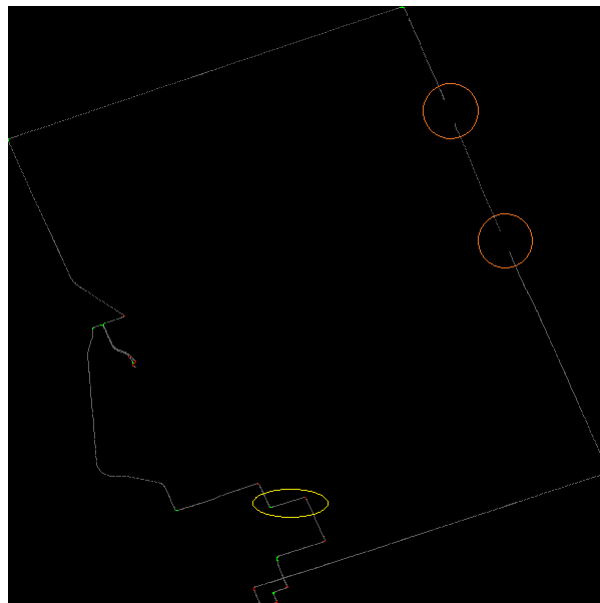


Figure 4.12: Plotted route of driver 4

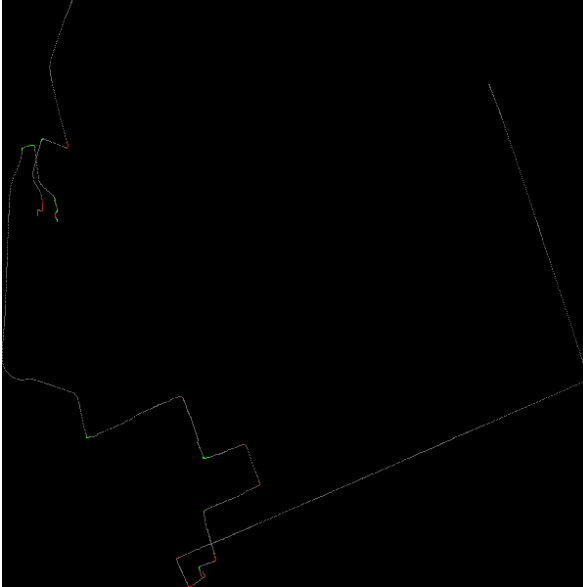


Figure 4.13: Plotted route of driver 5



Figure 4.14: Plotted route of driver 6

distortions, the results were not affected. However, turns that occurred where there was missing data were not detected. For example, the turns at Richmond Street and Sunningdale Road, and Sunningdale Road and Highbury Avenue were not detected. Since these turns were essentially missing due to GPS, they are not counted as true turns. So out of a total of 16 true turns for driver 5, 16 were detected by the algorithm.

In general, distorted GPS data will not have an affect on the analysis of turns, since the analysis only involves vehicle parameters during the turn; not latitude and longitude. Vehicle parameters will fluctuate within a turn which is why they are included in the analysis. Latitude and longitude, as discussed earlier, will only fluctuate by 0.0001, which is not useful for analysis. Hence they will be excluded, so distorted GPS data will not have an affect on the end results.

Figure 4.14 shows the route taken by driver 6. There are a few differences to highlight. First, there are a few parking lot turns along Sunningdale Road that were excluded. Second, driver 6 went from York Street to Richmond Street, which skipped the two turns from York Street to Talbot Street and Talbot Street to King Street. Lastly, there was missing data from Highbury Avenue to Dundas Street, so the algorithm was not able to detect this turn. Despite having three less true turns than the official route, all the turns were detected for driver 6.

Driver 7 started in the Middlesex parking lot, however the RoadLab vehicle came online after the turn onto Richmond Street as verified by Steve Beauchemin, the first observant in the vehicle at the time (see Figure 4.15). This means that two turns were ignored: one from Perth Drive to Windermere Road, and another from Windermere Road to Richmond Street. Additionally, a detour was taken slightly off the official route along Richmond Street, and there were a few parking lot turns that were excluded. After coming out of the parking lot, driver 7 turned from Fanshawe Park Road back onto Richmond Street. This turn was included since it

did not occur in a parking lot. In total, driver 7 has 17 true turns out of which 17 were detected by the algorithm.



Figure 4.15: Plotted route of driver 7

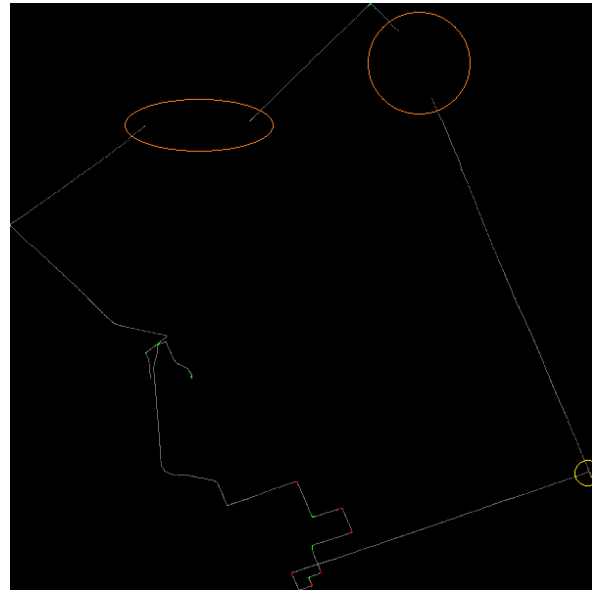


Figure 4.16: Plotted route of driver 8

Figure 4.16 shows distortions in GPS coordinates for driver 8. It is difficult to conclude if these distortions also caused some missing data, although it appears that if the coordinates were oriented properly, the cut-off ends would meet. This is speculated by matching the distance along Sunningdale Road and Highbury Avenue in Figure 4.16 to the distance of those roads in Figure 4.15. Driver 8 also had a slight detour. After looking at the video sequences for driver 8, it appears that they missed the right turn from Highbury Avenue to Dundas Street and had to turn around by going into a parking lot. These parking lot turns were excluded, but the left turn from Highbury Avenue back onto Dundas Street was included. This caused driver 8 to have the same amount of turns as the official route, with the turn from Highbury Avenue to Dundas Street being a left turn instead of a right turn.

Figure 4.17 shows that there is missing data for driver 9. This caused the turn from Richmond Street to Oxford Street to go undetected, leaving 17 true turns for driver 9 of which 17 were detected.

There was one false negative, i.e. missed turn, for driver 10 (see Figure 4.18). This was the left turn from Dufferin Avenue to Waterloo Street. Table 4.5 shows the raw data frames of where the turn should have been detected. In Section 4.1, the mathematics behind the PBDT algorithm was explained as a fluctuation in latitude and longitude values. Table 4.5 shows that, based on this concept, a turn should be detected because the longitude values fluctuate. In the PBDT algorithms themselves, *BEND\_THRESHOLD* is also employed to discriminate turns from bends. The average steering wheel position between frames 69822 and 69882 is  $-41.2$ , which falls below the threshold. This causes the turn to remain undetected. Unfortunately,



if the value of *BEND\_THRESHOLD* was changed to accommodate this turn, it would cause more false positives to be detected and hurt the accuracy of the algorithm.



Figure 4.17: Plotted route of driver 9



Figure 4.18: Plotted route of driver 10 with 1 FN

Frame Number	Latitude	Longitude	Speed	Brake Pressure	Gas Pressure	Steering Wheel Position
69822	42.9883	-81.2439	24	1	26	-152
69823	42.9884	-81.2438	24	1	26	-139
...						
69851	42.9884	-81.2438	26	1	32	-33
69852	42.9885	-81.2438	26	1	32	-32
...						
69881	42.9885	-81.2438	28	1	26	3
69882	42.9885	-81.2439	28	1	26	4

Table 4.5: Raw data of driver 10 where a turn should have been detected

The data for drivers 11 and 12 (see Figures 4.19 to 4.20) did not have any issues, except some missing data for driver 12 along Sunningdale Road. The official route was taken by these 2 drivers with no GPS distortions and all turn events were detected.

Figure 4.21 shows the route taken by driver 13 and their results. There was missing data along parts of Western Road and Windermere Road, which caused 2 missing turns. The PBDT algorithm also failed to detect 2 turns at York Street to Talbot Street and Talbot Street to King Street. There is also a false positive that was detected along Central Avenue. Table 4.6 shows the raw data where the false positive was detected along Central. The turn was detected by Algorithm 3 where the coordinates were rotated by 90°. There is considerable variation in the steering wheel position by just looking at the start and end of the FP turn, however the map



Figure 4.19: Plotted route of driver 11



Figure 4.20: Plotted route of driver 12

view (shown in Figure 4.22) does not seem to indicate that a turn occurred, but perhaps a lane change.

<i>Frame Number</i>	<i>Latitude</i>	<i>Longitude</i>	<i>Speed</i>	<i>Brake Pressure</i>	<i>Gas Pressure</i>	<i>Steering Wheel Position</i>
76488	42.9910	-81.2482	12	46	0	-116
76489	42.9910	-81.2483	12	44	0	-120
...						
76547	42.9910	-81.2483	11	1	33	-103
76548	42.9910	-81.2484	11	1	33	-100

Table 4.6: Raw data of driver 13 where a false turn was detected

Tables 4.7 and 4.8 show where the two missed turns should have been detected by the algorithm. Both tables show that the reason the turns were not detected as the same reason a turn was not detected for driver 10: the average steering wheel position was too small to exceed *BEND\_THRESHOLD*. The average steering wheel position was -29.29 between frames 63676 and 64067 (Table 4.7) and -8.6 between frames 64726 and 65748 (Table 4.8). The duration of the second missed turn is just over 1000 frames, and it may have been this large duration that caused the average steering wheel position to be so small between those frames.

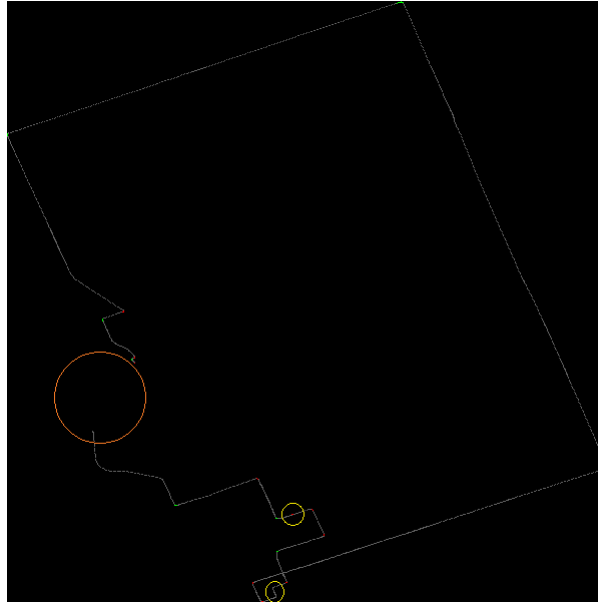


Figure 4.21: Plotted route of driver 13 with 1 FP and 2 FN



Figure 4.22: Map view of driver 13 where a false turn was detected

<i>Frame Number</i>	<i>Latitude</i>	<i>Longitude</i>	<i>Speed</i>	<i>Brake Pressure</i>	<i>Gas Pressure</i>	<i>Steering Wheel Position</i>
63676	42.9807	-81.2507	15	1	27	-406
63677	42.9807	-81.2506	15	1	23	-399
...						
63706	42.9807	-81.2506	18	1	0	-203
63707	42.9808	-81.2506	18	1	0	-200
...						
63766	42.9808	-81.2506	9	93	0	10
63767	42.9809	-81.2506	9	93	0	10
...						
64066	42.9809	-81.2506	14	1	39	3
64067	42.9810	-81.2507	14	1	39	3

Table 4.7: Raw data of driver 13 where the first FN should have been detected

<i>Frame Number</i>	<i>Latitude</i>	<i>Longitude</i>	<i>Speed</i>	<i>Brake Pressure</i>	<i>Gas Pressure</i>	<i>Steering Wheel Position</i>
64726	42.9818	-81.2510	1	83	0	-129
64727	42.9818	-81.2511	1	83	0	-128
...						
65506	42.9818	-81.2511	5	54	0	141
65507	42.9819	-81.2511	5	70	0	141
...						
65747	42.9819	-81.2511	23	1	80	142
65748	42.9820	-81.2510	23	1	80	136

Table 4.8: Raw data of driver 13 where the second FN should have been detected



Figure 4.23: Plotted route of driver 14



Figure 4.24: Plotted route of driver 15

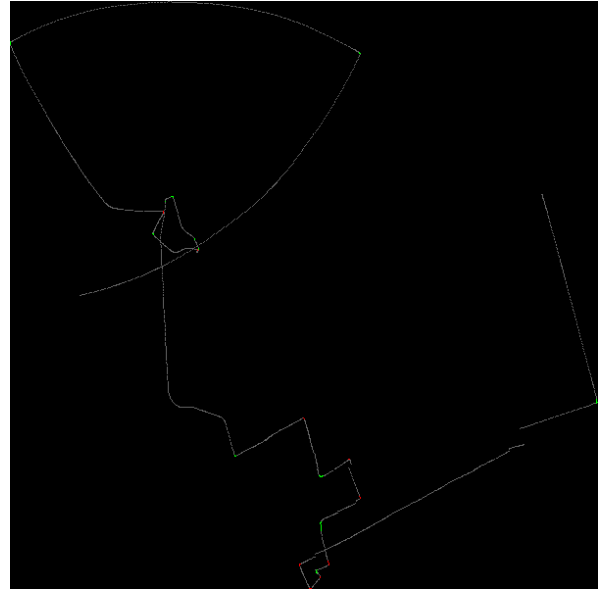


Figure 4.25: Plotted route of driver 16

Drivers 14 and 15 (see Figures 4.23 and 4.24) did not have any issues. There was some missing data along Richmond Street for driver 14, but this did not have an affect on the results. In Figure 4.25 it is clear that there are large GPS distortions for driver 16. But, like with drivers 5 and 8, these distortions did not affect the accuracy of the algorithm.

	<i>Driver</i>																<i>Total</i>
	<i>1</i>	<i>2</i>	<i>3</i>	<i>4</i>	<i>5</i>	<i>6</i>	<i>7</i>	<i>8</i>	<i>9</i>	<i>10</i>	<i>11</i>	<i>12</i>	<i>13</i>	<i>14</i>	<i>15</i>	<i>16</i>	
<i>True Turns</i>	18	18	18	18	16	16	17	18	17	18	18	18	16	16	18	18	278
<i>PBTD</i>	18	18	20	18	16	16	17	18	17	17	18	18	15	16	18	18	278
<i>FP</i>	0	0	2	0	0	0	0	0	0	0	0	0	1	0	0	0	3
<i>FN</i>	0	0	0	0	0	0	0	0	0	1	0	0	2	0	0	0	3

Table 4.9: Results of the Position-Based Turn Detection algorithm

Using Equation 4.15 and the results summarized in Table 4.9, the accuracy of the PBTD algorithm can be determined:

$$A = \frac{n_T - FP_T - FN_T}{n_T} \quad (4.16)$$

$$= \frac{278 - 3 - 3}{278} \quad (4.17)$$

$$= 0.9784 \quad (4.18)$$

$$= 97.84\% \quad (4.19)$$

Based on this equation, the algorithm achieves 97.84% accuracy.

There has been some debate over whether missed turns due to missing data, which has been seen with drivers 5, 6, 9 and 13, should be counted as true turns. From one perspective, these missing turns could argue that the PBTD algorithm should be modified to accommodate the possibility of missing data, or use a different method entirely that is able to impute when there is missing data. From another perspective, it is arguable that it is not the limitations of the algorithm but of the RoadLab dataset itself. In either case, Table 4.10 summarizes the results with missed turns due to missing data included. The accuracy of the algorithm then becomes 95.77%.

	<i>Driver</i>																
	1	2	3	4	5	6	7	8	9	10	11	12	13	14	15	16	Total
<i>True Turns</i>	18	18	18	18	18	17	17	18	18	18	18	18	18	16	18	18	284
<i>PBTD</i>	18	18	20	18	16	16	17	18	17	17	18	18	15	16	18	18	278
<i>FP</i>	0	0	2	0	0	0	0	0	0	0	0	0	1	0	0	0	3
<i>FN</i>	0	0	0	0	2	1	0	0	1	1	0	0	4	0	0	0	9

Table 4.10: Results of the Position-Based Turn Detection algorithm with missed turns (due to missing data) included as actual turns

An accuracy of 97.84% and 95.77% holds promise, however there are a couple areas that need to be considered to improve the algorithm in the future:

1. *BEND\_THRESHOLD*,
2. *FRAME\_THRESHOLD* and
3. Distortion of GPS data.

The optimal values of both *BEND\_THRESHOLD* and *FRAME\_THRESHOLD* contribute to the accuracy of the PBTD algorithm since *BEND\_THRESHOLD* successfully eliminates

bends and *FRAME\_THRESHOLD* successfully removes duplicate turns. It is possible that the value of these thresholds may have overfitted the results for this specific route, especially *FRAME\_THRESHOLD*. *FRAME\_THRESHOLD* assumed turns could not occur less than 11.3 seconds apart, which isn't necessarily true of all routes. The algorithm is supposed to work optimally given any route, and it is difficult to prove that the value of *BEND\_THRESHOLD* would work accordingly. Future research could focus on choosing thresholds independent of the route taken.

The distortion of GPS data could also pose a threat for other routes. It did not affect the results for the route used in this research since the distortions did not largely affect the angle going from one road to another. But that doesn't mean it isn't possible for the GPS coordinates to be warped enough so that it smooths the transition from road to another, causing a turn to be missed by the algorithm. This could prove to be a second limitation to the algorithm.

# Chapter 5

## Cluster Analysis

As the turn detection methods identified  $(f_{start}, f_{end})$  turn pairs, it also extracted information about the turn. Algorithms 2 and 3 calculated the average, standard deviation, kurtosis and skewness of:

1. speed,
2. brake pressure,
3. gas pressure, and
4. steering wheel position.

They also calculated the acceleration of each turn, which was defined as:

$$a = \frac{v_{f_{end}} - v_{f_{start}}}{d}, \quad (5.1)$$

where  $v_{f_{end}}$  is the speed at the end of the turn and  $v_{f_{start}}$  is the speed at the start of the turn. The duration,  $d$ , was defined in Equation 4.12. Duration is also used to analyze the time it takes to complete a turn. The last two descriptors are the age and gender of the driver, as they may be useful in categorizing driver behaviour.

Kurtosis and skewness are computed as metrics which, along with the average and standard deviation, become part of the set of descriptors for input to the clustering algorithm. These two metrics - kurtosis and skewness - will only be used as measures to characterize turns, while average and standard deviation will be used to analyze the cluster results.

The rest of the chapter is organized as follows. In the next section, all the preprocessing steps will be explained. In this section, normalization is performed on the data, and files are generated in order to analyze driving behaviour prior to a turn, during a turn, and after a turn. In Section 5.2, K-Means clustering is introduced and is performed on all preprocessed files generated from Section 5.1 using the most optimal value for  $K$ . Finally, in Section 5.3, cluster assignments are evaluated for consistency across pre-, during and post- turns. An optimal time



will be selected before and after a turn that will be most suitable for cluster analysis in the future.

## 5.1 Preprocessing

In total, there are 20 descriptors for each turn. This research will analyze driving behaviour across all drivers by averaging all the turns of each driver into one set of descriptors. This will create one file for analysis with 16 entries representing each driver, where each entry contains the average of each of the 20 descriptors. The aim of this research is to analyze driver behaviour in relation to other drivers in order to build towards a computational model of driver behaviour. This is why all the turns are averaged for each driver instead of looking at turns within each driver, and then each driver is analyzed against one another.

Before the averaging takes place, the values of 18 descriptors need to be normalized (excluding age and gender) so that analysis is done on the same scale, which will prevent any of the descriptors from skewing the results. To do this, the MinMaxScaler method was used from the scikit-learn Python library to normalize all descriptor values for all drivers between 0 and 1. Steering wheel and acceleration are the only descriptors that can have negative values, so the following equation was used to extract the zero value after normalization:

$$zero\_value = \frac{-min}{max - min}, \quad (5.2)$$

where *min* is the lowest value for that descriptor and *max* is the highest value. Table 5.1 shows the zero values for the average, standard deviation, kurtosis and skewness of the steering wheel descriptor, as well as acceleration.

	<i>Zero value</i>
<i>Average of wheel position</i>	0.42291678
<i>Standard deviation of wheel position</i>	0.5061441
<i>Kurtosis of wheel position</i>	0.12448418
<i>Skewness of wheel position</i>	0.32532348
<i>Acceleration</i>	0.3485342

Table 5.1: Zero values of steering wheel position and acceleration during turns

The raw RoadLab data was not normalized because it would reduce the capability of choosing an optimal value for *BEND\_THRESHOLD*.

After normalization, the descriptors are averaged, and the standard deviation, skewness and kurtosis of acceleration and duration are calculated. The analysis file now contains 26 descriptors, including age and gender. To generate this file, descriptors were produced from the vehicle parameters *within* each turn for every frame that was part of the turn, which created the average, standard deviation, skewness and kurtosis of the vehicle parameters. But these could

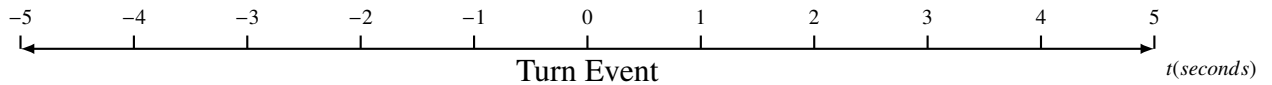
not be calculated for acceleration and duration since they are derivatives of the vehicle parameters. The average, standard deviation, skewness and kurtosis of acceleration and duration were able to be calculated by averaging all the turns together, creating a set of descriptors *across* all turns.

Table 5.2 shows how each descriptor should be interpreted during analysis based on all the calculations that were made to generate the file.

<i>Descriptor</i>	<i>Interpretation</i>
Average [wheel, brake, gas, speed]	Average of the averages of [wheel, brake, gas, speed]
Standard Deviation [wheel, brake, gas, speed]	Average standard deviation of [wheel, brake, gas, speed]
Kurtosis [wheel, brake, gas, speed]	Average kurtosis of [wheel, brake, gas, speed]
Skewness [wheel, brake, gas, speed]	Average skewness of [wheel, brake, gas, speed]
Average [acceleration, duration]	Average [acceleration, duration]
Standard Deviation [acceleration, duration]	Standard deviation of [acceleration, duration]
Kurtosis [acceleration, duration]	Kurtosis of [acceleration, duration]
Skewness [acceleration, duration]	Skewness of [acceleration, duration]

Table 5.2: Summary of how the final set of descriptors are to be interpreted

Analysis files will also need to be created for pre- and post-turns. The vehicle parameters should be analyzed before and after a turn to expose underlying driving behaviours before and after each turn event. This research will analyze the average turn descriptors of each driver between 1 and 5 seconds before and after a turn, in 1-second increments. This means there will be a file for 5 seconds, 4 seconds, 3 seconds, 2 seconds and 1 second prior to a turn, and a file for 1 second, 2 seconds, 3 seconds, 4 seconds and 5 seconds after a turn. This creates a timeline for the analysis, where there is a file representing the average turn descriptors for each driver at a certain point in time:



In the above diagram, 0 represents the time of the actual turn event, even though the duration of a turn event is longer than 0 seconds. The timeline should be interpreted relative to a turn, so even though this timeline does not consider turn duration, it shows the different time intervals pre- and post- turns.

The pre- and post- turn files for 1 to 5 seconds are generated from the original 16 turn files of each driver. Each turn had a start frame and end frame, which is another representation of time. If  $t = 1$  second, then that represents 15 frames of data (see Table 5.3).

The vehicle parameters were taken up to  $t * 15$  number of frames before and after each turn defined in the turn file, depending on  $t$  (see Algorithms 6 and 7). This is where the average, standard deviation, skewness and kurtosis of steering wheel position, brake pressure, gas pressure and speed were calculated. The duration was excluded as a descriptor since it is defined by  $t$ , hence it would be constant. Acceleration was calculated based on the time interval and

$t$	Number of Frames
1	15
2	30
3	45
4	60
5	75

Table 5.3: Translation of 1-second intervals to number of frames

speed. Then the average was calculated again on all descriptors, as well as standard deviation, skewness and kurtosis for acceleration, which produced one final set of descriptors that represents a single driver. The resulting file contained a set of 22 descriptors for each driver for the given value of  $t$ .

---

**Algorithm 6:**  $pre(t)$ 


---

```

1 Input: files, dData % 16 files of turn events, raw data of all drivers
2 Output:  $pre_t$  % file containing turn descriptors t-seconds prior to each turn event
3 for turns in files do
4   for turn in turns do
5     for i in ( $turn[f_{start}] - (t * 15)$ ,  $turn[f_{start}]$ ) do
6       descriptors.storeVehicleParameters(dData)
7       S'.write()
8       descriptors.calculateAverage()
9       descriptors.calculateStd()
10      descriptors.calculateKurtosis()
11      descriptors.calculateSkewness()
12      descriptors.append(acceleration)
13    acceleration.calculateAverage()
14    acceleration.calculateStd()
15    acceleration.calculateKurtosis()
16    acceleration.calculateSkewness()
17    descriptors.append(acceleration)
18 descriptors.normalize()
19  $pre_t.write(descriptors.averageDescriptors())$ 

```

---

Algorithms 6 and 7 were executed on each of the values for  $t$ . In total, there are 11 files for analysis that contain information on driver behaviour. Each of these files can be found in Appendix A.

**Algorithm 7:** *post(t)*


---

```

1 Input: files, dData % 16 files of turn events, raw data of all drivers
2 Output: postt % file containing turn descriptors t-seconds after each turn event
3 for turns in files do
4   for turn in turns do
5     for i in (turn[fend], turn[fend] + (t * 15)) do
6       descriptors.storeVehicleParameters(dData)
7       S'.write()
8     descriptors.calculateAverage()
9     descriptors.calculateStd()
10    descriptors.calculateKurtosis()
11    descriptors.calculateSkewness()
12    descriptors.append(acceleration)
13  acceleration.calculateAverage()
14  acceleration.calculateStd()
15  acceleration.calculateKurtosis()
16  acceleration.calculateSkewness()
17  descriptors.append(acceleration)
18 descriptors.normalize()
19 pret.write(descriptors.averageDescriptors())

```

---

## 5.2 K-Means Clustering

The K-Means clustering algorithm was the chosen clustering method for this analysis. The algorithm can be modelled in 4 steps:

1. Choose the number  $K$  of clusters for set of points  $x_1 \dots x_n$ .
2. Place centroids  $c_1 \dots c_K$  at random locations.
3. Repeat until convergence:
  - (a) For each point  $x_i$ :
    - i. Find nearest centroid  $c_j$ .
    - ii. Assign the point  $x_i$  to cluster  $j$ .
  - (b) For each cluster  $j = 1 \dots K$ :
    - i. Recompute new centroid  $c_j$  as mean of all points  $x_i$  assigned to cluster  $j$  in previous step.
4. Stop when none of the cluster assignments change.

The K-Means algorithm requires two inputs:  $K$ , the number of clusters, and a set of points in  $n$ -dimensional space. The algorithm was performed in both 26-dimensional space and 22-

dimensional space, since those are the number of descriptors available throughout all turns, and before and after every turn taken by each driver.

There are two approaches that will be used to pick a value for  $K$  for each of the analysis files. The Elbow method is a validation method to help find the appropriate number of clusters in a dataset. The method computes the average within-cluster sum of squares (WCSS) for different values of  $K$ . The WCSS-values and  $K$ -values are plotted which reveals a sharp angle in the graph. This “elbow” indicates the value of  $K$  most suited to the dataset, or file, that is going to be analyzed.

The second approach, called the Silhouette analysis, measures the separation distance between clusters for different  $K$ -values. A silhouette coefficient is computed for each cluster which ranges from -1 to 1. The closer the silhouette coefficient is to 1, the more separation there is between neighbouring clusters. The average silhouette score is the computed average of the silhouette coefficients. The higher the average, the more separation there is, on average, between a cluster and its neighbours. In the Silhouette analysis, the value for  $K$  is chosen with the highest average silhouette score.

Both approaches were implemented in Python 3.5. The matplotlib and pandas libraries were used for the Elbow method, and the scikit-learn library was used for the Silhouette analysis.

The data in each analysis file (shown in Tables A.1 to A.11) were passed to both implementations of the Elbow method and the Silhouette analysis. Figures 5.1 to 5.11 show the results of the Elbow method. With Figures 5.1 to 5.4, which show 5, 4, 3 and 2 seconds pre-turns, it is difficult to determine if the number of clusters should be 2 or 3, since the angle between 2 and 3 clusters look similar by visually looking at the figures. This is why two approaches are being used, since the Elbow method may not necessarily produce a clear “elbow”. The Silhouette analysis will help decide whether to use 2 or 3 clusters for these files. With Figures 5.5 to 5.11 it is clear that the “elbow” occurs at 2 clusters, so this is the chosen  $K$ -value for the rest of the files.

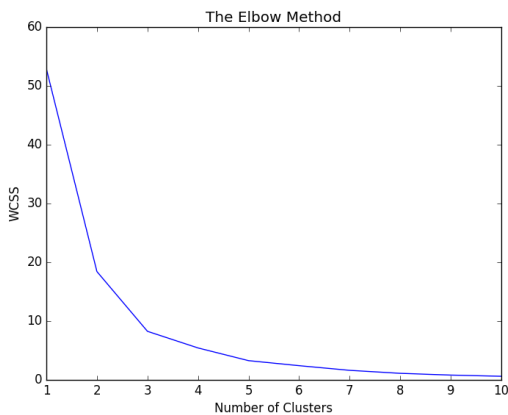


Figure 5.1: Result of the elbow method for all drivers 5 seconds prior to all turns

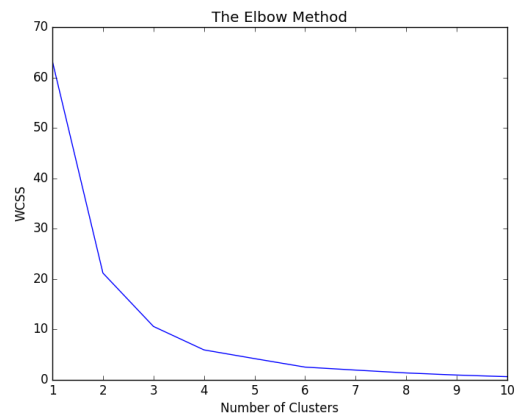


Figure 5.2: Result of the elbow method for all drivers 4 seconds prior to all turns

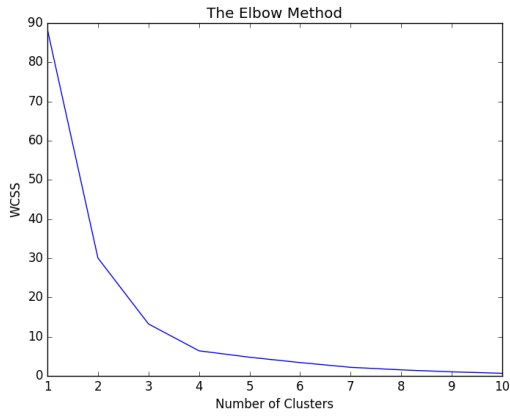


Figure 5.3: Result of the elbow method for all drivers 3 seconds prior to all turns

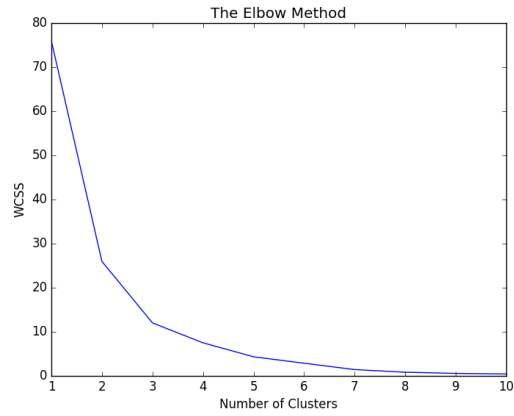


Figure 5.4: Result of the elbow method for all drivers 2 seconds prior to all turns

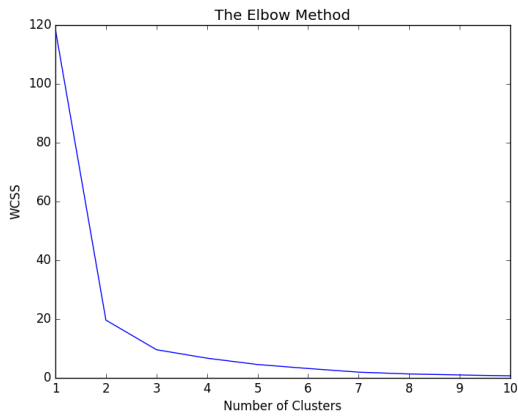


Figure 5.5: Result of the elbow method for all drivers 1 second prior to all turns

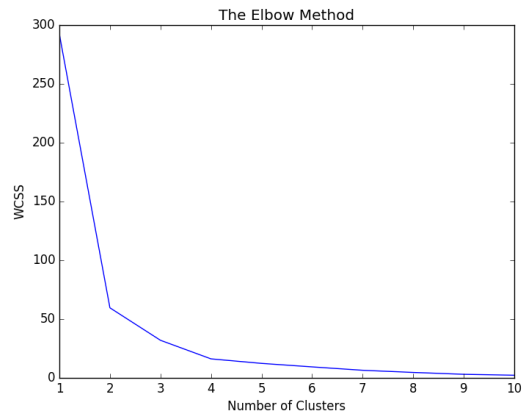


Figure 5.6: Result of the elbow method for all drivers during turns

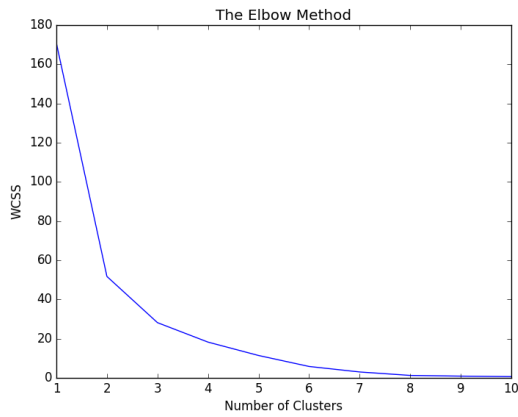


Figure 5.7: Result of the elbow method for all drivers 1 second after all turns

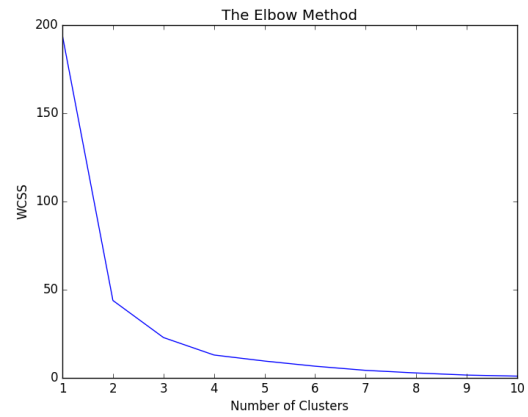


Figure 5.8: Result of the elbow method for all drivers 2 seconds after all turns

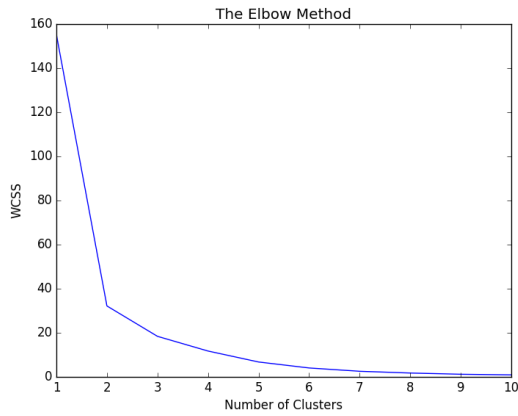


Figure 5.9: Result of the elbow method for all drivers 3 seconds after all turns

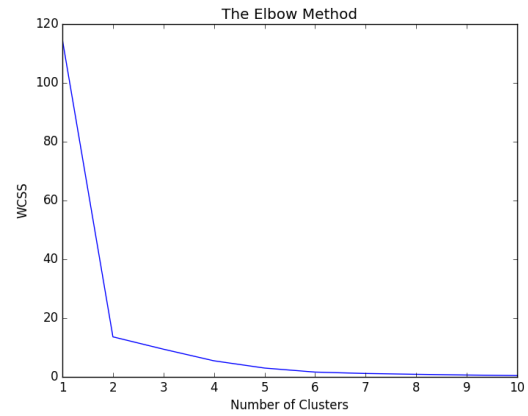


Figure 5.10: Result of the elbow method for all drivers 4 seconds after all turns

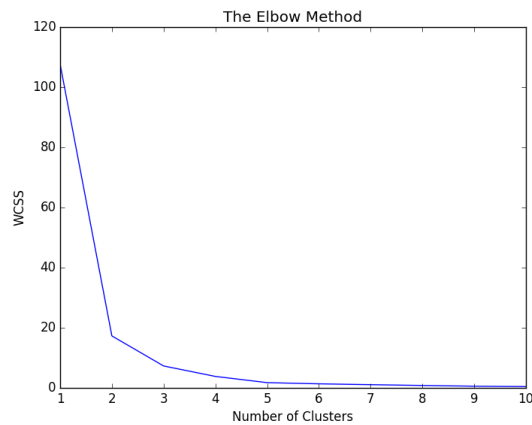


Figure 5.11: Result of the elbow method for all drivers 5 seconds after all turns

Table 5.4 shows the average silhouette scores for each file for up to and including 6 clusters. The cells that are highlighted represent the highest average silhouette scores for each file. Here, the Silhouette analysis recommends 3 clusters for 5 seconds pre-turns, and 2 clusters for the rest. In general, the average silhouette score decreases the more clusters there are, with a few exceptions. This could be because there are only 16 observations, which is a relatively small sample, which could have caused the scores to be sensitive based on the number of clusters.

n_clusters	Pre-					During	Post-				
	5 secs.	4 secs.	3 secs.	2 secs.	1 sec.		1 sec.	2 secs.	3 secs.	4 secs.	5 secs.
2	0.56	0.57	0.68	0.65	0.76	0.64	0.60	0.62	0.64	0.75	0.71
3	0.58	0.54	0.53	0.52	0.54	0.53	0.54	0.52	0.53	0.60	0.62
4	0.51	0.55	0.57	0.53	0.52	0.51	0.56	0.49	0.50	0.46	0.67
5	0.48	0.46	0.51	0.51	0.49	0.48	0.59	0.43	0.51	0.52	0.57
6	0.44	0.48	0.47	0.37	0.39	0.44	0.52	0.44	0.45	0.50	0.50

Table 5.4: Silhouette scores of all analysis files for 1 to 6 clusters

Table 5.5 summarizes what  $K$ -values will be passed to the K-Means algorithm. The first file, the 5 seconds pre-turn file, will use both 2 and 3. The Silhouette analysis suggests to use 3 clusters, however the rest of the files are using 2. To maintain consistency, both 2 and 3 will be used for this file.

n_clusters	Pre-					During	Post-				
	5 secs.	4 secs.	3 secs.	2 secs.	1 sec.		1 sec.	2 secs.	3 secs.	4 secs.	5 secs.
	2, 3	2	2	2	2	2	2	2	2	2	2

Table 5.5: The chosen  $K$ -value(s) for each file

The  $K$ -values have been determined for each of the files. There are two other parameters of the K-Means algorithm that will be modified for the analysis. The 2nd step of the algorithm states “Place centroids  $c_1 \dots c_K$  at random locations”. It has been found that placing centroids randomly can create what is known as the Random Initialization Trap. If centroids are placed close together, this could take longer processing time and possibly give different results. The `kmeans++` parameter will be used to avoid this trap. Given this parameter, the algorithm will choose initial values with a certain separation distance. This will increase processing time, but, more importantly, the results will stay consistent if the algorithm was executed on the same data multiple times.

The next step of the algorithm is to “Find nearest centroid  $c_j$  for each point  $x_i$ ”. For the second parameter, a choice has been made to use Euclidean distance over Manhattan distance. It has been found that both measures produced the same clustering results, so the decision to use Euclidean distance was arbitrary.

Weka 3.8 was the software used for the K-Means cluster analysis on each file. All of the descriptors were included in the analysis, except for `sub_no`, `age` and `gender`. `Gender` was



ignored because K-Means can only accept numeric attributes, and because it could have skewed the results. Sub\_no simply identifies the driver which is not useful for K-Means. Age was ignored because it could also have skewed the results. While not used for clustering, sub\_no, age and gender will help interpret the results and find patterns between clusters.

### 5.3 Results and Cluster Descriptions

The K-Means clustering algorithm was performed on all 11 preprocessed files. The results of the clustering algorithm can be found in Appendix B.

The angle between clusters will be used as a measure to quantify their separation. These clusters will be represented as two vectors,  $v$  and  $w$ :

$$\vartheta = \cos^{-1} \frac{v \cdot w}{|v||w|} \quad (5.3)$$

where  $v$  is the vector of the centroid of cluster0 and  $w$  is the vector of the centroid for cluster1. The centroids represent the average value of each of the descriptors in each cluster. This means that  $v$  and  $w$  represent vectors in 20-dimensional space for clusters derived from pre- and post-turns, and 24-dimensional space for clusters during turns.

Table 5.6 shows the centroids at 5 seconds prior to turns for three clusters. Here, vector  $z$  is introduced as the vector for cluster2. The angle will need to be calculated in cluster-pairs, so it will need to be computed between  $v$  and  $w$ ,  $w$  and  $z$  and  $v$  and  $z$ .

		Centroids													
			avg_sp	std_sp	kurt_sp	skew_sp	avg_br	std_br	kurt_br	skew_br	avg_gas	std_gas	kurt_gas	...	
<b>Pre-</b>	5 s	$v$	0.39	0.32	0.07	0.61	0.34	0.24	0.10	0.51	0.17	0.20	0.05	...	
		$w$	0.33	0.35	0.06	0.62	0.29	0.16	0.10	0.53	0.26	0.20	0.04	...	
		$z$	0.40	0.35	0.08	0.60	0.35	0.17	0.12	0.54	0.23	0.16	0.03	...	
		Centroids													
			skew_gas	avg_wh	std_wh	kurt_wh	skew_wh	avg_ac	std_ac	kurt_ac	skew_ac	avg_dur	std_dur	kurt_dur	skew_dur
...			0.35	0.47	0.16	0.12	0.51	0.47	0.10	1.04	0.07				
...			0.33	0.44	0.18	0.12	0.53	0.50	0.11	1.87	0.93				
...			0.31	0.43	0.17	0.13	0.53	0.48	0.09	-0.54	0.11				

Table 5.6: Cluster centroids for cluster0 ( $v$ ), cluster1 ( $w$ ) and cluster2 ( $z$ ) at 5 seconds pre-turns

Table 5.7 shows the calculated results of the angle,  $\vartheta$ , between each cluster-pair. There appears to be some separation in cluster-pairs by looking at  $\vartheta$ . The lowest angle is 25.63 degrees, which is fairly separable given the vectors are in 20-dimensional space. The other two values, 73.28 and 57.13, also indicate considerable separation.

Table 5.8 shows the centroids for cluster0 and cluster1 for each interval of time. This table will be used later in this section to associate driving behaviours with each cluster. Table 5.9 summarizes the angles based on these centroids. The angle is at its lowest during turns and 4 seconds post-turns. It is believed that drivers are subjected to similar conditions during turns as

	<b>Pre-</b>		
	<i>5 secs.</i>		
<b>Clusters</b>	<i>0, 1</i>	<i>1, 2</i>	<i>0, 2</i>
$\vartheta$	25.63	73.28	57.13

Table 5.7: Angle between the 3 clusters 5 seconds pre-turns

		Centroids												
		avg_sp	std_sp	kurt_sp	skew_sp	avg_br	std_br	kurt_br	skew_br	avg_gas	std_gas	kurt_gas	...	
<b>Pre-</b>	5 s	v	0.39	0.33	0.08	0.61	0.34	0.22	0.11	0.52	0.18	0.19	0.05	...
		w	0.35	0.35	0.06	0.62	0.31	0.18	0.10	0.53	0.24	0.19	0.04	...
	4 s	v	0.39	0.35	0.12	0.51	0.34	0.19	0.12	0.51	0.21	0.16	0.05	...
		w	0.35	0.33	0.11	0.53	0.27	0.13	0.09	0.52	0.25	0.14	0.07	...
	3 s	v	0.37	0.31	0.06	0.65	0.31	0.13	0.12	0.51	0.20	0.11	0.06	...
		w	0.36	0.36	0.06	0.65	0.32	0.14	0.12	0.51	0.26	0.13	0.06	...
	2 s	v	0.36	0.27	0.10	0.50	0.27	0.15	0.13	0.53	0.20	0.10	0.09	...
		w	0.37	0.33	0.09	0.49	0.32	0.09	0.10	0.48	0.23	0.07	0.05	...
	1 s	v	0.35	0.29	0.13	0.48	0.28	0.07	0.12	0.50	0.21	0.08	0.09	...
		w	0.37	0.32	0.18	0.52	0.30	0.04	0.15	0.48	0.23	0.13	0.12	...
	<b>During</b>	v	0.49	0.25	0.08	0.46	0.25	0.37	0.07	0.51	0.27	0.25	0.04	...
		w	0.59	0.21	0.06	0.45	0.21	0.34	0.06	0.52	0.33	0.24	0.02	...
<b>Post-</b>	1 s	v	0.54	0.50	0.16	0.49	0.03	0.03	0.10	0.52	0.35	0.12	0.20	...
		w	0.49	0.39	0.19	0.52	0.03	0.02	0.08	0.49	0.27	0.10	0.16	...
	2 s	v	0.56	0.45	0.09	0.65	0.07	0.07	0.06	0.51	0.34	0.14	0.14	...
		w	0.53	0.40	0.08	0.67	0.03	0.02	0.11	0.51	0.30	0.08	0.11	...
	3 s	v	0.56	0.41	0.05	0.59	0.11	0.08	0.11	0.49	0.30	0.10	0.08	...
		w	0.56	0.43	0.05	0.60	0.03	0.02	0.14	0.52	0.34	0.12	0.08	...
	4 s	v	0.58	0.39	0.06	0.41	0.13	0.09	0.12	0.51	0.30	0.10	0.06	...
		w	0.58	0.41	0.06	0.42	0.03	0.02	0.18	0.53	0.34	0.11	0.06	...
	5 s	v	0.60	0.42	0.05	0.23	0.04	0.04	0.18	0.54	0.34	0.14	0.10	...
		w	0.56	0.40	0.04	0.23	0.07	0.06	0.19	0.52	0.30	0.11	0.09	...

Centroids													
skew_gas	avg_wh	std_wh	kurt_wh	skew_wh	avg_ac	std_ac	kurt_ac	skew_ac	avg_dur	std_dur	kurt_dur	skew_dur	
...	0.34	0.46	0.16	0.11	0.52	0.47	0.09	0.42	-0.10				
...	0.33	0.45	0.17	0.14	0.53	0.50	0.11	1.76	0.92				
...	0.44	0.44	0.14	0.14	0.53	0.47	0.11	0.96	0.13				
...	0.43	0.42	0.17	0.13	0.55	0.49	0.09	1.25	0.64				
...	0.33	0.42	0.16	0.13	0.50	0.40	0.07	0.82	0.16				
...	0.32	0.44	0.15	0.15	0.51	0.42	0.15	2.41	0.54				
...	0.45	0.44	0.18	0.12	0.39	0.41	0.07	0.40	-0.06				
...	0.43	0.42	0.18	0.09	0.44	0.41	0.10	1.19	0.34				
...	0.50	0.43	0.19	0.20	0.42	0.45	0.08	2.86	1.22				
...	0.49	0.42	0.21	0.15	0.41	0.43	0.10	0.37	-0.22				
...	0.35	0.44	0.63	0.08	0.36	0.45	0.15	-0.49	0.45	0.11	0.14	3.97	2.04
...	0.33	0.43	0.62	0.08	0.35	0.45	0.17	-0.63	-0.15	0.07	0.09	4.49	2.11
...	0.48	0.50	0.23	0.17	0.53	0.38	0.10	-0.43	0.52				
...	0.48	0.51	0.23	0.16	0.50	0.35	0.12	3.97	1.26				
...	0.48	0.49	0.18	0.09	0.66	0.27	0.12	3.31	1.38				
...	0.47	0.50	0.23	0.09	0.63	0.27	0.12	2.31	1.28				
...	0.50	0.53	0.20	0.16	0.55	0.29	0.11	1.38	0.94				
...	0.49	0.50	0.24	0.12	0.55	0.34	0.13	2.28	1.25				
...	0.50	0.54	0.21	0.18	0.40	0.27	0.13	1.79	1.00				
...	0.48	0.50	0.26	0.13	0.42	0.32	0.14	1.56	1.11				
...	0.46	0.51	0.23	0.13	0.46	0.28	0.13	0.14	0.69				
...	0.44	0.56	0.22	0.13	0.42	0.28	0.21	4.34	2.08				

Table 5.8: Cluster centroids for cluster0 (v) and cluster1 (w)

the course of action is restricted. Drivers are forced to do a turn maneuver as that is their goal. This assumption could explain why the angle is only 7.7 degrees. At 4 seconds post-turns, it is more difficult to rationalize why the angle is 6.65 degrees. Further analysis is needed to explain this.

The highest angles are at 1 second pre-turns, 1 second post-turns and 5 seconds post-turns. It is assumed that more distinct behaviours will arise immediately before a turn and immediately after a turn. These behaviours span 1 second before and after a turn, so this is the point in time when there is more activity in vehicle parameters such as braking and acceleration. Table 5.8 will be used later in this section for confirmation. Again, it is difficult to explain an angle of 59.87 degrees 5 seconds post-turns without further analysis. It is probable that the reason for this is because of outside influences.

	Pre-					During	Post-				
	5 secs.	4 secs.	3 secs.	2 secs.	1 sec.		1 sec.	2 secs.	3 secs.	4 secs.	5 secs.
$\theta$	42.87	16.99	29.17	28.86	57.38	7.77	81.63	8.94	12.78	6.65	59.87

Table 5.9: Angle between the 2 clusters at each point in time

Tables 5.10 to 5.15 summarize the results and show which drivers fall under which clusters. It does not appear as though there is a relationship between age or gender between clusters; there is a good mix, approximately 50/50, between male and female drivers in each cluster. Although one exception can be found in Table 5.13, where all drivers in cluster0 are female except for one male. Since there are more females in cluster0, the next step then requires looking at the ages of these females and comparing them to the ages of the females in cluster1. It turns out that there is a variety of age values for females in each cluster, so this remains inconclusive.

There are some observations in age that are worth noting. In Table 5.10, every driver in cluster1 is in their 20s (see cluster1 for 5 seconds pre-turns for 3 clusters). However, there are also drivers in their 20s in clusters 0 and 2. There is also no distinction in gender between drivers in their 20s in cluster 1, and drivers in their 20s in clusters 0 and 2. In Table 5.12, almost every driver in cluster0 (1 second pre-turns) is in their 20s, except for one driver who is 41. But, like with the previous observation, there is no relationship that can distinguish these drivers from the other 20-year-olds in cluster1.

	sub_no	age	gender		sub_no	age	gender
cluster0	1	37	Male	cluster0	1	37	Male
	3	41	Female		4	41	Male
	5	37	Female		5	37	Female
	7	31	Female		6	22	Female
	10	20	Male		7	31	Female
	12	24	Female		10	20	Male
	14	47	Female		12	24	Female
	15	44	Female		14	47	Female
cluster1	8	21	Male	cluster1	2	37	Male
	9	21	Female		3	41	Female
	11	22	Female		8	21	Male
	13	23	Male		9	21	Female
	16	25	Male		11	22	Female
cluster2	2	37	Male	13	23	Male	
	4	41	Male	16	25	Male	
	6	22	Female				

Table 5.10: Cluster assignments of drivers pre-turns of 5 seconds with 3 clusters and 5 seconds with 2 clusters

	sub_no	age	gender		sub_no	age	gender
cluster0	1	37	Male	cluster0	1	37	Male
	2	37	Male		2	37	Male
	3	41	Female		4	41	Male
	4	41	Male		5	37	Female
	6	22	Female		6	22	Female
	7	31	Female		8	21	Male
	10	20	Male		9	21	Female
	12	24	Female		10	20	Male
	14	47	Female		11	22	Female
	15	44	Female		12	24	Female
	16	25	Male		14	47	Female
cluster1	5	37	Female	cluster1	3	41	Female
	8	21	Male		7	31	Female
	9	21	Female		13	23	Male
	11	22	Female		16	25	Male
	13	23	Male				

Table 5.11: Cluster assignments of drivers pre-turns of 4 and 3 seconds with 2 clusters

	sub_no	age	gender		sub_no	age	gender
cluster0	1	37	Male	cluster0	3	41	Female
	5	37	Female		8	21	Male
	9	21	Female		9	21	Female
	10	20	Male		10	20	Male
	12	24	Female		11	22	Female
	16	25	Male		12	24	Female
cluster1	2	37	Male	cluster1	1	37	Male
	3	41	Female		2	37	Male
	4	41	Male		4	41	Male
	6	22	Female		5	37	Female
	7	31	Female		6	22	Female
	8	21	Male		7	31	Female
	11	22	Female		13	23	Male
	13	23	Male		14	47	Female
	14	47	Female		15	44	Female
	15	44	Female		16	25	Male

Table 5.12: Cluster assignments of drivers pre-turns of 2 and 1 seconds with 2 clusters

	sub_no	age	gender		sub_no	age	gender
cluster0	3	41	Female	cluster0	1	37	Male
	5	37	Female		2	37	Male
	11	22	Female		6	22	Female
	12	24	Female		8	21	Male
	15	44	Female		12	24	Female
	16	25	Male		13	23	Male
cluster1	1	37	Male	cluster1	3	41	Female
	2	37	Male		4	41	Male
	4	41	Male		5	37	Female
	6	22	Female		7	31	Female
	7	31	Female		9	21	Female
	8	21	Male		10	20	Male
	9	21	Female		11	22	Female
	10	20	Male		14	47	Female
	13	23	Male		16	25	Male
	14	47	Female				

Table 5.13: Cluster assignments of drivers during turns and post-turns of 1 second with 2 clusters

	sub_no	age	gender		sub_no	age	gender
cluster0	1	37	Male	cluster0	8	21	Male
	3	41	Female		12	24	Female
	8	21	Male	cluster1	1	37	Male
	12	24	Female		2	37	Male
cluster1	2	37	Male		3	41	Female
	4	41	Male		4	41	Male
	5	37	Female		5	37	Female
	6	22	Female		6	22	Female
	7	31	Female		7	31	Female
	9	21	Female		9	21	Female
	10	20	Male		10	20	Male
	11	22	Female		11	22	Female
	13	23	Male		13	23	Male
	14	47	Female		14	47	Female
	15	44	Female		15	44	Female
	16	25	Male		16	25	Male

Table 5.14: Cluster assignments of drivers post-turns of 2 and 3 seconds with 2 clusters

	sub_no	age	gender		sub_no	age	gender	
cluster0	8	21	Male	cluster0	1	37	Male	
	12	24	Female		2	37	Male	
cluster1	1	37	Male		3	41	Female	
	2	37	Male		5	37	Female	
	3	41	Female		6	22	Female	
	4	41	Male		7	31	Female	
	5	37	Female		9	21	Female	
	6	22	Female		10	20	Male	
	7	31	Female		12	24	Female	
	9	21	Female		13	23	Male	
	10	20	Male		14	47	Female	
	11	22	Female		15	44	Female	
	13	23	Male		cluster1	4	41	Male
	14	47	Female			8	21	Male
	15	44	Female			11	22	Female
	16	25	Male	16		25	Male	

Table 5.15: Cluster assignments of drivers post-turns of 4 and 5 seconds with 2 clusters

There does not appear to be a clear distinction between age and gender in any of the clusters. The next step is to use Table 5.8 to describe each cluster and associate behaviours by comparing the centroids. These observations are summarized in Table 5.16. A difference of  $\geq 5$  was used to differentiate between cluster0 and cluster1 as having “more” or “less” of some descriptor. Average and standard deviation helped distinguish between clusters. Kurtosis and skewness were excluded as observations since they cannot be described in terms of driver behaviour. Instead, they are simply used for the clustering algorithm which computationally decides the clustering for kurtosis and skewness.

		<b>cluster0</b>	<b>cluster1</b>
<b>Pre-</b>	5 s	Less average gas pedal pressure	More average gas pedal pressure
	4 s	More average braking More variation in braking	Less average braking Less variation in braking
		3 s	Less variation in speed Less average gas pedal pressure Less variation in acceleration
	2 s	Less variation in speed Less average braking More variation in braking	More variation in speed More average braking Less variation in braking
	1 s	Less variation in gas pedal pressure	More variation in gas pedal pressure
<b>During</b>		Less average speed Less average gas pedal pressure More variation in turn duration	More average speed More average gas pedal pressure Less variation in turn duration
<b>Post-</b>	1 s	More average speed More variation in speed More average gas pedal pressure	Less average speed Less variation in speed Less average gas pedal pressure
		2 s	More variation in speed More average braking More variation in braking More variation in gas pedal pressure Less variation in wheel position
	3 s	More average braking More variation in braking Less average acceleration	Less average braking Less variation in braking More average acceleration
	4 s	More average braking More variation in braking Less variation in wheel position Less average acceleration	Less average braking Less variation in braking More variation in wheel position More average acceleration
		5 s	Less average change in wheel position Less variation in acceleration

Table 5.16: Observations about cluster0 and cluster1 at each point in time

Based on these observations, it appears that cluster0 displays consistent behaviour over time as well as cluster1. The observations are also consistent within each time frame. For example, if

there is more braking (on average), then it is expected that there is also less pressure on the gas pedal. If there is more speed (on average) then it is possible for there to be more variation in speed. Speed and gas pedal pressure are almost synonymous, so if there is more average speed then more gas pedal pressure (on average) is also expected. Finally, if there is more braking (on average) then it is also possible that there is more variation in speed as more braking causes less speed.

Each cluster represents a certain pattern of behaviour and the drivers that fall under each cluster generally exhibit the behaviour of that cluster. The first cluster, cluster0, can be summarized as follows:

*Drivers in this cluster brake earlier and execute the turn with less speed. This causes their turns to take longer. After the turn, they immediately apply pressure to the gas pedal and gain speed. After gaining speed, pressure is applied to the brake pedal, perhaps to stabilize the speed of the vehicle.*

The second cluster, cluster1, can be summarized like so:

*Drivers in this cluster still apply gas pressure and start braking more just before the turn. This causes the speed to vary considerably. They take the turn at a slightly faster speed and they are left with less speed coming out of the turn. The vehicle coasts for 2 seconds and then the driver begins to accelerate.*

Based on these descriptions it appears that drivers in cluster0 are more cautious when approaching a turn. However after a turn, they waste no time in speeding up again. Drivers in cluster1 brake later, but they take more time accelerating after the turn. While cluster0 seems more cautious, it does not seem appropriate to classify cluster1 as aggressive driving. If the driving behaviour were aggressive, then it would be expected that the drivers accelerate faster coming out of the turn, which they don't. Drivers in cluster0 actually gain speed faster than drivers in cluster1. Thus, cluster0 will simply be described as "brake earlier; speed up earlier" and cluster1 will be described as "brake later; speed up later".

## 5.4 Driver Characterization

Now that behaviour classification has been established for each cluster, each driver will be inspected in terms of which cluster they fall under over time. Table 5.17 shows the cluster assignments of all drivers in each time frame. There is only one driver that consistently appears in cluster0 at each point in time: driver 12. This driver, therefore, falls under the "brake earlier; speed up earlier" category. Since there is only one driver that consistently belongs to one cluster for each point in time, it will not be enough to categorize drivers using just cluster0 and cluster1. For this reason, four *categories* will be used to categorize drivers. Clusters 0 and 1 identify two categories of driving behaviour. For this analysis of drivers over time, two other categories are introduced: "brake earlier; speed up later" and "brake later; speed up earlier". The first category out of the two describes a driver who is cautious, while the second describes



a driver who is more aggressive. The four categories are shown in Table 5.18.

These four categories are believed to best represent all possible driving behaviours in terms of braking and speed. Braking and speed will largely contribute to the categorization of drivers and enhance the capability of driver modelling. Each driver will be assigned to a category based on their braking and speed behaviours, and this will bring to light how these categories can benefit driver models and make driver characterization easier.

		<b>cluster0</b>	<b>cluster1</b>
<b>Pre-</b>	<i>5 secs.</i>	1, 4, 5, 6, 7, 10, 12, 14, 15	2, 3, 8, 9, 11, 13, 16
	<i>4 secs.</i>	1, 2, 3, 4, 6, 7, 10, 12, 14, 15, 16	5, 8, 9, 11, 13
	<i>3 secs.</i>	1, 2, 4, 5, 6, 8, 9, 10, 11, 12, 14, 15	3, 7, 13, 16
	<i>2 secs.</i>	1, 5, 9, 10, 12, 16	2, 3, 4, 6, 7, 8, 11, 13, 14, 15
	<i>1 sec.</i>	3, 8, 9, 10, 11, 12	1, 2, 4, 5, 6, 7, 13, 14, 15, 16
<b>During</b>		3, 5, 11, 12, 15, 16	1, 2, 4, 6, 7, 8, 9, 10, 13, 14
<b>Post-</b>	<i>1 sec.</i>	1, 2, 6, 8, 12, 13, 15	3, 4, 5, 7, 9, 10, 11, 14, 16
	<i>2 secs.</i>	1, 3, 8, 12	2, 4, 5, 6, 7, 9, 10, 11, 13, 14, 15, 16
	<i>3 secs.</i>	8, 12	1, 2, 3, 4, 5, 6, 7, 9, 10, 11, 13, 14, 15, 16
	<i>4 secs.</i>	8, 12	1, 2, 3, 4, 5, 6, 7, 9, 10, 11, 13, 14, 15, 16
	<i>5 secs.</i>	1, 2, 3, 5, 6, 7, 9, 10, 12, 13, 14, 15	4, 8, 11, 16

Table 5.17: Cluster assignments over time

	<b>Description</b>
<b>Category I (cluster0)</b>	Brake earlier; speed up earlier
<b>Category II (cluster1)</b>	Brake later; speed up later
<b>Category III (cluster0;cluster1)</b>	Brake earlier; speed up later
<b>Category IV (cluster1;cluster0)</b>	Brake later; speed up earlier

Table 5.18: The 4 categories of driving behaviour

Driver 1 remains in cluster0 before turning and brakes earlier. But then they switch to cluster1 and increase speed during the turn. After the turn, they switch back to cluster0 and start to gain speed, and instead of braking they switch again to cluster1 and continue to accelerate. In short, driver 1 brakes earlier and accelerates earlier, and even starts to gain speed during the turn versus waiting until after the turn. For this reason, driver 1 belongs to Category I.

Driver 2 applies more gas pedal pressure and starts in cluster1, but then immediately switches to cluster0 and brakes earlier. Before the turn, they switch back to the cluster1 and continue to brake, and then somehow take the turn with more speed. After the turn, driver 2 goes back to cluster0 and speeds up earlier. This puts driver 2 under Category I.

Driver 3 goes back and forth between cluster0 and cluster1 before the turn. They apply more gas pedal pressure, then more brake pedal pressure, then more gas pressure. Right before the

turn, they apply brake pressure again and execute the turn with less speed. Driver 3 then speeds up later. It is unclear if driver 3 brakes earlier or brakes later since they go back and forth before the turn. However, driver 3 will be put into Category II because at the start they are applying gas pressure and brake just before the turn.

Driver 4 starts in cluster0 and brakes earlier, and then switches to cluster1 before the turn and continue to brake. They take the turn with more speed and afterwards they remain in cluster1 and speed up later. Driver 4 therefore also falls under Category III.

Driver 5 has the opposite behaviour compared to driver 3 before the turn. Driver 5 applies more brake pedal pressure, then less brake pressure, then less gas pedal pressure and, right before the turn, less brake pressure. Then they take the turn at lower speed and accelerate later coming out of the turn. Because driver 5 started braking earlier, this puts them in Category III.

Driver 6 brakes earlier and starts in cluster0 and then continues to brake and switches to cluster1. They take the turn with slightly more speed, and then immediately speed up and go back to cluster0. Driver 6 then switches back to cluster1 and continues to accelerate. Driver 6 thus belongs to Category I as they brake earlier and speed up faster.

Driver 7 starts to brake earlier, and then they apply some gas pressure and begin braking again just before the turn. They drive through the turn with more speed and accelerate later. At the very beginning, driver 7 was in cluster0 and then remained in cluster1. They applied gas pressure before the turn which is why they fall under Category II.

Driver 8 starts in cluster1 and then moves to cluster0 when they have less gas pedal pressure. They go back to cluster1 and brake just before the turn, and take the turn with more speed. After the turn, they switch to cluster0 and remain there, indicating they speed up earlier. This puts driver 8 in Category IV.

Driver 9 started in cluster1 and did not brake. They switched to cluster0 and eased up on the gas pedal, and then they braked considerably due to the higher variation in braking. They took the turn at a higher speed and then waited before accelerating again. Driver 9 braked later and sped up later, so they belong in Category II.

Driver 10 remained in cluster0 for each time frame before the turn, and then switched over to cluster1 during and after the turn. This puts driver 10 in Category III.

Driver 11, like driver 8, also starts in cluster1 and moves to cluster0 when they have less gas pressure. They go back to cluster1 and brake just before the turn. Driver 11 brakes enough that they switch back to cluster0 and take the turn at less speed. After the turn, they wait to speed up. Driver 11 therefore belongs to Category II.

Driver 12 stayed in cluster0 for every point in time, so they belong to Category I.

Driver 13 is in cluster1 for each time frame before the turn and during the turn. They then

briefly switch over to cluster0 and speed up earlier, and go back to cluster1 and continue to accelerate. Driver 13 braked later and gained speed faster, which puts them in Category IV.

Driver 14 brakes earlier and then speeds up during the turn. They do not immediately speed up after the turn but wait to accelerate. Because of this, driver 14 falls under Category III.

Driver 15 brakes earlier and takes the turn with less speed. Right after the turn they begin to speed up and continue to accelerate. Therefore, driver 15 is classified in Category I.

Finally, driver 16 goes back and forth between cluster0 and 1 before the turn. They apply more gas pedal pressure, then more brake pedal pressure, the more gas pressure. Right before the turn, there is more variation in braking. They take the turn with less speed, and then switch back to cluster1 and remain there, indicating that they speed up later. This puts driver 16 in Category II.

The categorization of each driver is summarized in Table 5.19. The bulk of drivers fall under the first three categories, while only drivers 8 and 13 belong to Category IV. This category is considered the more aggressive category since drivers in this category brake just before the turn and speed up soon after the turn. There could be less drivers in this category because the RoadLab drivers were operating the vehicle under supervision, which could have caused them to behave more cautiously. Or, there are simply less “aggressive” drivers in the RoadLab dataset.

	<b>Driver</b>
<b>Category I (cluster0)</b>	1, 2, 6, 12, 15
<b>Category II (cluster1)</b>	3, 7, 9, 11, 16
<b>Category III (cluster0;cluster1)</b>	4, 5, 10, 14
<b>Category IV (cluster1;cluster0)</b>	8, 13

Table 5.19: Driver classification

## 5.5 Optimal Time for Analysis

The aim of this research is to provide the building blocks for driver characterization of turn maneuvers, and part of this requires choosing an optimal time for analysis. A naïve approach would be to select the time frame that contains the set of drivers for cluster0 and the set of drivers for cluster1 that proceeded to be classified into the equivalent category. This means that all drivers in cluster0 were classified in Category I, and all drivers in cluster1 were classified in Category II. But since there are only two clusters and four categories, a one-to-one correspondence will not work.

Another naïve approach would be to look at the number of times each driver was assigned to each cluster (see Table 5.20), and eliminate the categories by assigning each driver to the cluster

where they have the greater count (see Table 5.21). This enables a one-to-one correspondence between matching cluster assignments at one desired point in time to the classified drivers based on cluster count. The optimal time for analysis then becomes the point in time that has the best match.

	Driver															
Count	1	2	3	4	5	6	7	8	9	10	11	12	13	14	15	16
<i>cluster0</i>	7	4	5	3	5	5	3	6	4	6	3	11	2	4	6	3
<i>cluster1</i>	4	7	6	8	6	6	8	5	7	5	8	0	9	7	5	8

Table 5.20: Number of times each driver occurs in cluster0 and cluster1

	Driver															
Count	1	2	3	4	5	6	7	8	9	10	11	12	13	14	15	16
<i>cluster0</i>	1							1		1		1			1	
<i>cluster1</i>		1	1	1	1	1	1		1		1		1	1		1

Table 5.21: Cluster assignment based on count

The best match is simply defined as the highest number of correct assignments. Using Table 5.17, the best match occurs at 2, 3 and 4 seconds post-turns with a score of 13/16 correctly identified drivers. However 2-4 seconds after a turn does not seem relevant when the most activity occurs closer to a turn. It would also be useful to select a time prior to a turn to have the capability of predicting driving behaviours.

The approach this research will take requires looking back at the rationales behind putting drivers in a particular category. There are points in time that have become the deciding factor when it comes to classifying drivers. For example, 4 seconds and 3 seconds pre-turns were used to determine if a driver braked earlier. This characterization was applied to all the drivers in their rationales. Also, 1 second post-turns was used to label every driver as speeding up earlier or speeding up later. Based on these dependencies, 4 seconds and 3 seconds pre-turns, and 1 second post-turns are potential candidates for optimal analysis.

Table 5.22 shows a matrix of the cluster assignments for these 3 points in time, and highlight which assignments are found in the wrong cluster based on their category (see Table 5.19).

All the drivers assigned to the “speed up earlier” category were also found in the cluster assignment matrix for 1 second post-turns, as well as all drivers assigned to the “speed up later” category. This makes 1 second post-turns the perfect candidate for an optimal time for analysis. There are four misclassifications for 4 seconds pre-turns: drivers 3, 5, 7 and 16. Drivers 3, 7 and 16 were supposed to be among the cluster assignments in the “brake later” category, and driver 5 should have been with the cluster assignments in the “brake earlier” category. Again, this is all compared to the category they were assigned to which is shown in Table 5.19.

	<b>Brake earlier</b>	<b>Brake later</b>
<i>4 seconds</i>	1, 2, [3], 4, 6, [7], 10, 12, 14, 15, [16]	[5], 8, 9, 11, 13
<i>3 seconds</i>	1, 2, 4, 5, 6, [8], [9], 10, [11], 12, 14, 15	3, 7, 13, 16
<i>1 second</i>	1, 2, 6, 8, 12, 13, 15	3, 4, 5, 7, 9, 10, 11, 14, 16
	<b>Speed up earlier</b>	<b>Speed up later</b>

Table 5.22: Cluster assignments at 4 and 3 seconds pre-turns and 1 second post-turns compared to their categorization

There are three misclassifications for 3 seconds pre-turns: drivers 8, 9 and 11. These drivers, based on their classification, are supposed to be in the “brake later” category in the matrix. Between 4 seconds pre-turns and 3 seconds pre-turns, 3 seconds is more accurate with only three misclassified drivers. Ideally, the optimal analysis time should be prior to a turn in order to incorporate driver prediction and possible accident prevention in the future. But, because 1 second post-turns is so accurate, both 3-seconds pre-turns and 1 second post-turns will be chosen as the optimal time for analysis. Conceptually, these times are compatible with what is expected to occur near a turn. Before a turn, the driver has to take extra time to prepare, such as giving enough time to brake, checking if the light is green, spotting any walking pedestrians or cyclists, how far the vehicle is ahead, etc. Since the preparation for a turn takes time, it makes sense that the optimal time pre-turns is 3 seconds. Once the driver finishes the turn maneuver, there is less for them to check until they perform the next maneuver. This is why 1 second is a good time for analysis post-turns, since the driver can immediately take action once a turn is completed.

## 5.6 Key Observations

This chapter is summarized with three key observations:

1. Cluster0 and cluster1 represent two particular driving behaviours: brake earlier; speed up earlier and brake later; speed up later, respectively.
2. The optimal times for analysis are 3 seconds pre-turns and 1 second post-turns.
3. The categorization of drivers contributes to driver modelling with the use of four categories representing different types of behaviour.

# Chapter 6

## Conclusion and Future Work

This thesis made two major contributions for the modelling of drivers performing turn maneuvers:

1. A position-based turn detection algorithm with 97.84% accuracy, and
2. An analysis of turns  $t - 5$  to  $t + 5$  seconds to find an optimal time for modelling driver behaviour.

The PBTD algorithm used geographic latitude and longitude to detect turns on a frame-by-frame basis. The algorithm was executed with and without rotating the coordinates to identify turns occurring at less than 90 degrees. Both of these results were combined to produce a full set of turns for each driver. Prior to analysis, parking lot turns were manually removed, and the results were normalized and averaged for each driver.

Files were generated for each value of  $t$  up to and including 5 seconds pre- and post-turns. These files were passed to the K-Means clustering algorithm using the appropriate  $K$ -value as determined by the Elbow method and Silhouette analysis. The cluster assignments were examined and certain behaviours were associated with each cluster based on their centroids. From there, four categories were defined: brake earlier; speed up earlier, brake later; speed up later, brake earlier; speed up later and brake later; speed up earlier. The cluster assignments were then examined for each driver to assess how they changed from cluster to cluster over time, and this assessment was used to assign each driver to one of the four categories. This process helped determine two optimal times for behaviour analysis: 3 seconds pre-turns and 1 second post-turns.

Future work will include automating the entire process covered by this thesis. This may require eliminating Weka 3.8 and implementing K-Means clustering in Python 3.5, as the PBTD algorithm was also implemented in Python 3.5. An automated method would make it easier to construct driver models and classify driver behaviour more efficiently. In order to automate the entire process, parts of this thesis would also need to be modified. Currently, the PBTD algorithm is arguably overfitted to the RoadLab route with the use of *BEND\_THRESHOLD* and *FRAME\_THRESHOLD*. For this research, these thresholds were determined by trial and

error, however they should be set dynamically. They can be set dynamically for each route, or they can be tested on multiple routes and a fixed value can be decided for each threshold that gives the best overall accuracy for all tested routes. These constant values would then be used every time the process is computed. In short, a separate analysis would need to be performed to determine a proper value for *BEND\_THRESHOLD* and *FRAME\_THRESHOLD*.

Another useful modification would be to include automatic detection of turns within parking lots. This eliminates the need to manually remove parking lot turns, which were validated individually using geographic coordinates, from the turn files of each driver. A parking lot turn detection algorithm could be incorporated after the PBTD algorithm and before normalization and averaging of turn events. This also allows research to extend to the analysis of parking lot turns. They were excluded in the analysis for this thesis, but can be used for a separate analysis and see how the results compare to the clustering results of the turns analyzed in this paper. There may be parallels in driver behaviour between turns and turns in a parking lot.

Turns from one road to another was the chosen driving maneuver for this research, but the entire process covered here can be generalized for any driving maneuver, such as parking lot turns, lane changes, overtaking a vehicle, approaching a vehicle, and many more. The only component that would change is the maneuver detection algorithm, and analysis would still be conducted  $t - 5$  to  $t + 5$  seconds before and after each maneuver. This accelerates the work needed for driver modelling.

Analysis can also be performed across multiple driving maneuvers to check for consistency in driving behaviour. The clusters generated from the analysis of each maneuver can represent a type of behaviour and these labels can determine if a driver behaves similarly for other driving maneuvers. The more kinds of analyses that are done on drivers the more driver models can be improved. This also helps automobile manufacturers and researchers understand drivers better.

A key element that was excluded from this research was the driving environment. Elements in the environment, such as weather conditions, pedestrians, type of intersection (i.e. a yield, stop or traffic light intersection), and oncoming traffic, can explain why a turn is taking so long, sudden braking, sudden acceleration and any other reactive behaviour. The RoadLab dataset provides video sequences of the front of the vehicle as well as information about driver gaze. This part of the dataset can reveal the field of vision for each driver and where their attention (gaze) is focused. Computer vision techniques could extract environmental conditions and be cross-referenced with turn events, or any driving maneuver, to understand driving situations that may cause certain behaviour. The driving environment could also explain certain clustering results and expose particular turns that may skew these results.

The more ambitious avenue for future work is integrating automated modelling methods on an in-vehicle i-ADAS. The driver model would then be dynamic and constantly changing as the driver uses the vehicle and provides the model with more data with each passing second. This may introduce other research areas such as storage capacity, instrumentation and vehicle-to-vehicle communication. Machine learning methods can be used to learn any new driving behaviours and update the behaviour model in real time.

Finally, as discussed in Section 4.3, the PBTD algorithm could suffer when there is other distorted geographical data. With more routes, it can be determined if these distortions would affect the results of the algorithm. Also, the false negatives that the algorithm did not detect had abnormally low average steering wheel positions, which is what caused these turns to go undetected. The PBTD algorithm can be improved by adding another metric that decides if a turn occurred in conjunction with average wheel position.

This section concludes the research shown in this paper with future work for the position-based turn detection algorithm as well as a discussion on automating the entire process. The aim of this research was to provide insight on how to detect and analyze turn maneuvers and contribute to driver behaviour modelling, and provide footing for any future work on the topic.



# Bibliography

- [1] R. Abou-Jaoude. ACC radar sensor technology, test requirements, and test solutions. *IEEE Trans. on Intelligent Transportation Systems*, 4(3):115–122, 2003.
- [2] C. Bauer. A driver specific maneuver prediction model based on fuzzy logic. PhD Thesis, 2012.
- [3] M. Baumann and J. Krems. *A comprehension based cognitive model of situation awareness*. Springer, 2009.
- [4] S.S. Beauchemin, M.A. Bauer, D. Laurendeau, T. Kowsari, J. Cho, M. Hunter, K. Charbonneau, and O. McCarthy. Roadlab: An in-vehicle laboratory for developing on-board i-adas. In *Proceedings of the ISCA 23rd International Conference on Computer Applications in Industry and Engineering*, Imperial Palace Hotel, Las Vegas, Nevada, USA, November 2010. CAINE.
- [5] L. Bergasa, J. Nuevo, M. Sotelo, R. Barea, and M. Lopez. Real-time system for monitoring driver vigilance. *IEEE Trans. on Intelligent Transportation Systems*, 7(1):63–77, 2006.
- [6] H. Berndt and K. Dietmayer. Driver intention inference with vehicle onboard sensors. In *IEEE Int. Conf. on Vehicular Electronics and Safety ICVE*, pages 102–107. IEEE, 2009.
- [7] R. Chandler, R. Herman, and E. Montroll. Traffic dynamics: Studies in car following. *Operations Research*, 6(2):165–184, 1958.
- [8] S. Cheng and M. Trivedi. Turn-intent analysis using body pose for intelligent driver assistance. *IEEE Pervasive Computing*, 5(4):28–37, 2006.
- [9] S. Dermann and R. Isermann. Nonlinear distance and cruise control for passenger cars. In *Proceedings of the American Control Conference*, pages 3081–3085. IEEE, 1995.
- [10] S. Hamdar. *Driver behavior modeling*, pages 537–558. 2012.
- [11] Q. Ji, Z. Zhu, and P. Lan. Real-time nonintrusive monitoring and prediction of driver fatigue. *IEEE Trans. on Vehicular Technology*, 53(4):1052–1068, 2004.
- [12] S. Jin, S-Y Park, and J-J Lee. Driver fatigue detection using a genetic algorithm. *Artificial Life and Robotics*, 11(1):87–90, 2007.

- [13] D. Kasper, G. Weidl, T. Dang, G. Breuel, A. Tamke, A. Wedel, and W. Rosenstiel. Object-oriented bayesian networks for detection of lane change maneuvers. *IEEE Intelligent Transportation Systems Magazine*, 4(3):19–31, Fall 2012.
- [14] N. Kuge, T. Yamamura, O. Shimoyama, and A. Liu. A driver behavior recognition method based on a driver model framework. *SAE Transactions*, 109(6):469–476, 2000.
- [15] M. Land. Eye movements and the control of actions in everyday life. *Progress and Retinal and Eye Research*, 25(3):296–324, 2006.
- [16] Y-C. Lee, J. Lee, and L. Boyle. Visual attention in driving: the effects of cognitive load and visual disruption. *Human Factors: The Journal of the Human Factors and Ergonomics Society*, 49(4):721–733, 2007.
- [17] J. Lowenau, P. Venhovens, and J. Bernasch. Advanced vehicle navigation in the BMW real time light simulation. *Journal of Navigation*, 53(1):30–41, 2000.
- [18] M. Lu, K. Wevers, and R. van der Heijden. Technical feasibility of advanced driver assistance systems (ADAS) for road traffic safety. *Transportation Planning and Technology*, 28(3):167–187, 2005.
- [19] Hiren M. Mandalia and Dario D. Salvucci. Using support vector machines for lane-change detection. *Proceedings of the Human Factors and Ergonomics Society Annual Meeting*, 49(22):1965–1969, 2005.
- [20] J. McCall, D. Wipf, M. Trivedi, and B. Rao. Lane change intent analysis using robust operators and sparse bayesian learning. *IEEE Trans. on Intelligent Transportation Systems*, 8(3):431–440, 2007.
- [21] S. Metari, F. Prel, T. Moszkowicz, D. Laurendeau, N. Teasdale, S. Beauchemin, and Martin Simoneau. A computer vision framework for the analysis and interpretation of the cephalocular behavior of drivers. *Machine Vision and Applications*, 24(1):159–173, 2013.
- [22] Y. Noguchi, R. Nopsuwanchai, M. Ohsuga, and Y. Kamakura. Classification of blink waveforms towards the assessment of driver’s arousal level—an approach for HMM based classification from blinking video sequence. *Engineering Psychology and Cognitive Ergonomics*, pages 779–786, 2007.
- [23] M. Plochl and J. Edelmann. Driver models in automobile dynamics application. *Vehicle System Dynamics*, 45(7-8):688–741, 2007.
- [24] C. Rodemerck, H. Winner, and R. Kastner. Predicting the driver’s turn intentions at urban intersections using context-based indicators. In *2015 IEEE Intelligent Vehicles Symposium (IV)*, pages 964–969, June 2015.
- [25] D. Salvucci. Modeling driver behavior in a cognitive architecture. *Human Factors: The Journal of the Human Factors and Ergonomics Society*, 48(2):362–380, 2006.

- [26] Dario D. Salvucci, Hiren M. Mandalia, Nobuyuki Kuge, and Tomohiro Yamamura. Lane-change detection using a computational driver model. *Human Factors*, 49(3):532–542, 2007. PMID: 17552315.
- [27] D. Sandberg and M. Wahde. Particle swarm optimization of feed forward neural networks for the detection of drowsy driving. *Int. Journal Comp. Neural Networks*, 38:788–793, 2008.
- [28] D. Sanpeng, X. Xiaoli, Y. Xuecui, and M. Dehua. Research on the driver fatigue monitoring method based on the Dempster-Shafer theory. In *Proceedings of the Control and Decision Conference (CCDC)*, pages 4176–4179. IEEE, 2010.
- [29] J. Schmitt, A. Breu, M. Maurer, and B. Farber. Simulation des bremsverhaltens in gefahrensituationen mittels experimentell validiertem fahrermodell. *VDI BERICHTE*, 75, 2007.
- [30] J. Schmitt and B. Farber. Verbesserung von fas durch fahrerabsichtserkennung mit fuzzy logic. *VDI BERICHTE*, 2005.
- [31] L. Vlacic, M. Parent, and F. Harashima. *Intelligent Vehicle Technologies: Theory and Applications*. Butterworth-Heinemann, 2001.
- [32] K. Weiss, N. Kaempchen, and A. Kirchner. Multiple-model tracking for the detection of lane change maneuvers. In *IEEE Intelligent Vehicles Symposium, 2004*, pages 937–942, June 2004.
- [33] Seyed Mohsen Zabihi. *Developing Predictive Models of Driver Behaviour for the Design of Advanced Driving Assistance Systems*. PhD thesis, University of Western Ontario, 2017.
- [34] Mahboubeh Zardosht. Identifying individual driver behaviour using in-vehicle can-bus signals of pre-turning maneuvers. Master’s thesis, University of Western Ontario, 2016.

# Appendix A

## Preprocessed Files for Analysis

sub_no	avg_speed	std_speed	kurt_speed	skew_speed	avg_brake	std_brake	kurt_brake	skew_brake	avg_gas	std_gas	kurt_gas
1	0.3945	0.3896	0.0685	0.619	0.3859	0.2419	0.1078	0.5473	0.1846	0.242	0.0397
2	0.3931	0.3569	0.059	0.6142	0.3347	0.2308	0.1189	0.5435	0.267	0.1623	0.0304
3	0.3776	0.3117	0.0764	0.6112	0.3693	0.2368	0.0474	0.5253	0.1536	0.1687	0.0427
4	0.394	0.3462	0.0621	0.6029	0.3359	0.1615	0.0852	0.5047	0.2051	0.195	0.0456
5	0.3671	0.216	0.0663	0.6026	0.2372	0.2453	0.116	0.5451	0.1399	0.147	0.0951
6	0.4148	0.3602	0.1197	0.5821	0.3705	0.1259	0.1427	0.5608	0.2174	0.1296	0.0277
7	0.4075	0.3934	0.0612	0.6151	0.3375	0.1911	0.1537	0.4828	0.2372	0.2053	0.0327
8	0.3205	0.2754	0.0687	0.6089	0.2362	0.2089	0.0248	0.4982	0.262	0.1983	0.0522
9	0.3457	0.3101	0.0501	0.6478	0.31	0.1251	0.1597	0.5257	0.2279	0.1354	0.0528
10	0.3847	0.2593	0.0702	0.6264	0.2384	0.2859	0.056	0.5109	0.1938	0.2513	0.0531
11	0.348	0.3472	0.0505	0.6191	0.3016	0.1029	0.0815	0.5296	0.208	0.1389	0.0329
12	0.3781	0.3628	0.0885	0.5953	0.3797	0.2427	0.2011	0.4696	0.1732	0.2641	0.0213
13	0.3404	0.4679	0.048	0.6147	0.312	0.1377	0.0981	0.5445	0.3244	0.2992	0.0485
14	0.3837	0.2959	0.1029	0.6108	0.336	0.2659	0.0326	0.5004	0.1343	0.1538	0.0433
15	0.4211	0.3657	0.0576	0.6364	0.4176	0.2322	0.1081	0.5305	0.1507	0.1443	0.0697
16	0.3155	0.35	0.0705	0.5918	0.303	0.233	0.1353	0.5545	0.2605	0.2228	0.0331

skew_gas	avg_wheel	std_wheel	kurt_wheel	skew_wheel	avg_acceleration	std_acceleration	kurt_acceleration	skew_acceleration	age	gender
0.3518	0.457	0.1493	0.1184	0.4763	0.4833	0.1028	2.2911	1.6668	37	Male
0.3189	0.4427	0.1612	0.1873	0.5293	0.4976	0.1052	0.1858	0.4352	37	Male
0.3624	0.5032	0.1736	0.1575	0.5199	0.4885	0.1483	2.7952	1.3605	41	Female
0.3167	0.4211	0.1658	0.0903	0.5548	0.4776	0.0971	-0.6667	-0.1211	41	Male
0.3923	0.4616	0.1843	0.0914	0.5186	0.4393	0.0658	-0.7265	-0.6151	37	Female
0.3083	0.418	0.1867	0.1034	0.5198	0.474	0.0682	-1.1477	0.026	22	Female
0.3431	0.4667	0.1524	0.1409	0.5716	0.4827	0.1827	1.2561	-0.4396	31	Female
0.3594	0.4346	0.2227	0.0954	0.5477	0.4979	0.0898	4.178	1.7037	21	Male
0.3215	0.4528	0.176	0.1081	0.5427	0.4874	0.0605	0.6148	1.0823	21	Female
0.3441	0.4724	0.143	0.1188	0.5042	0.4651	0.0831	1.2828	-0.7696	20	Male
0.2986	0.4156	0.1639	0.1096	0.5255	0.5114	0.0822	2.6523	1.563	22	Female
0.3195	0.4745	0.158	0.1176	0.4593	0.4743	0.0533	-0.4856	0.3592	24	Female
0.3054	0.4324	0.2169	0.1615	0.5808	0.5164	0.1378	-0.7025	-0.4216	23	Male
0.354	0.4785	0.2016	0.1045	0.5198	0.4272	0.1109	2.0834	-1.3102	47	Female
0.3518	0.48	0.1251	0.0832	0.5354	0.4713	0.0844	-0.1495	0.282	44	Female
0.3509	0.4581	0.1089	0.1426	0.4741	0.5075	0.1801	2.621	0.7262	25	Male

Table A.1: Average driver descriptors 5 seconds pre-turns

sub_no	avg_speed	std_speed	kurt_speed	skew_speed	avg_brake	std_brake	kurt_brake	skew_brake	avg_gas	std_gas	kurt_gas
1	0.3912	0.3842	0.0998	0.5328	0.3758	0.224	0.1436	0.5486	0.2006	0.2365	0.048
2	0.3939	0.3653	0.1023	0.5211	0.3288	0.1892	0.1114	0.53	0.2891	0.1336	0.0309
3	0.3729	0.3303	0.1168	0.5126	0.3537	0.183	0.1041	0.4925	0.1681	0.1063	0.0322
4	0.3915	0.3642	0.1205	0.4956	0.3377	0.1412	0.1041	0.4525	0.2223	0.12	0.0552
5	0.3643	0.2183	0.1209	0.5308	0.2109	0.2258	0.0871	0.53	0.1395	0.1274	0.1073
6	0.4125	0.3763	0.1443	0.4963	0.3751	0.1104	0.1493	0.5587	0.2283	0.1165	0.0321
7	0.4073	0.388	0.1058	0.5203	0.3318	0.178	0.159	0.4925	0.2431	0.1765	0.0364
8	0.3238	0.2654	0.1203	0.542	0.2238	0.1896	0.0395	0.4996	0.2639	0.1613	0.0519
9	0.3455	0.3088	0.0954	0.5532	0.2975	0.113	0.1556	0.5052	0.2401	0.116	0.0595
10	0.3849	0.2828	0.1071	0.5155	0.2238	0.1848	0.0938	0.5261	0.1964	0.1963	0.114
11	0.3493	0.3717	0.0934	0.5169	0.3061	0.0524	0.0823	0.5206	0.2306	0.1001	0.0532
12	0.3742	0.3661	0.1253	0.513	0.3801	0.1681	0.1642	0.4522	0.1862	0.2322	0.0271
13	0.3421	0.4816	0.1008	0.5158	0.3095	0.0905	0.0813	0.5293	0.3569	0.1939	0.0728
14	0.3783	0.2844	0.1449	0.5007	0.3157	0.2193	0.0927	0.5223	0.1432	0.1441	0.0556
15	0.4154	0.3789	0.0993	0.5378	0.4091	0.2165	0.0304	0.5018	0.1677	0.1171	0.0697
16	0.317	0.3396	0.1641	0.5016	0.2927	0.2299	0.143	0.5595	0.2819	0.2081	0.0443
skew_gas	avg_wheel	std_wheel	kurt_wheel	skew_wheel	avg_acceleration	std_acceleration	kurt_acceleration	skew_acceleration	age	gender	
0.4409	0.4357	0.1322	0.1316	0.4662	0.4767	0.0981	1.8731	1.5113	37	Male	
0.427	0.4242	0.1456	0.156	0.56	0.4899	0.105	-0.0089	0.2859	37	Male	
0.4522	0.486	0.1544	0.1962	0.5156	0.4847	0.1615	3.784	1.6224	41	Female	
0.4284	0.4004	0.147	0.1057	0.5695	0.4689	0.1004	-0.6637	-0.2389	41	Male	
0.4951	0.442	0.1694	0.1114	0.525	0.4384	0.0582	-0.5798	-0.7085	37	Female	
0.4405	0.3967	0.1567	0.0983	0.5447	0.4651	0.0695	-1.0633	-0.074	22	Female	
0.414	0.4446	0.1405	0.1514	0.5913	0.4735	0.1835	1.2014	-0.3229	31	Female	
0.4348	0.4132	0.2016	0.1025	0.5402	0.4914	0.0859	4.7951	1.9337	21	Male	
0.4257	0.4335	0.1456	0.1262	0.5491	0.4813	0.0583	-0.0526	0.7681	21	Female	
0.4684	0.4567	0.1418	0.1327	0.4962	0.4562	0.0825	1.1066	-0.7559	20	Male	
0.3931	0.3961	0.1483	0.1285	0.5343	0.5016	0.0785	2.7912	1.5077	22	Female	
0.4203	0.4533	0.1543	0.1353	0.4876	0.4674	0.0501	-0.4599	-0.0742	24	Female	
0.4012	0.4107	0.1807	0.1815	0.5942	0.5126	0.1466	-0.6797	-0.2969	23	Male	
0.4457	0.4588	0.2008	0.1148	0.5306	0.423	0.1128	2.399	-1.5179	47	Female	
0.4528	0.4597	0.1079	0.1215	0.545	0.4684	0.0908	-0.1499	0.2975	44	Female	
0.4383	0.4402	0.1111	0.1609	0.4895	0.4995	0.1699	2.5447	0.6667	25	Male	

Table A.2: Average driver descriptors 4 seconds pre-turns

sub_no	avg_speed	std_speed	kurt_speed	skew_speed	avg_brake	std_brake	kurt_brake	skew_brake	avg_gas	std_gas	kurt_gas
1	0.387	0.3432	0.0464	0.6519	0.3587	0.1875	0.1503	0.5775	0.1879	0.2042	0.0504
2	0.3938	0.3399	0.0449	0.6441	0.318	0.1263	0.0477	0.5162	0.2769	0.1012	0.0352
3	0.3677	0.3248	0.0466	0.6429	0.348	0.1602	0.091	0.4729	0.1704	0.0915	0.0481
4	0.3878	0.3543	0.0413	0.6495	0.3403	0.1066	0.1199	0.4381	0.2174	0.0602	0.0385
5	0.3601	0.1888	0.0528	0.6806	0.184	0.2072	0.1915	0.5376	0.1289	0.0882	0.1245
6	0.4081	0.3677	0.0611	0.6376	0.378	0.0943	0.1543	0.5655	0.2218	0.0987	0.0726
7	0.4054	0.3597	0.0512	0.6527	0.3258	0.1131	0.2244	0.5127	0.243	0.1555	0.0527
8	0.3265	0.2269	0.1026	0.6288	0.211	0.1284	0.0925	0.5367	0.2446	0.116	0.0576
9	0.3444	0.2753	0.0467	0.6624	0.2821	0.1153	0.1198	0.5009	0.2287	0.0878	0.0785
10	0.3831	0.2756	0.0721	0.621	0.2246	0.1615	0.1184	0.534	0.1854	0.1335	0.0529
11	0.3495	0.3601	0.0463	0.6421	0.3082	0.038	0.086	0.5325	0.2289	0.0561	0.0391
12	0.3695	0.3499	0.0598	0.65	0.3805	0.0883	0.1162	0.4904	0.1821	0.1737	0.0313
13	0.3435	0.4574	0.0596	0.6421	0.3131	0.087	0.0225	0.4953	0.3409	0.1079	0.0464
14	0.3724	0.2596	0.0795	0.6436	0.3044	0.14	0.1056	0.4737	0.1392	0.1211	0.0414
15	0.4086	0.3574	0.0466	0.6598	0.3938	0.1821	0.0931	0.4746	0.1629	0.0965	0.0845
16	0.3176	0.3079	0.0724	0.6502	0.281	0.207	0.1441	0.5507	0.2836	0.1566	0.0869
skew_gas	avg_wheel	std_wheel	kurt_wheel	skew_wheel	avg_acceleration	std_acceleration	kurt_acceleration	skew_acceleration	age	gender	
0.352	0.4234	0.1334	0.1184	0.4342	0.4063	0.0767	1.3127	1.2311	37	Male	
0.3228	0.4163	0.1472	0.1445	0.5242	0.4163	0.0902	-0.2178	0.2672	37	Male	
0.3193	0.4781	0.1586	0.1501	0.4906	0.4205	0.1633	5.7975	2.2075	41	Female	
0.3297	0.3908	0.1418	0.1275	0.5325	0.4009	0.093	-0.6358	0.0036	41	Male	
0.38	0.4327	0.1778	0.1267	0.4827	0.3744	0.049	-0.4313	-0.8784	37	Female	
0.3446	0.386	0.1448	0.1115	0.5329	0.3925	0.0626	-1.0887	-0.0953	22	Female	
0.2956	0.4324	0.1427	0.1311	0.545	0.396	0.148	1.244	-0.5637	31	Female	
0.329	0.4015	0.2091	0.1348	0.4926	0.4195	0.0697	5.9252	2.2811	21	Male	
0.3266	0.4268	0.145	0.1612	0.51	0.4073	0.0491	-0.0456	0.7587	21	Female	
0.3013	0.4531	0.1547	0.1395	0.4291	0.3858	0.0692	0.7986	-0.8533	20	Male	
0.3358	0.3875	0.1505	0.1309	0.5173	0.4262	0.0652	2.2208	1.3344	22	Female	
0.3255	0.44	0.1746	0.1324	0.4927	0.3974	0.0447	0.0468	-0.4881	24	Female	
0.3152	0.4023	0.1668	0.1796	0.5485	0.4355	0.138	-0.3717	-0.0308	23	Male	
0.3283	0.4484	0.2327	0.1135	0.5024	0.358	0.0891	2.2785	-1.6264	47	Female	
0.3338	0.4479	0.0995	0.1759	0.5139	0.3963	0.0767	-0.3555	0.0429	44	Female	
0.3365	0.4313	0.133	0.1475	0.4529	0.4216	0.1456	2.981	0.5479	25	Male	

Table A.3: Average driver descriptors 3 seconds pre-turns

sub_no	avg_speed	std_speed	kurt_speed	skew_speed	avg_brake	std_brake	kurt_brake	skew_brake	avg_gas	std_gas	kurt_gas
1	0.3823	0.2966	0.0864	0.508	0.3319	0.1465	0.1635	0.5889	0.1833	0.1729	0.0622
2	0.3938	0.3125	0.0664	0.4863	0.3089	0.0864	0.0497	0.4847	0.2774	0.095	0.0299
3	0.3626	0.3208	0.0693	0.4885	0.3433	0.1425	0.0588	0.4987	0.1761	0.0708	0.0327
4	0.383	0.3488	0.0651	0.5037	0.3314	0.0818	0.1324	0.4463	0.2229	0.0512	0.0418
5	0.3558	0.1816	0.0732	0.5178	0.1455	0.1724	0.1539	0.513	0.1268	0.068	0.0775
6	0.4029	0.3712	0.0815	0.4923	0.3805	0.0872	0.1876	0.5529	0.2279	0.0796	0.03
7	0.4021	0.3431	0.0947	0.5119	0.3315	0.0816	0.1231	0.4445	0.2616	0.1252	0.056
8	0.3287	0.2081	0.117	0.5379	0.2024	0.0923	0.091	0.532	0.2476	0.0854	0.0544
9	0.3431	0.2378	0.1468	0.5045	0.2594	0.1222	0.1471	0.5091	0.2188	0.0561	0.1174
10	0.3815	0.2591	0.0841	0.4666	0.2258	0.1866	0.1467	0.5602	0.189	0.0835	0.0784
11	0.3488	0.3449	0.0939	0.466	0.3044	0.0314	0.0459	0.4964	0.2299	0.046	0.0495
12	0.3648	0.3428	0.0969	0.4796	0.3787	0.0907	0.0504	0.5064	0.1822	0.1223	0.0461
13	0.3448	0.4305	0.1379	0.4618	0.3182	0.061	0.0466	0.4776	0.3357	0.0512	0.0665
14	0.3657	0.2556	0.1063	0.4968	0.2965	0.1274	0.1465	0.4391	0.1487	0.0847	0.0663
15	0.401	0.3483	0.0637	0.4989	0.3728	0.1177	0.1144	0.4763	0.1707	0.0529	0.081
16	0.3182	0.2908	0.0969	0.5055	0.2603	0.1781	0.0987	0.5228	0.2955	0.1044	0.1287
skew_gas	avg_wheel	std_wheel	kurt_wheel	skew_wheel	avg_acceleration	std_acceleration	kurt_acceleration	skew_acceleration	age	gender	
0.4738	0.4226	0.1359	0.1097	0.3549	0.4121	0.0696	1.3862	1.1194	37	Male	
0.4311	0.4191	0.1894	0.0814	0.4283	0.4243	0.0859	-0.2475	-0.0023	37	Male	
0.4444	0.48	0.175	0.095	0.4188	0.4282	0.1572	6.3955	2.3494	41	Female	
0.4164	0.3944	0.1504	0.0933	0.4318	0.4078	0.1003	-0.3878	-0.0772	41	Male	
0.4598	0.4335	0.2116	0.0917	0.4121	0.3851	0.0454	-0.1199	-0.9931	37	Female	
0.4261	0.3886	0.1399	0.0722	0.4411	0.4007	0.0637	-0.9947	-0.0127	22	Female	
0.4154	0.4311	0.1692	0.0884	0.4488	0.3993	0.1475	1.1466	-0.714	31	Female	
0.4158	0.4013	0.2335	0.0909	0.4399	0.4244	0.0572	3.9526	1.7932	21	Male	
0.4689	0.4314	0.1624	0.1578	0.4348	0.4169	0.0449	-0.9397	0.412	21	Female	
0.4051	0.4621	0.1729	0.0892	0.3551	0.3967	0.0667	-0.1244	-0.6094	20	Male	
0.4692	0.3914	0.1615	0.0855	0.4345	0.4325	0.0626	1.6994	1.2122	22	Female	
0.455	0.4356	0.1976	0.1669	0.4022	0.4073	0.0476	-0.2801	-0.3094	24	Female	
0.4573	0.4095	0.2084	0.1154	0.4614	0.4442	0.1432	-0.643	0.0865	23	Male	
0.4135	0.4459	0.2943	0.1357	0.4503	0.3702	0.0833	1.3589	-1.3734	47	Female	
0.4164	0.4465	0.0998	0.0672	0.4341	0.4067	0.0855	-0.3777	0.0927	44	Female	
0.4522	0.4322	0.1765	0.0904	0.378	0.4267	0.1292	2.4765	0.0484	25	Male	

Table A.4: Average driver descriptors 2 seconds pre-turns

sub_no	avg_speed	std_speed	kurt_speed	skew_speed	avg_brake	std_brake	kurt_brake	skew_brake	avg_gas	std_gas	kurt_gas
1	0.3736	0.2623	0.2078	0.5422	0.3217	0.0596	0.2848	0.6191	0.1969	0.1983	0.1389
2	0.3887	0.3062	0.1094	0.4935	0.3102	0.0278	0.1003	0.4475	0.2977	0.127	0.0789
3	0.3535	0.3025	0.1048	0.5083	0.3436	0.0969	0.1184	0.4809	0.1683	0.0472	0.1093
4	0.3732	0.3357	0.1636	0.5367	0.3174	0.0538	0.1416	0.4516	0.2341	0.0812	0.1509
5	0.3486	0.177	0.1817	0.4954	0.1131	0.0447	0.1274	0.4713	0.1243	0.1296	0.1445
6	0.392	0.4038	0.1813	0.5383	0.3951	0.0287	0.1802	0.539	0.2257	0.0927	0.1251
7	0.3945	0.3471	0.2661	0.5195	0.3332	0.0214	0.1516	0.4506	0.2688	0.2367	0.1044
8	0.3274	0.2367	0.125	0.4878	0.2073	0.0664	0.1364	0.5303	0.2572	0.0687	0.118
9	0.3392	0.213	0.0763	0.4753	0.2422	0.0692	0.1429	0.485	0.2188	0.1105	0.0523
10	0.3762	0.2544	0.2012	0.4488	0.2247	0.1335	0.1455	0.4971	0.1843	0.0749	0.1024
11	0.3429	0.338	0.1487	0.4857	0.305	0.0189	0.0746	0.4983	0.2359	0.0636	0.0953
12	0.3554	0.3683	0.1299	0.4989	0.3835	0.0643	0.1012	0.5037	0.1951	0.1287	0.0675
13	0.3411	0.4057	0.2065	0.497	0.3259	0.0162	0.1089	0.4462	0.3464	0.0662	0.1102
14	0.3544	0.3095	0.1707	0.5336	0.3008	0.0535	0.178	0.4341	0.1625	0.1388	0.0494
15	0.3892	0.3492	0.1155	0.4904	0.3631	0.0348	0.2033	0.4316	0.1631	0.1096	0.1814
16	0.3147	0.2728	0.2323	0.5133	0.2406	0.0525	0.0684	0.5023	0.3144	0.1186	0.1377
skew_gas	avg_wheel	std_wheel	kurt_wheel	skew_wheel	avg_acceleration	std_acceleration	kurt_acceleration	skew_acceleration	age	gender	
0.4959	0.4148	0.1252	0.1484	0.3903	0.4415	0.0637	0.1353	0.6554	37	Male	
0.4749	0.4143	0.2595	0.1421	0.4106	0.4493	0.0872	-0.3188	-0.2709	37	Male	
0.4919	0.4742	0.1737	0.1995	0.4527	0.4582	0.1525	5.7164	2.2642	41	Female	
0.5246	0.392	0.1744	0.1555	0.4391	0.4353	0.111	0.832	0.327	41	Male	
0.4666	0.426	0.2534	0.1402	0.4556	0.4194	0.0507	0.0318	-0.7028	37	Female	
0.5262	0.387	0.1612	0.1502	0.3907	0.4258	0.0706	-1.2611	-0.1039	22	Female	
0.4787	0.4231	0.211	0.1417	0.4161	0.422	0.1462	1.7363	-1.0792	31	Female	
0.4537	0.3949	0.2562	0.2258	0.4683	0.4587	0.0732	7.4299	2.575	21	Male	
0.5219	0.4275	0.1751	0.1834	0.4427	0.4388	0.0318	-0.6476	0.5274	21	Female	
0.491	0.4626	0.1719	0.1728	0.3479	0.4246	0.0695	-0.3285	0.2021	20	Male	
0.5224	0.3893	0.1726	0.1687	0.4401	0.4609	0.0781	5.0602	2.2076	22	Female	
0.4987	0.4241	0.1911	0.2245	0.3775	0.4313	0.0557	-0.0487	-0.443	24	Female	
0.48	0.4113	0.2973	0.1728	0.423	0.4618	0.1468	-0.3632	-0.1552	23	Male	
0.4819	0.4335	0.3323	0.1423	0.4147	0.4005	0.0899	1.2824	-1.2457	47	Female	
0.4787	0.4385	0.0843	0.1577	0.3977	0.4359	0.0907	-0.4684	0.1664	44	Female	
0.4751	0.4264	0.2126	0.1442	0.4049	0.4567	0.1179	2.1197	0.2581	25	Male	

Table A.5: Average driver descriptors 1 second pre-turns



sub_no	avg_duration	std_duration	kurt_duration	skew_duration	avg_speed	std_speed	kurt_speed	skew_speed	avg_brake	std_brake	kurt_brake	skew_brake	avg_gas
1	0.0726	0.1074	11.0869	3.4749	0.6097	0.2387	0.0663	0.4419	0.2316	0.3953	0.0498	0.4677	0.4175
2	0.0864	0.1433	7.357	2.8464	0.5883	0.2002	0.0705	0.4597	0.2585	0.3825	0.082	0.5194	0.3451
3	0.0779	0.0853	5.9509	2.3346	0.4958	0.2589	0.1127	0.4954	0.2676	0.4105	0.0101	0.4969	0.2936
4	0.0554	0.0644	3.4282	1.9528	0.5763	0.1814	0.0637	0.4425	0.2058	0.3208	0.1143	0.5512	0.3
5	0.0889	0.1095	2.1219	1.7489	0.5028	0.179	0.0635	0.4809	0.19	0.2822	0.0832	0.5396	0.1814
6	0.061	0.0484	0.3183	1.2884	0.6304	0.25	0.0603	0.4613	0.2345	0.3951	0.0071	0.4988	0.3586
7	0.0689	0.1273	10.3995	3.3952	0.6391	0.1755	0.0655	0.4574	0.2192	0.3691	0.0261	0.497	0.313
8	0.0567	0.0386	-0.2312	0.7591	0.61	0.2373	0.0547	0.4433	0.1935	0.2831	0.0874	0.551	0.309
9	0.1089	0.1852	8.7273	3.1008	0.5636	0.1892	0.0689	0.4597	0.1961	0.2717	0.0287	0.4964	0.3163
10	0.0661	0.0751	5.6213	2.4525	0.5727	0.2127	0.0629	0.4581	0.1863	0.3551	0.086	0.5019	0.2847
11	0.1331	0.1468	1.5866	1.6107	0.4441	0.3141	0.0659	0.4583	0.2365	0.3143	0.1406	0.4725	0.3007
12	0.1409	0.1912	2.0729	1.9168	0.5154	0.2728	0.0832	0.4408	0.2812	0.4069	0.0921	0.5403	0.2956
13	0.0373	0.0353	-0.8904	0.9815	0.5775	0.1907	0.0657	0.4508	0.1702	0.3345	0.037	0.5265	0.4244
14	0.0546	0.049	-0.8717	0.8053	0.5627	0.1843	0.058	0.427	0.1923	0.3088	0.0876	0.5491	0.2648
15	0.077	0.0637	1.5696	1.2464	0.5075	0.2984	0.0637	0.4397	0.2564	0.4609	0.0231	0.5184	0.3016
16	0.1241	0.2219	10.5115	3.364	0.5034	0.2009	0.075	0.4481	0.2494	0.3496	0.0443	0.4703	0.2616
std_gas	kurt_gas	skew_gas	avg_wheel	std_wheel	kurt_wheel	skew_wheel	avg_acceleration	std_acceleration	kurt_acceleration	skew_acceleration	age	gender	
0.4197	0.028	0.3714	0.4211	0.6467	0.0579	0.3535	0.4946	0.1749	-0.6624	-0.0444	37	Male	
0.2182	0.0229	0.3462	0.4395	0.6052	0.1113	0.3326	0.4416	0.1808	-0.0617	-0.4627	37	Male	
0.2467	0.0846	0.363	0.472	0.6695	0.0749	0.3608	0.4553	0.2067	-0.8022	0.1929	41	Female	
0.2134	0.0148	0.3345	0.439	0.6053	0.0773	0.3804	0.4234	0.1694	-0.3491	-0.5227	41	Male	
0.1815	0.0195	0.345	0.4261	0.5932	0.0942	0.4062	0.3946	0.0967	0.6135	0.7831	37	Female	
0.2737	0.0201	0.3185	0.441	0.6828	0.0562	0.304	0.4582	0.1813	0.3856	-0.8007	22	Female	
0.197	0.0189	0.3176	0.4203	0.5913	0.0928	0.3779	0.4306	0.2047	-1.0665	-0.3178	31	Female	
0.2243	0.0311	0.3342	0.4287	0.6206	0.067	0.327	0.4503	0.1725	-1.349	-0.3043	21	Male	
0.2213	0.0184	0.3233	0.4432	0.622	0.1053	0.3591	0.464	0.124	-1.0173	0.0815	21	Female	
0.2154	0.0289	0.3406	0.4427	0.6558	0.074	0.354	0.4263	0.1808	-0.6071	0.3384	20	Male	
0.2101	0.0311	0.3503	0.4361	0.629	0.067	0.3205	0.4859	0.1782	-1.0332	0.3323	22	Female	
0.2697	0.0339	0.3655	0.4237	0.6522	0.1243	0.3931	0.4598	0.1629	-1.1899	0.5796	24	Female	
0.2561	0.0147	0.3302	0.4207	0.5576	0.111	0.2954	0.5281	0.2255	-0.6725	0.5396	23	Male	
0.189	0.0148	0.3197	0.4401	0.6227	0.0702	0.3751	0.4238	0.1295	-0.9216	0.0138	47	Female	
0.3522	0.014	0.3299	0.4375	0.5934	0.0535	0.3209	0.4355	0.1529	-0.2434	0.3137	44	Female	
0.2146	0.0405	0.3598	0.423	0.6329	0.06	0.3497	0.4471	0.132	-0.3008	0.5046	25	Male	

Table A.6: Average driver descriptors during turns

sub_no	avg_speed	std_speed	kurt_speed	skew_speed	avg_brake	std_brake	kurt_brake	skew_brake	avg_gas	std_gas	kurt_gas
1	0.5954	0.5907	0.1259	0.498	0.0131	0.0151	0.1445	0.5194	0.5037	0.2721	0.1549
2	0.5086	0.4559	0.1566	0.5194	0.0116	0.0014	0.1111	0.5556	0.3251	0.0979	0.1749
3	0.4785	0.4281	0.19	0.4957	0.0512	0.0341	0.0229	0.5013	0.2753	0.1565	0.2702
4	0.4958	0.4157	0.129	0.5272	0.0352	0.0337	0.1284	0.503	0.291	0.0838	0.2209
5	0.4466	0.276	0.2318	0.5474	0.0115	0.0024	0.0426	0.5059	0.2203	0.0741	0.1332
6	0.5806	0.4328	0.1864	0.4726	0.0117	0.003	0.1166	0.5076	0.3148	0.1016	0.1958
7	0.5254	0.396	0.1989	0.5236	0.0603	0.0054	0.0079	0.5049	0.2579	0.1672	0.1167
8	0.5027	0.3977	0.1588	0.5009	0.0808	0.0629	0.0283	0.5189	0.2489	0.0427	0.1397
9	0.516	0.351	0.112	0.5089	0.0195	0.0067	0.0937	0.524	0.2837	0.0421	0.1057
10	0.5029	0.3921	0.1821	0.5247	0.0111	0.0028	0.0141	0.4899	0.27	0.0876	0.1461
11	0.4844	0.4943	0.1657	0.4997	0.007	0.0021	0.1667	0.4722	0.2879	0.0727	0.1307
12	0.5479	0.4921	0.1575	0.475	0.0689	0.0297	0.0861	0.4878	0.2972	0.1116	0.2409
13	0.5434	0.5903	0.1961	0.4884	0.0117	0.0012	0.0288	0.5207	0.403	0.1328	0.3219
14	0.4891	0.3824	0.2449	0.5512	0.0448	0.0408	0.1118	0.4971	0.259	0.0522	0.158
15	0.5213	0.5304	0.1289	0.5068	0.0403	0.0743	0.2046	0.5208	0.3335	0.0738	0.1379
16	0.4454	0.3941	0.2171	0.5413	0.0372	0.0203	0.1338	0.451	0.2573	0.1258	0.1822
skew_gas	avg_wheel	std_wheel	kurt_wheel	skew_wheel	avg_acceleration	std_acceleration	kurt_acceleration	skew_acceleration	age	gender	
0.458	0.4743	0.2037	0.1562	0.5305	0.4104	0.1245	1.12	1.1383	37	Male	
0.4515	0.5176	0.2291	0.1727	0.5314	0.3877	0.0963	0.0038	0.7101	37	Male	
0.476	0.4674	0.198	0.1442	0.5148	0.3642	0.1612	9.1982	3.0048	41	Female	
0.413	0.5566	0.2488	0.1376	0.486	0.3637	0.1781	6.298	2.3552	41	Male	
0.4788	0.5109	0.151	0.1294	0.4974	0.2995	0.0588	6.2489	2.5135	37	Female	
0.444	0.5368	0.1968	0.1856	0.513	0.3599	0.0806	-1.1838	0.3927	22	Female	
0.4785	0.4907	0.2508	0.1502	0.5097	0.3364	0.1189	1.5346	-0.9292	31	Female	
0.5184	0.531	0.1679	0.1537	0.5259	0.3278	0.0804	-0.1324	0.2237	21	Male	
0.4464	0.5039	0.1849	0.1556	0.4701	0.3283	0.0643	0.7929	1.0076	21	Female	
0.587	0.4778	0.3935	0.1622	0.5037	0.3577	0.103	0.5546	1.1431	20	Male	
0.4446	0.5206	0.2002	0.1887	0.481	0.3651	0.1273	3.6239	2.0639	22	Female	
0.5447	0.506	0.2347	0.1491	0.5396	0.3281	0.0542	-1.4292	-0.1701	24	Female	
0.4002	0.4486	0.2581	0.2197	0.5704	0.4663	0.1532	-0.3521	1.0621	23	Male	
0.4755	0.5185	0.2545	0.1527	0.5222	0.3355	0.1038	3.6764	-1.6075	47	Female	
0.5214	0.4637	0.3029	0.1423	0.4801	0.3638	0.0787	-1.0588	0.2899	44	Female	
0.4884	0.5237	0.1852	0.1808	0.5196	0.3613	0.2025	3.7996	1.8237	25	Male	

Table A.7: Average driver descriptors 1 second post-turns

sub_no	avg_speed	std_speed	kurt_speed	skew_speed	avg_brake	std_brake	kurt_brake	skew_brake	avg_gas	std_gas	kurt_gas
1	0.6286	0.5951	0.0732	0.6478	0.0295	0.0563	0.114	0.5018	0.5204	0.2676	0.1423
2	0.5339	0.4243	0.0807	0.6435	0.0117	0.0013	0.1272	0.5698	0.3349	0.0693	0.1011
3	0.502	0.3982	0.0926	0.6623	0.0616	0.0524	0.0052	0.4995	0.2866	0.125	0.1553
4	0.5193	0.4041	0.0579	0.6657	0.0438	0.0345	0.1308	0.4896	0.3043	0.0732	0.1524
5	0.4652	0.2701	0.1166	0.6252	0.0116	0.0018	0.0932	0.5343	0.2277	0.0832	0.0723
6	0.6044	0.4209	0.085	0.6835	0.0117	0.0018	0.0932	0.4977	0.316	0.0844	0.1563
7	0.5434	0.3587	0.067	0.6678	0.0616	0.0045	0.0036	0.4969	0.2608	0.1492	0.0976
8	0.5194	0.3554	0.1001	0.6581	0.103	0.0864	0.0205	0.5147	0.2571	0.0629	0.1168
9	0.538	0.3527	0.0736	0.679	0.0195	0.0054	0.135	0.5097	0.2872	0.0314	0.0913
10	0.5241	0.3587	0.0792	0.6891	0.0115	0.0043	0.0829	0.5383	0.2801	0.0774	0.1094
11	0.5113	0.4466	0.0753	0.6708	0.0079	0.006	0.2977	0.4623	0.2875	0.0766	0.1233
12	0.5719	0.4383	0.0909	0.6303	0.0885	0.0776	0.1159	0.506	0.2982	0.1062	0.1513
13	0.5778	0.5904	0.0691	0.673	0.0116	0.0006	0.0311	0.5223	0.4169	0.1051	0.0722
14	0.5107	0.3603	0.0662	0.6701	0.0288	0.0553	0.1014	0.5026	0.2667	0.0684	0.1542
15	0.5507	0.4893	0.0561	0.6556	0.0479	0.064	0.1626	0.5263	0.3376	0.0533	0.0775
16	0.4685	0.3754	0.078	0.6756	0.0436	0.0272	0.0164	0.4873	0.2672	0.0869	0.0864
skew_gas	avg_wheel	std_wheel	kurt_wheel	skew_wheel	avg_acceleration	std.acceleration	kurt_acceleration	skew_acceleration	age	gender	
0.4464	0.4649	0.1785	0.0858	0.6702	0.3448	0.171	2.2176	1.4818	37	Male	
0.4569	0.5097	0.1999	0.087	0.6036	0.294	0.1149	0.0207	0.7768	37	Male	
0.509	0.4514	0.1614	0.0825	0.6722	0.2573	0.1517	9.3527	2.9536	41	Female	
0.3936	0.5426	0.2635	0.086	0.6061	0.2891	0.1978	6.4572	2.5086	41	Male	
0.5412	0.4982	0.167	0.1008	0.6112	0.2028	0.0823	7.6521	2.8388	37	Female	
0.4225	0.5181	0.1923	0.1094	0.6188	0.27	0.0789	-1.2218	0.4071	22	Female	
0.4747	0.4812	0.2114	0.0768	0.6414	0.2563	0.1041	-1.1604	0.1134	31	Female	
0.4681	0.5239	0.1572	0.1019	0.6216	0.2308	0.1148	2.8214	1.2754	21	Male	
0.4706	0.4927	0.1937	0.0849	0.6484	0.2417	0.0962	4.9565	2.2015	21	Female	
0.5382	0.4737	0.3177	0.0776	0.6342	0.2609	0.1111	1.2164	1.3378	20	Male	
0.501	0.5127	0.1887	0.1205	0.6052	0.2717	0.1748	5.6881	2.5105	22	Female	
0.4947	0.5007	0.212	0.0931	0.6643	0.2295	0.0618	-1.1502	-0.1725	24	Female	
0.4916	0.4366	0.2451	0.0788	0.6638	0.4053	0.1583	-0.398	0.924	23	Male	
0.4521	0.5036	0.2766	0.0776	0.6247	0.245	0.092	0.7117	-0.9618	47	Female	
0.4951	0.4624	0.2774	0.0757	0.6517	0.2694	0.1014	-0.1126	0.7876	44	Female	
0.4499	0.5159	0.2245	0.098	0.6555	0.2621	0.1833	3.9029	1.9432	25	Male	

Table A.8: Average driver descriptors 2 seconds post-turns

sub_no	avg_speed	std_speed	kurt_speed	skew_speed	avg_brake	std_brake	kurt_brake	skew_brake	avg_gas	std_gas	kurt_gas
1	0.6577	0.6237	0.0454	0.5876	0.0435	0.0562	0.1685	0.5271	0.5538	0.3197	0.0547
2	0.557	0.4334	0.0577	0.5763	0.0117	0.001	0.1835	0.5427	0.3622	0.0902	0.0877
3	0.5235	0.4233	0.0527	0.6059	0.0712	0.0441	0.0045	0.4986	0.3153	0.1547	0.1058
4	0.5405	0.42	0.0458	0.6045	0.0486	0.0262	0.1193	0.4933	0.3278	0.1098	0.1347
5	0.4815	0.2749	0.1182	0.5755	0.0117	0.0015	0.1468	0.566	0.2529	0.1118	0.0723
6	0.6254	0.4241	0.0434	0.5902	0.0129	0.0103	0.2395	0.515	0.3304	0.1148	0.0625
7	0.5593	0.3605	0.0491	0.583	0.0623	0.0054	0.0069	0.5054	0.2813	0.15	0.0876
8	0.5351	0.385	0.0472	0.5977	0.1202	0.0794	0.0646	0.4682	0.2828	0.0813	0.0421
9	0.5572	0.3591	0.0455	0.6015	0.0197	0.004	0.1022	0.4976	0.3091	0.0388	0.0955
10	0.5442	0.3741	0.0478	0.6126	0.017	0.0215	0.0508	0.5171	0.3068	0.0809	0.0828
11	0.5344	0.4453	0.0462	0.5897	0.008	0.0048	0.3502	0.4608	0.3036	0.1003	0.0549
12	0.5922	0.4402	0.0439	0.5782	0.1065	0.0808	0.1571	0.5214	0.3162	0.1154	0.1089
13	0.6099	0.6237	0.0429	0.6001	0.0118	0.001	0.1536	0.5845	0.4569	0.1279	0.0597
14	0.5311	0.3774	0.0718	0.6202	0.0234	0.0389	0.1778	0.5223	0.2863	0.0845	0.0639
15	0.5769	0.5025	0.0414	0.5992	0.0492	0.0492	0.1568	0.5326	0.3703	0.0766	0.0931
16	0.4897	0.397	0.0444	0.5971	0.0486	0.0245	0.0767	0.4715	0.294	0.0749	0.0811
skew_gas	avg_wheel	std_wheel	kurt_wheel	skew_wheel	avg_acceleration	std_acceleration	kurt_acceleration	skew_acceleration	age	gender	
0.4782	0.4735	0.2035	0.1192	0.5866	0.4159	0.188	1.8851	1.3312	37	Male	
0.4948	0.5153	0.2478	0.1215	0.5291	0.3442	0.1043	-0.9225	0.3567	37	Male	
0.4887	0.4548	0.1634	0.1408	0.5959	0.3097	0.1489	7.6437	2.5544	41	Female	
0.3975	0.5511	0.2654	0.1155	0.5281	0.3458	0.1792	5.6334	2.2489	41	Male	
0.539	0.5029	0.1989	0.1175	0.5543	0.269	0.0939	5.144	2.3704	37	Female	
0.5059	0.5212	0.2259	0.1791	0.5399	0.3212	0.0807	-1.125	0.4062	22	Female	
0.5084	0.4892	0.2164	0.1261	0.553	0.3293	0.1169	-0.7273	0.2603	31	Female	
0.4847	0.5377	0.17	0.152	0.5309	0.3038	0.1494	4.1139	1.7939	21	Male	
0.5192	0.501	0.2176	0.1075	0.5727	0.2978	0.0926	2.6874	1.7765	21	Female	
0.5079	0.4834	0.3201	0.1276	0.5446	0.3192	0.1018	0.4353	1.1076	20	Male	
0.4811	0.5228	0.1965	0.1218	0.5392	0.3242	0.1893	6.3888	2.6568	22	Female	
0.5231	0.5133	0.227	0.1669	0.5661	0.2775	0.0699	-1.3556	0.0817	24	Female	
0.4572	0.4443	0.2739	0.1278	0.57	0.4703	0.1623	-0.8368	0.7292	23	Male	
0.4946	0.5071	0.305	0.0989	0.5305	0.2972	0.105	1.4725	-1.2079	47	Female	
0.4963	0.4768	0.2714	0.115	0.5606	0.3273	0.0939	-0.1656	0.7205	44	Female	
0.4472	0.5309	0.2756	0.0968	0.5588	0.3324	0.1935	4.3678	2.2221	25	Male	

Table A.9: Average driver descriptors 3 seconds post-turns

sub_no	avg_speed	std_speed	kurt_speed	skew_speed	avg_brake	std_brake	kurt_brake	skew_brake	avg_gas	std_gas	kurt_gas
1	0.683	0.6058	0.0557	0.4001	0.0534	0.0563	0.2238	0.5535	0.5421	0.3001	0.0438
2	0.577	0.3992	0.0603	0.4185	0.0122	0.0009	0.184	0.543	0.3654	0.0995	0.0516
3	0.5425	0.4075	0.0564	0.4235	0.0775	0.0431	0.0541	0.5243	0.3231	0.1512	0.0394
4	0.5594	0.3991	0.0555	0.4306	0.053	0.0247	0.2289	0.5483	0.3311	0.1124	0.1068
5	0.4962	0.2517	0.081	0.4398	0.0121	0.0017	0.1713	0.5453	0.2617	0.1134	0.0507
6	0.644	0.3897	0.0524	0.4043	0.0189	0.023	0.278	0.5302	0.3264	0.1096	0.1062
7	0.5737	0.3319	0.057	0.4127	0.0636	0.0084	0.1219	0.4396	0.2883	0.1359	0.0664
8	0.5491	0.3701	0.0548	0.4292	0.1335	0.086	0.0908	0.4969	0.2879	0.1032	0.0387
9	0.5742	0.327	0.0496	0.4206	0.0205	0.0038	0.0888	0.4958	0.3133	0.0422	0.0643
10	0.5625	0.3554	0.06	0.4311	0.0266	0.0405	0.0453	0.515	0.3157	0.0784	0.07
11	0.5543	0.408	0.0555	0.4024	0.0081	0.0056	0.4443	0.5153	0.3001	0.0975	0.0678
12	0.6099	0.4085	0.0557	0.3978	0.1209	0.084	0.1493	0.5233	0.3209	0.1044	0.0903
13	0.6401	0.6185	0.0486	0.4235	0.0124	0.0033	0.2099	0.6135	0.4656	0.1269	0.0422
14	0.5485	0.3475	0.1111	0.4466	0.0217	0.0392	0.2579	0.5916	0.2897	0.0784	0.0365
15	0.6011	0.4904	0.0898	0.4119	0.0528	0.0477	0.1452	0.5401	0.377	0.0949	0.0411
16	0.5091	0.3816	0.0496	0.4232	0.0544	0.0327	0.081	0.4742	0.3031	0.0688	0.0867
skew_gas	avg_wheel	std_wheel	kurt_wheel	skew_wheel	avg_acceleration	std_acceleration	kurt_acceleration	skew_acceleration	age	gender	
0.4863	0.4802	0.2183	0.1237	0.4453	0.3968	0.1925	0.2652	0.8077	37	Male	
0.4503	0.5174	0.2958	0.1331	0.3918	0.3247	0.1066	-0.8958	0.4314	37	Male	
0.501	0.4569	0.1727	0.1476	0.4659	0.2809	0.1524	4.6718	1.8254	41	Female	
0.4226	0.5551	0.2887	0.1399	0.3689	0.3344	0.1863	4.9991	2.1208	41	Male	
0.5139	0.5062	0.2347	0.1245	0.4257	0.2578	0.0981	3.613	2.038	37	Female	
0.4764	0.5238	0.2502	0.1325	0.4388	0.2934	0.0794	-1.3342	0.224	22	Female	
0.5184	0.4937	0.2597	0.1293	0.4394	0.3268	0.1383	-1.2803	0.09	31	Female	
0.4715	0.5475	0.1839	0.1864	0.3452	0.2835	0.1645	4.3075	1.8261	21	Male	
0.5006	0.5074	0.2162	0.1151	0.4296	0.2816	0.1126	3.7072	1.9887	21	Female	
0.5292	0.4901	0.3162	0.1332	0.3998	0.3035	0.1102	-0.0643	0.9321	20	Male	
0.5247	0.5287	0.209	0.142	0.3997	0.3001	0.2	5.8079	2.5502	22	Female	
0.5325	0.523	0.237	0.1676	0.4456	0.2513	0.0922	-0.7319	0.1823	24	Female	
0.459	0.4509	0.2989	0.1433	0.4336	0.4633	0.165	-1.1789	0.4908	23	Male	
0.5023	0.5092	0.3248	0.1124	0.3688	0.2781	0.1072	0.4121	-0.8853	47	Female	
0.469	0.4872	0.2782	0.1361	0.4216	0.3093	0.1011	0.3289	0.9313	44	Female	
0.4351	0.5412	0.2967	0.1038	0.3991	0.3203	0.2192	2.8481	1.9434	25	Male	

Table A.10: Average driver descriptors 4 seconds post-turns

sub_no	avg_speed	std_speed	kurt_speed	skew_speed	avg_brake	std_brake	kurt_brake	skew_brake	avg_gas	std_gas	kurt_gas
1	0.7046	0.6004	0.0429	0.2016	0.0596	0.0563	0.1968	0.5804	0.5098	0.3388	0.093
2	0.5947	0.4023	0.0425	0.2236	0.0123	0.0008	0.1795	0.5408	0.3613	0.1141	0.1023
3	0.5588	0.4154	0.0439	0.2312	0.0803	0.0435	0.2283	0.5165	0.323	0.1669	0.0652
4	0.5753	0.4006	0.0399	0.2287	0.0536	0.0234	0.2548	0.5856	0.3265	0.1262	0.0862
5	0.5091	0.2712	0.043	0.2519	0.0124	0.0031	0.1516	0.5591	0.2615	0.1221	0.0887
6	0.6595	0.3844	0.0408	0.2058	0.0249	0.033	0.2433	0.5171	0.3183	0.1217	0.1322
7	0.5865	0.3428	0.0468	0.2186	0.0633	0.0108	0.1789	0.4688	0.2874	0.163	0.1435
8	0.5613	0.3863	0.042	0.243	0.1367	0.1072	0.1494	0.5206	0.2851	0.137	0.0737
9	0.5886	0.3283	0.0373	0.2238	0.0209	0.0057	0.0686	0.5159	0.3084	0.0594	0.1502
10	0.578	0.3708	0.045	0.2253	0.0357	0.0538	0.1058	0.4749	0.3159	0.0832	0.1102
11	0.5716	0.4062	0.0416	0.2096	0.0221	0.0707	0.2958	0.5165	0.2935	0.1056	0.0943
12	0.6253	0.4123	0.0452	0.2125	0.1221	0.0903	0.235	0.5391	0.3187	0.1113	0.1348
13	0.6673	0.6238	0.0381	0.2272	0.0218	0.0415	0.1523	0.5888	0.4573	0.156	0.082
14	0.5637	0.3477	0.1019	0.2614	0.0294	0.0737	0.2061	0.5855	0.2877	0.085	0.0854
15	0.6215	0.4891	0.0479	0.2196	0.0555	0.0489	0.1904	0.5744	0.3672	0.1375	0.07
16	0.5256	0.3918	0.04	0.2356	0.0633	0.053	0.0701	0.4692	0.301	0.0844	0.1013
skew_gas	avg_wheel	std_wheel	kurt_wheel	skew_wheel	avg_acceleration	std_acceleration	kurt_acceleration	skew_acceleration	age	gender	
0.4487	0.4975	0.1899	0.121	0.4732	0.3606	0.2006	-0.199	0.6418	37	Male	
0.4252	0.5315	0.2817	0.1253	0.4429	0.2944	0.1156	-0.9763	0.4171	37	Male	
0.4704	0.471	0.1731	0.1437	0.5022	0.2491	0.1544	3.4131	1.5203	41	Female	
0.4091	0.5701	0.2566	0.1301	0.4314	0.3057	0.2003	4.2334	1.9283	41	Male	
0.4854	0.5221	0.2185	0.117	0.4615	0.2354	0.1226	1.5752	1.5322	37	Female	
0.4325	0.539	0.2139	0.125	0.4867	0.2539	0.0869	-1.2697	0.1732	22	Female	
0.4992	0.5083	0.2534	0.1243	0.491	0.3014	0.1555	-1.3552	0.0881	31	Female	
0.4303	0.5668	0.1735	0.1726	0.3835	0.2557	0.1943	5.23	2.0654	21	Male	
0.4431	0.5239	0.1782	0.1213	0.4696	0.2412	0.1143	3.813	1.9758	21	Female	
0.489	0.5089	0.2645	0.1221	0.436	0.2707	0.1123	-0.4274	0.5973	20	Male	
0.4804	0.5455	0.1838	0.1314	0.4504	0.2645	0.2103	5.7277	2.5126	22	Female	
0.4825	0.5433	0.1983	0.161	0.4791	0.2198	0.1069	-0.3886	0.4996	24	Female	
0.4122	0.468	0.2624	0.1412	0.4366	0.4412	0.1777	-1.1882	0.4013	23	Male	
0.4658	0.5233	0.2713	0.1092	0.4146	0.2507	0.1057	-1.0879	-0.2124	47	Female	
0.4222	0.5067	0.2321	0.1502	0.4478	0.2775	0.1031	-0.2517	0.6654	44	Female	
0.4203	0.5626	0.2583	0.0997	0.4216	0.2927	0.2339	2.1821	1.8153	25	Male	

Table A.11: Average driver descriptors 5 seconds post-turns

# Appendix B

## Cluster Assignments of Drivers

instance_no	sub_no	avg_speed	std_speed	kurt_speed	skew_speed	avg_brake	std_brake	kurt_brake	skew_brake	avg_gas	std_gas	kurt_gas
0	1	0.3945	0.3896	0.0685	0.619	0.3859	0.2419	0.1078	0.5473	0.1846	0.242	0.0397
2	3	0.3776	0.3117	0.0764	0.6112	0.3693	0.2368	0.0474	0.5253	0.1536	0.1687	0.0427
4	5	0.3671	0.216	0.0663	0.6026	0.2372	0.2453	0.116	0.5451	0.1399	0.147	0.0951
6	7	0.4075	0.3934	0.0612	0.6151	0.3375	0.1911	0.1537	0.4828	0.2372	0.2053	0.0327
9	10	0.3847	0.2593	0.0702	0.6264	0.2384	0.2859	0.056	0.5109	0.1938	0.2513	0.0531
11	12	0.3781	0.3628	0.0885	0.5953	0.3797	0.2427	0.2011	0.4696	0.1732	0.2641	0.0213
13	14	0.3837	0.2959	0.1029	0.6108	0.336	0.2659	0.0326	0.5004	0.1343	0.1538	0.0433
14	15	0.4211	0.3657	0.0576	0.6364	0.4176	0.2322	0.1081	0.5305	0.1507	0.1443	0.0697
7	8	0.3205	0.2754	0.0687	0.6089	0.2362	0.2089	0.0248	0.4982	0.262	0.1983	0.0522
8	9	0.3457	0.3101	0.0501	0.6478	0.31	0.1251	0.1597	0.5257	0.2279	0.1354	0.0528
10	11	0.348	0.3472	0.0505	0.6191	0.3016	0.1029	0.0815	0.5296	0.208	0.1389	0.0329
12	13	0.3404	0.4679	0.048	0.6147	0.312	0.1377	0.0981	0.5445	0.3244	0.2992	0.0485
15	16	0.3155	0.35	0.0705	0.5918	0.303	0.233	0.1353	0.5545	0.2605	0.2228	0.0331
1	2	0.3931	0.3569	0.059	0.6142	0.3347	0.2308	0.1189	0.5435	0.267	0.1623	0.0304
3	4	0.394	0.3462	0.0621	0.6029	0.3359	0.1615	0.0852	0.5047	0.2051	0.195	0.0456
5	6	0.4148	0.3602	0.1197	0.5821	0.3705	0.1259	0.1427	0.5608	0.2174	0.1296	0.0277
skew_gas	avg_wheel	std_wheel	kurt_wheel	skew_wheel	avg_acceleration	std_acceleration	kurt.acceleration	skew_acceleration	age	gender	cluster	
0.3518	0.457	0.1493	0.1184	0.4763	0.4833	0.1028	2.2911	1.6668	37	Male	cluster0	
0.3624	0.5032	0.1736	0.1575	0.5199	0.4885	0.1483	2.7952	1.3605	41	Female	cluster0	
0.3923	0.4616	0.1843	0.0914	0.5186	0.4393	0.0658	-0.7265	-0.6151	37	Female	cluster0	
0.3431	0.4667	0.1524	0.1409	0.5716	0.4827	0.1827	1.2561	-0.4396	31	Female	cluster0	
0.3441	0.4724	0.143	0.1188	0.5042	0.4651	0.0831	1.2828	-0.7696	20	Male	cluster0	
0.3195	0.4745	0.158	0.1176	0.4593	0.4743	0.0533	-0.4856	0.3592	24	Female	cluster0	
0.354	0.4785	0.2016	0.1045	0.5198	0.4272	0.1109	2.0834	-1.3102	47	Female	cluster0	
0.3518	0.48	0.1251	0.0832	0.5354	0.4713	0.0844	-0.1495	0.282	44	Female	cluster0	
0.3594	0.4346	0.2227	0.0954	0.5477	0.4979	0.0898	4.178	1.7037	21	Male	cluster1	
0.3215	0.4528	0.176	0.1081	0.5427	0.4874	0.0605	0.6148	1.0823	21	Female	cluster1	
0.2986	0.4156	0.1639	0.1096	0.5255	0.5114	0.0822	2.6523	1.563	22	Female	cluster1	
0.3054	0.4324	0.2169	0.1615	0.5808	0.5164	0.1378	-0.7025	-0.4216	23	Male	cluster1	
0.3509	0.4581	0.1089	0.1426	0.4741	0.5075	0.1801	2.621	0.7262	25	Male	cluster1	
0.3189	0.4427	0.1612	0.1873	0.5293	0.4976	0.1052	0.1858	0.4352	37	Male	cluster2	
0.3167	0.4211	0.1658	0.0903	0.5548	0.4776	0.0971	-0.6667	-0.1211	41	Male	cluster2	
0.3083	0.418	0.1867	0.1034	0.5198	0.474	0.0682	-1.1477	0.026	22	Female	cluster2	

Table B.1: Cluster assignments of drivers pre-turns of 5 seconds with 3 clusters

instance_no	sub_no	avg_speed	std_speed	kurt_speed	skew_speed	avg_brake	std_brake	kurt_brake	skew_brake	avg_gas	std_gas	kurt_gas
0	1	0.3945	0.3896	0.0685	0.619	0.3859	0.2419	0.1078	0.5473	0.1846	0.242	0.0397
3	4	0.394	0.3462	0.0621	0.6029	0.3359	0.1615	0.0852	0.5047	0.2051	0.195	0.0456
4	5	0.3671	0.216	0.0663	0.6026	0.2372	0.2453	0.116	0.5451	0.1399	0.147	0.0951
5	6	0.4148	0.3602	0.1197	0.5821	0.3705	0.1259	0.1427	0.5608	0.2174	0.1296	0.0277
6	7	0.4075	0.3934	0.0612	0.6151	0.3375	0.1911	0.1537	0.4828	0.2372	0.2053	0.0327
9	10	0.3847	0.2593	0.0702	0.6264	0.2384	0.2859	0.056	0.5109	0.1938	0.2513	0.0531
11	12	0.3781	0.3628	0.0885	0.5953	0.3797	0.2427	0.2011	0.4696	0.1732	0.2641	0.0213
13	14	0.3837	0.2959	0.1029	0.6108	0.336	0.2659	0.0326	0.5004	0.1343	0.1538	0.0433
14	15	0.4211	0.3657	0.0576	0.6364	0.4176	0.2322	0.1081	0.5305	0.1507	0.1443	0.0697
1	2	0.3931	0.3569	0.059	0.6142	0.3347	0.2308	0.1189	0.5435	0.267	0.1623	0.0304
2	3	0.3776	0.3117	0.0764	0.6112	0.3693	0.2368	0.0474	0.5253	0.1536	0.1687	0.0427
7	8	0.3205	0.2754	0.0687	0.6089	0.2362	0.2089	0.0248	0.4982	0.262	0.1983	0.0522
8	9	0.3457	0.3101	0.0501	0.6478	0.31	0.1251	0.1597	0.5257	0.2279	0.1354	0.0528
10	11	0.348	0.3472	0.0505	0.6191	0.3016	0.1029	0.0815	0.5296	0.208	0.1389	0.0329
12	13	0.3404	0.4679	0.048	0.6147	0.312	0.1377	0.0981	0.5445	0.3244	0.2992	0.0485
15	16	0.3155	0.35	0.0705	0.5918	0.303	0.233	0.1353	0.5545	0.2605	0.2228	0.0331
skew_gas	avg_wheel	std_wheel	kurt_wheel	skew_wheel	avg_acceleration	std_acceleration	kurt_acceleration	skew_acceleration	age	gender	cluster	
0.3518	0.457	0.1493	0.1184	0.4763	0.4833	0.1028	2.2911	1.6668	37	Male	cluster0	
0.3167	0.4211	0.1658	0.0903	0.5548	0.4776	0.0971	-0.6667	-0.1211	41	Male	cluster0	
0.3923	0.4616	0.1843	0.0914	0.5186	0.4393	0.0658	-0.7265	-0.6151	37	Female	cluster0	
0.3083	0.418	0.1867	0.1034	0.5198	0.474	0.0682	-1.1477	0.026	22	Female	cluster0	
0.3431	0.4667	0.1524	0.1409	0.5716	0.4827	0.1827	1.2561	-0.4396	31	Female	cluster0	
0.3441	0.4724	0.143	0.1188	0.5042	0.4651	0.0831	1.2828	-0.7696	20	Male	cluster0	
0.3195	0.4745	0.158	0.1176	0.4593	0.4743	0.0533	-0.4856	0.3592	24	Female	cluster0	
0.354	0.4785	0.2016	0.1045	0.5198	0.4272	0.1109	2.0834	-1.3102	47	Female	cluster0	
0.3518	0.48	0.1251	0.0832	0.5354	0.4713	0.0844	-0.1495	0.282	44	Female	cluster0	
0.3189	0.4427	0.1612	0.1873	0.5293	0.4976	0.1052	0.1858	0.4352	37	Male	cluster1	
0.3624	0.5032	0.1736	0.1575	0.5199	0.4885	0.1483	2.7952	1.3605	41	Female	cluster1	
0.3594	0.4346	0.2227	0.0954	0.5477	0.4979	0.0898	4.178	1.7037	21	Male	cluster1	
0.3215	0.4528	0.176	0.1081	0.5427	0.4874	0.0605	0.6148	1.0823	21	Female	cluster1	
0.2986	0.4156	0.1639	0.1096	0.5255	0.5114	0.0822	2.6523	1.563	22	Female	cluster1	
0.3054	0.4324	0.2169	0.1615	0.5808	0.5164	0.1378	-0.7025	-0.4216	23	Male	cluster1	
0.3509	0.4581	0.1089	0.1426	0.4741	0.5075	0.1801	2.621	0.7262	25	Male	cluster1	

Table B.2: Cluster assignments of drivers pre-turns of 5 seconds with 2 clusters



instance_no	sub_no	avg_speed	std_speed	kurt_speed	skew_speed	avg_brake	std_brake	kurt_brake	skew_brake	avg_gas	std_gas	kurt_gas
0	1	0.3912	0.3842	0.0998	0.5328	0.3758	0.224	0.1436	0.5486	0.2006	0.2365	0.048
1	2	0.3939	0.3653	0.1023	0.5211	0.3288	0.1892	0.1114	0.53	0.2891	0.1336	0.0309
2	3	0.3729	0.3303	0.1168	0.5126	0.3537	0.183	0.1041	0.4925	0.1681	0.1063	0.0322
3	4	0.3915	0.3642	0.1205	0.4956	0.3377	0.1412	0.1041	0.4525	0.2223	0.12	0.0552
5	6	0.4125	0.3763	0.1443	0.4963	0.3751	0.1104	0.1493	0.5587	0.2283	0.1165	0.0321
6	7	0.4073	0.388	0.1058	0.5203	0.3318	0.178	0.159	0.4925	0.2431	0.1765	0.0364
9	10	0.3849	0.2828	0.1071	0.5155	0.2238	0.1848	0.0938	0.5261	0.1964	0.1963	0.114
11	12	0.3742	0.3661	0.1253	0.513	0.3801	0.1681	0.1642	0.4522	0.1862	0.2322	0.0271
13	14	0.3783	0.2844	0.1449	0.5007	0.3157	0.2193	0.0927	0.5223	0.1432	0.1441	0.0556
14	15	0.4154	0.3789	0.0993	0.5378	0.4091	0.2165	0.0304	0.5018	0.1677	0.1171	0.0697
15	16	0.317	0.3396	0.1641	0.5016	0.2927	0.2299	0.143	0.5595	0.2819	0.2081	0.0443
4	5	0.3643	0.2183	0.1209	0.5308	0.2109	0.2258	0.0871	0.53	0.1395	0.1274	0.1073
7	8	0.3238	0.2654	0.1203	0.542	0.2238	0.1896	0.0395	0.4996	0.2639	0.1613	0.0519
8	9	0.3455	0.3088	0.0954	0.5532	0.2975	0.113	0.1556	0.5052	0.2401	0.116	0.0595
10	11	0.3493	0.3717	0.0934	0.5169	0.3061	0.0524	0.0823	0.5206	0.2306	0.1001	0.0532
12	13	0.3421	0.4816	0.1008	0.5158	0.3095	0.0905	0.0813	0.5293	0.3569	0.1939	0.0728
skew_gas	avg_wheel	std_wheel	kurt_wheel	skew_wheel	avg_acceleration	std_acceleration	kurt_acceleration	skew_acceleration	age	gender	cluster	
0.4409	0.4357	0.1322	0.1316	0.4662	0.4767	0.0981	1.8731	1.5113	37	Male	cluster0	
0.427	0.4242	0.1456	0.156	0.56	0.4899	0.105	-0.0089	0.2859	37	Male	cluster0	
0.4522	0.486	0.1544	0.1962	0.5156	0.4847	0.1615	3.784	1.6224	41	Female	cluster0	
0.4284	0.4004	0.147	0.1057	0.5695	0.4689	0.1004	-0.6637	-0.2389	41	Male	cluster0	
0.4405	0.3967	0.1567	0.0983	0.5447	0.4651	0.0695	-1.0633	-0.074	22	Female	cluster0	
0.414	0.4446	0.1405	0.1514	0.5913	0.4735	0.1835	1.2014	-0.3229	31	Female	cluster0	
0.4684	0.4567	0.1418	0.1327	0.4962	0.4562	0.0825	1.1066	-0.7559	20	Male	cluster0	
0.4203	0.4533	0.1543	0.1353	0.4876	0.4674	0.0501	-0.4599	-0.0742	24	Female	cluster0	
0.4457	0.4588	0.2008	0.1148	0.5306	0.423	0.1128	2.399	-1.5179	47	Female	cluster0	
0.4528	0.4597	0.1079	0.1215	0.545	0.4684	0.0908	-0.1499	0.2975	44	Female	cluster0	
0.4383	0.4402	0.1111	0.1609	0.4895	0.4995	0.1699	2.5447	0.6667	25	Male	cluster0	
0.4951	0.442	0.1694	0.1114	0.525	0.4384	0.0582	-0.5798	-0.7085	37	Female	cluster1	
0.4348	0.4132	0.2016	0.1025	0.5402	0.4914	0.0859	4.7951	1.9337	21	Male	cluster1	
0.4257	0.4335	0.1456	0.1262	0.5491	0.4813	0.0583	-0.0526	0.7681	21	Female	cluster1	
0.3931	0.3961	0.1483	0.1285	0.5343	0.5016	0.0785	2.7912	1.5077	22	Female	cluster1	
0.4012	0.4107	0.1807	0.1815	0.5942	0.5126	0.1466	-0.6797	-0.2969	23	Male	cluster1	

Table B.3: Cluster assignments of drivers pre-turns of 4 seconds with 2 clusters

instance_no	sub_no	avg_speed	std_speed	kurt_speed	skew_speed	avg_brake	std_brake	kurt_brake	skew_brake	avg_gas	std_gas	kurt_gas
0	1	0.387	0.3432	0.0464	0.6519	0.3587	0.1875	0.1503	0.5775	0.1879	0.2042	0.0504
1	2	0.3938	0.3399	0.0449	0.6441	0.318	0.1263	0.0477	0.5162	0.2769	0.1012	0.0352
3	4	0.3878	0.3543	0.0413	0.6495	0.3403	0.1066	0.1199	0.4381	0.2174	0.0602	0.0385
4	5	0.3601	0.1888	0.0528	0.6806	0.184	0.2072	0.1915	0.5376	0.1289	0.0882	0.1245
5	6	0.4081	0.3677	0.0611	0.6376	0.378	0.0943	0.1543	0.5655	0.2218	0.0987	0.0726
7	8	0.3265	0.2269	0.1026	0.6288	0.211	0.1284	0.0925	0.5367	0.2446	0.116	0.0576
8	9	0.3444	0.2753	0.0467	0.6624	0.2821	0.1153	0.1198	0.5009	0.2287	0.0878	0.0785
9	10	0.3831	0.2756	0.0721	0.621	0.2246	0.1615	0.1184	0.534	0.1854	0.1335	0.0529
10	11	0.3495	0.3601	0.0463	0.6421	0.3082	0.038	0.086	0.5325	0.2289	0.0561	0.0391
11	12	0.3695	0.3499	0.0598	0.65	0.3805	0.0883	0.1162	0.4904	0.1821	0.1737	0.0313
13	14	0.3724	0.2596	0.0795	0.6436	0.3044	0.14	0.1056	0.4737	0.1392	0.1211	0.0414
14	15	0.4086	0.3574	0.0466	0.6598	0.3938	0.1821	0.0931	0.4746	0.1629	0.0965	0.0845
2	3	0.3677	0.3248	0.0466	0.6429	0.348	0.1602	0.091	0.4729	0.1704	0.0915	0.0481
6	7	0.4054	0.3597	0.0512	0.6527	0.3258	0.1131	0.2244	0.5127	0.243	0.1555	0.0527
12	13	0.3435	0.4574	0.0596	0.6421	0.3131	0.087	0.0225	0.4953	0.3409	0.1079	0.0464
15	16	0.3176	0.3079	0.0724	0.6502	0.281	0.207	0.1441	0.5507	0.2836	0.1566	0.0869
skew_gas	avg_wheel	std_wheel	kurt_wheel	skew_wheel	avg_acceleration	std_acceleration	kurt_acceleration	skew_acceleration	age	gender	cluster	
0.352	0.4234	0.1334	0.1184	0.4342	0.4063	0.0767	1.3127	1.2311	37	Male	cluster0	
0.3228	0.4163	0.1472	0.1445	0.5242	0.4163	0.0902	-0.2178	0.2672	37	Male	cluster0	
0.3297	0.3908	0.1418	0.1275	0.5325	0.4009	0.093	-0.6358	0.0036	41	Male	cluster0	
0.38	0.4327	0.1778	0.1267	0.4827	0.3744	0.049	-0.4313	-0.8784	37	Female	cluster0	
0.3446	0.386	0.1448	0.1115	0.5329	0.3925	0.0626	-1.0887	-0.0953	22	Female	cluster0	
0.329	0.4015	0.2091	0.1348	0.4926	0.4195	0.0697	5.9252	2.2811	21	Male	cluster0	
0.3266	0.4268	0.145	0.1612	0.51	0.4073	0.0491	-0.0456	0.7587	21	Female	cluster0	
0.3013	0.4531	0.1547	0.1395	0.4291	0.3858	0.0692	0.7986	-0.8533	20	Male	cluster0	
0.3358	0.3875	0.1505	0.1309	0.5173	0.4262	0.0652	2.2208	1.3344	22	Female	cluster0	
0.3255	0.44	0.1746	0.1324	0.4927	0.3974	0.0447	0.0468	-0.4881	24	Female	cluster0	
0.3283	0.4484	0.2327	0.1135	0.5024	0.358	0.0891	2.2785	-1.6264	47	Female	cluster0	
0.3338	0.4479	0.0995	0.1759	0.5139	0.3963	0.0767	-0.3555	0.0429	44	Female	cluster0	
0.3193	0.4781	0.1586	0.1501	0.4906	0.4205	0.1633	5.7975	2.2075	41	Female	cluster1	
0.2956	0.4324	0.1427	0.1311	0.545	0.396	0.148	1.244	-0.5637	31	Female	cluster1	
0.3152	0.4023	0.1668	0.1796	0.5485	0.4355	0.138	-0.3717	-0.0308	23	Male	cluster1	
0.3365	0.4313	0.133	0.1475	0.4529	0.4216	0.1456	2.981	0.5479	25	Male	cluster1	

Table B.4: Cluster assignments of drivers pre-turns of 3 seconds with 2 clusters

instance_no	sub_no	avg_speed	std_speed	kurt_speed	skew_speed	avg_brake	std_brake	kurt_brake	skew_brake	avg_gas	std_gas	kurt_gas
0	1	0.3823	0.2966	0.0864	0.508	0.3319	0.1465	0.1635	0.5889	0.1833	0.1729	0.0622
4	5	0.3558	0.1816	0.0732	0.5178	0.1455	0.1724	0.1539	0.513	0.1268	0.068	0.0775
8	9	0.3431	0.2378	0.1468	0.5045	0.2594	0.1222	0.1471	0.5091	0.2188	0.0561	0.1174
9	10	0.3815	0.2591	0.0841	0.4666	0.2258	0.1866	0.1467	0.5602	0.189	0.0835	0.0784
11	12	0.3648	0.3428	0.0969	0.4796	0.3787	0.0907	0.0504	0.5064	0.1822	0.1223	0.0461
15	16	0.3182	0.2908	0.0969	0.5055	0.2603	0.1781	0.0987	0.5228	0.2955	0.1044	0.1287
1	2	0.3938	0.3125	0.0664	0.4863	0.3089	0.0864	0.0497	0.4847	0.2774	0.095	0.0299
2	3	0.3626	0.3208	0.0693	0.4885	0.3433	0.1425	0.0588	0.4987	0.1761	0.0708	0.0327
3	4	0.383	0.3488	0.0651	0.5037	0.3314	0.0818	0.1324	0.4463	0.2229	0.0512	0.0418
5	6	0.4029	0.3712	0.0815	0.4923	0.3805	0.0872	0.1876	0.5529	0.2279	0.0796	0.03
6	7	0.4021	0.3431	0.0947	0.5119	0.3315	0.0816	0.1231	0.4445	0.2616	0.1252	0.056
7	8	0.3287	0.2081	0.117	0.5379	0.2024	0.0923	0.091	0.532	0.2476	0.0854	0.0544
10	11	0.3488	0.3449	0.0939	0.466	0.3044	0.0314	0.0459	0.4964	0.2299	0.046	0.0495
12	13	0.3448	0.4305	0.1379	0.4618	0.3182	0.061	0.0466	0.4776	0.3357	0.0512	0.0665
13	14	0.3657	0.2556	0.1063	0.4968	0.2965	0.1274	0.1465	0.4391	0.1487	0.0847	0.0663
14	15	0.401	0.3483	0.0637	0.4989	0.3728	0.1177	0.1144	0.4763	0.1707	0.0529	0.081
skew_gas	avg_wheel	std_wheel	kurt_wheel	skew_wheel	avg_acceleration	std_acceleration	kurt_acceleration	skew_acceleration	age	gender	cluster	
0.4738	0.4226	0.1359	0.1097	0.3549	0.4121	0.0696	1.3862	1.1194	37	Male	cluster0	
0.4598	0.4335	0.2116	0.0917	0.4121	0.3851	0.0454	-0.1199	-0.9931	37	Female	cluster0	
0.4689	0.4314	0.1624	0.1578	0.4348	0.4169	0.0449	-0.9397	0.412	21	Female	cluster0	
0.4051	0.4621	0.1729	0.0892	0.3551	0.3967	0.0667	-0.1244	-0.6094	20	Male	cluster0	
0.455	0.4356	0.1976	0.1669	0.4022	0.4073	0.0476	-0.2801	-0.3094	24	Female	cluster0	
0.4522	0.4322	0.1765	0.0904	0.378	0.4267	0.1292	2.4765	0.0484	25	Male	cluster0	
0.4311	0.4191	0.1894	0.0814	0.4283	0.4243	0.0859	-0.2475	-0.0023	37	Male	cluster1	
0.4444	0.48	0.175	0.095	0.4188	0.4282	0.1572	6.3955	2.3494	41	Female	cluster1	
0.4164	0.3944	0.1504	0.0933	0.4318	0.4078	0.1003	-0.3878	-0.0772	41	Male	cluster1	
0.4261	0.3886	0.1399	0.0722	0.4411	0.4007	0.0637	-0.9947	-0.0127	22	Female	cluster1	
0.4154	0.4311	0.1692	0.0884	0.4488	0.3993	0.1475	1.1466	-0.714	31	Female	cluster1	
0.4158	0.4013	0.2335	0.0909	0.4399	0.4244	0.0572	3.9526	1.7932	21	Male	cluster1	
0.4692	0.3914	0.1615	0.0855	0.4345	0.4325	0.0626	1.6994	1.2122	22	Female	cluster1	
0.4573	0.4095	0.2084	0.1154	0.4614	0.4442	0.1432	-0.643	0.0865	23	Male	cluster1	
0.4135	0.4459	0.2943	0.1357	0.4503	0.3702	0.0833	1.3589	-1.3734	47	Female	cluster1	
0.4164	0.4465	0.0998	0.0672	0.4341	0.4067	0.0855	-0.3777	0.0927	44	Female	cluster1	

Table B.5: Cluster assignments of drivers pre-turns of 2 seconds with 2 clusters

instance_no	sub_no	avg_speed	std_speed	kurt_speed	skew_speed	avg_brake	std_brake	kurt_brake	skew_brake	avg_gas	std_gas	kurt_gas
2	3	0.3535	0.3025	0.1048	0.5083	0.3436	0.0969	0.1184	0.4809	0.1683	0.0472	0.1093
7	8	0.3274	0.2367	0.125	0.4878	0.2073	0.0664	0.1364	0.5303	0.2572	0.0687	0.118
8	9	0.3392	0.213	0.0763	0.4753	0.2422	0.0692	0.1429	0.485	0.2188	0.1105	0.0523
9	10	0.3762	0.2544	0.2012	0.4488	0.2247	0.1335	0.1455	0.4971	0.1843	0.0749	0.1024
10	11	0.3429	0.338	0.1487	0.4857	0.305	0.0189	0.0746	0.4983	0.2359	0.0636	0.0953
11	12	0.3554	0.3683	0.1299	0.4989	0.3835	0.0643	0.1012	0.5037	0.1951	0.1287	0.0675
0	1	0.3736	0.2623	0.2078	0.5422	0.3217	0.0596	0.2848	0.6191	0.1969	0.1983	0.1389
1	2	0.3887	0.3062	0.1094	0.4935	0.3102	0.0278	0.1003	0.4475	0.2977	0.127	0.0789
3	4	0.3732	0.3357	0.1636	0.5367	0.3174	0.0538	0.1416	0.4516	0.2341	0.0812	0.1509
4	5	0.3486	0.177	0.1817	0.4954	0.1131	0.0447	0.1274	0.4713	0.1243	0.1296	0.1445
5	6	0.392	0.4038	0.1813	0.5383	0.3951	0.0287	0.1802	0.539	0.2257	0.0927	0.1251
6	7	0.3945	0.3471	0.2661	0.5195	0.3332	0.0214	0.1516	0.4506	0.2688	0.2367	0.1044
12	13	0.3411	0.4057	0.2065	0.497	0.3259	0.0162	0.1089	0.4462	0.3464	0.0662	0.1102
13	14	0.3544	0.3095	0.1707	0.5336	0.3008	0.0535	0.178	0.4341	0.1625	0.1388	0.0494
14	15	0.3892	0.3492	0.1155	0.4904	0.3631	0.0348	0.2033	0.4316	0.1631	0.1096	0.1814
15	16	0.3147	0.2728	0.2323	0.5133	0.2406	0.0525	0.0684	0.5023	0.3144	0.1186	0.1377
skew_gas	avg_wheel	std_wheel	kurt_wheel	skew_wheel	avg_acceleration	std_acceleration	kurt_acceleration	skew_acceleration	age	gender	cluster	
0.4919	0.4742	0.1737	0.1995	0.4527	0.4582	0.1525	5.7164	2.2642	41	Female	cluster0	
0.4537	0.3949	0.2562	0.2258	0.4683	0.4587	0.0732	7.4299	2.575	21	Male	cluster0	
0.5219	0.4275	0.1751	0.1834	0.4427	0.4388	0.0318	-0.6476	0.5274	21	Female	cluster0	
0.491	0.4626	0.1719	0.1728	0.3479	0.4246	0.0695	-0.3285	0.2021	20	Male	cluster0	
0.5224	0.3893	0.1726	0.1687	0.4401	0.4609	0.0781	5.0602	2.2076	22	Female	cluster0	
0.4987	0.4241	0.1911	0.2245	0.3775	0.4313	0.0557	-0.0487	-0.443	24	Female	cluster0	
0.4959	0.4148	0.1252	0.1484	0.3903	0.4415	0.0637	0.1353	0.6554	37	Male	cluster1	
0.4749	0.4143	0.2595	0.1421	0.4106	0.4493	0.0872	-0.3188	-0.2709	37	Male	cluster1	
0.5246	0.392	0.1744	0.1555	0.4391	0.4353	0.111	0.832	0.327	41	Male	cluster1	
0.4666	0.426	0.2534	0.1402	0.4556	0.4194	0.0507	0.0318	-0.7028	37	Female	cluster1	
0.5262	0.387	0.1612	0.1502	0.3907	0.4258	0.0706	-1.2611	-0.1039	22	Female	cluster1	
0.4787	0.4231	0.211	0.1417	0.4161	0.422	0.1462	1.7363	-1.0792	31	Female	cluster1	
0.48	0.4113	0.2973	0.1728	0.423	0.4618	0.1468	-0.3632	-0.1552	23	Male	cluster1	
0.4819	0.4335	0.3323	0.1423	0.4147	0.4005	0.0899	1.2824	-1.2457	47	Female	cluster1	
0.4787	0.4385	0.0843	0.1577	0.3977	0.4359	0.0907	-0.4684	0.1664	44	Female	cluster1	
0.4751	0.4264	0.2126	0.1442	0.4049	0.4567	0.1179	2.1197	0.2581	25	Male	cluster1	

Table B.6: Cluster assignments of drivers pre-turns of 1 second with 2 clusters

instance_no	sub_no	avg_duration	std_duration	kurt_duration	skew_duration	avg_speed	std_speed	kurt_speed	skew_speed	avg_brake	std_brake	kurt_brake	skew_brake	avg_gas
2	3	0.0779	0.0853	5.9509	2.3346	0.4958	0.2589	0.1127	0.4954	0.2676	0.4105	0.0101	0.4969	0.2936
4	5	0.0889	0.1095	2.1219	1.7489	0.5028	0.179	0.0635	0.4809	0.19	0.2822	0.0832	0.5396	0.1814
10	11	0.1331	0.1468	1.5866	1.6107	0.4441	0.3141	0.0659	0.4583	0.2365	0.3143	0.1406	0.4725	0.3007
11	12	0.1409	0.1912	2.0729	1.9168	0.5154	0.2728	0.0832	0.4408	0.2812	0.4069	0.0921	0.5403	0.2956
14	15	0.077	0.0637	1.5696	1.2464	0.5075	0.2984	0.0637	0.4397	0.2564	0.4609	0.0231	0.5184	0.3016
15	16	0.1241	0.2219	10.5115	3.364	0.5034	0.2009	0.075	0.4481	0.2494	0.3496	0.0443	0.4703	0.2616
0	1	0.0726	0.1074	11.0869	3.4749	0.6097	0.2387	0.0663	0.4419	0.2316	0.3953	0.0498	0.4677	0.4175
1	2	0.0864	0.1433	7.357	2.8464	0.5883	0.2002	0.0705	0.4597	0.2585	0.3825	0.082	0.5194	0.3451
3	4	0.0554	0.0644	3.4282	1.9528	0.5763	0.1814	0.0637	0.4425	0.2058	0.3208	0.1143	0.5512	0.3
5	6	0.061	0.0484	0.3183	1.2884	0.6304	0.25	0.0603	0.4613	0.2345	0.3951	0.0071	0.4988	0.3586
6	7	0.0689	0.1273	10.3995	3.3952	0.6391	0.1755	0.0655	0.4574	0.2192	0.3691	0.0261	0.497	0.313
7	8	0.0567	0.0386	-0.2312	0.7591	0.61	0.2373	0.0547	0.4433	0.1935	0.2831	0.0874	0.551	0.309
8	9	0.1089	0.1852	8.7273	3.1008	0.5636	0.1892	0.0689	0.4597	0.1961	0.2717	0.0287	0.4964	0.3163
9	10	0.0661	0.0751	5.6213	2.4525	0.5727	0.2127	0.0629	0.4581	0.1863	0.3551	0.086	0.5019	0.2847
12	13	0.0373	0.0353	-0.8904	0.9815	0.5775	0.1907	0.0657	0.4508	0.1702	0.3345	0.037	0.5265	0.4244
13	14	0.0546	0.049	-0.8717	0.8053	0.5627	0.1843	0.058	0.427	0.1923	0.3088	0.0876	0.5491	0.2648
std_gas	kurt_gas	skew_gas	avg_wheel	std_wheel	kurt_wheel	skew_wheel	avg_acceleration	std_acceleration	kurt_acceleration	skew_acceleration	age	gender	cluster	
0.2467	0.0846	0.363	0.472	0.6695	0.0749	0.3608	0.4553	0.2067	-0.8022	0.1929	41	Female	cluster0	
0.1815	0.0195	0.345	0.4261	0.5932	0.0942	0.4062	0.3946	0.0967	0.6135	0.7831	37	Female	cluster0	
0.2101	0.0311	0.3503	0.4361	0.629	0.067	0.3205	0.4859	0.1782	-1.0332	0.3323	22	Female	cluster0	
0.2697	0.0339	0.3655	0.4237	0.6522	0.1243	0.3931	0.4598	0.1629	-1.1899	0.5796	24	Female	cluster0	
0.3522	0.014	0.3299	0.4375	0.5934	0.0535	0.3209	0.4355	0.1529	-0.2434	0.3137	44	Female	cluster0	
0.2146	0.0405	0.3598	0.423	0.6329	0.06	0.3497	0.4471	0.132	-0.3008	0.5046	25	Male	cluster0	
0.4197	0.028	0.3714	0.4211	0.6467	0.0579	0.3535	0.4946	0.1749	-0.6624	-0.0444	37	Male	cluster1	
0.2182	0.0229	0.3462	0.4395	0.6052	0.1113	0.3326	0.4416	0.1808	-0.0617	-0.4627	37	Male	cluster1	
0.2134	0.0148	0.3345	0.439	0.6053	0.0773	0.3804	0.4234	0.1694	-0.3491	-0.5227	41	Male	cluster1	
0.2737	0.0201	0.3185	0.441	0.6828	0.0562	0.304	0.4582	0.1813	0.3856	-0.8007	22	Female	cluster1	
0.197	0.0189	0.3176	0.4203	0.5913	0.0928	0.3779	0.4306	0.2047	-1.0665	-0.3178	31	Female	cluster1	
0.2243	0.0311	0.3342	0.4287	0.6206	0.067	0.327	0.4503	0.1725	-1.349	-0.3043	21	Male	cluster1	
0.2213	0.0184	0.3233	0.4432	0.622	0.1053	0.3591	0.464	0.124	-1.0173	0.0815	21	Female	cluster1	
0.2154	0.0289	0.3406	0.4427	0.6558	0.074	0.354	0.4263	0.1808	-0.6071	0.3384	20	Male	cluster1	
0.2561	0.0147	0.3302	0.4207	0.5576	0.111	0.2954	0.5281	0.2255	-0.6725	0.5396	23	Male	cluster1	
0.189	0.0148	0.3197	0.4401	0.6227	0.0702	0.3751	0.4238	0.1295	-0.9216	0.0138	47	Female	cluster1	

Table B.7: Cluster assignments of drivers during turns with 2 clusters

instance_no	sub_no	avg_speed	std_speed	kurt_speed	skew_speed	avg_brake	std_brake	kurt_brake	skew_brake	avg_gas	std_gas	kurt_gas
0	1	0.5954	0.5907	0.1259	0.498	0.0131	0.0151	0.1445	0.5194	0.5037	0.2721	0.1549
1	2	0.5086	0.4559	0.1566	0.5194	0.0116	0.0014	0.1111	0.5556	0.3251	0.0979	0.1749
5	6	0.5806	0.4328	0.1864	0.4726	0.0117	0.003	0.1166	0.5076	0.3148	0.1016	0.1958
7	8	0.5027	0.3977	0.1588	0.5009	0.0808	0.0629	0.0283	0.5189	0.2489	0.0427	0.1397
11	12	0.5479	0.4921	0.1575	0.475	0.0689	0.0297	0.0861	0.4878	0.2972	0.1116	0.2409
12	13	0.5434	0.5903	0.1961	0.4884	0.0117	0.0012	0.0288	0.5207	0.403	0.1328	0.3219
14	15	0.5213	0.5304	0.1289	0.5068	0.0403	0.0743	0.2046	0.5208	0.3335	0.0738	0.1379
2	3	0.4785	0.4281	0.19	0.4957	0.0512	0.0341	0.0229	0.5013	0.2753	0.1565	0.2702
3	4	0.4958	0.4157	0.129	0.5272	0.0352	0.0337	0.1284	0.503	0.291	0.0838	0.2209
4	5	0.4466	0.276	0.2318	0.5474	0.0115	0.0024	0.0426	0.5059	0.2203	0.0741	0.1332
6	7	0.5254	0.396	0.1989	0.5236	0.0603	0.0054	0.0079	0.5049	0.2579	0.1672	0.1167
8	9	0.516	0.351	0.112	0.5089	0.0195	0.0067	0.0937	0.524	0.2837	0.0421	0.1057
9	10	0.5029	0.3921	0.1821	0.5247	0.0111	0.0028	0.0141	0.4899	0.27	0.0876	0.1461
10	11	0.4844	0.4943	0.1657	0.4997	0.007	0.0021	0.1667	0.4722	0.2879	0.0727	0.1307
13	14	0.4891	0.3824	0.2449	0.5512	0.0448	0.0408	0.1118	0.4971	0.259	0.0522	0.158
15	16	0.4454	0.3941	0.2171	0.5413	0.0372	0.0203	0.1338	0.451	0.2573	0.1258	0.1822
skew_gas	avg_wheel	std_wheel	kurt_wheel	skew_wheel	avg_acceleration	std_acceleration	kurt_acceleration	skew_acceleration	age	gender	cluster	
0.458	0.4743	0.2037	0.1562	0.5305	0.4104	0.1245	1.12	1.1383	37	Male	cluster0	
0.4515	0.5176	0.2291	0.1727	0.5314	0.3877	0.0963	0.0038	0.7101	37	Male	cluster0	
0.444	0.5368	0.1968	0.1856	0.513	0.3599	0.0806	-1.1838	0.3927	22	Female	cluster0	
0.5184	0.531	0.1679	0.1537	0.5259	0.3278	0.0804	-0.1324	0.2237	21	Male	cluster0	
0.5447	0.506	0.2347	0.1491	0.5396	0.3281	0.0542	-1.4292	-0.1701	24	Female	cluster0	
0.4002	0.4486	0.2581	0.2197	0.5704	0.4663	0.1532	-0.3521	1.0621	23	Male	cluster0	
0.5214	0.4637	0.3029	0.1423	0.4801	0.3638	0.0787	-1.0588	0.2899	44	Female	cluster0	
0.476	0.4674	0.198	0.1442	0.5148	0.3642	0.1612	9.1982	3.0048	41	Female	cluster1	
0.413	0.5566	0.2488	0.1376	0.486	0.3637	0.1781	6.298	2.3552	41	Male	cluster1	
0.4788	0.5109	0.151	0.1294	0.4974	0.2995	0.0588	6.2489	2.5135	37	Female	cluster1	
0.4785	0.4907	0.2508	0.1502	0.5097	0.3364	0.1189	1.5346	-0.9292	31	Female	cluster1	
0.4464	0.5039	0.1849	0.1556	0.4701	0.3283	0.0643	0.7929	1.0076	21	Female	cluster1	
0.587	0.4778	0.3935	0.1622	0.5037	0.3577	0.103	0.5546	1.1431	20	Male	cluster1	
0.4446	0.5206	0.2002	0.1887	0.481	0.3651	0.1273	3.6239	2.0639	22	Female	cluster1	
0.4755	0.5185	0.2545	0.1527	0.5222	0.3355	0.1038	3.6764	-1.6075	47	Female	cluster1	
0.4884	0.5237	0.1852	0.1808	0.5196	0.3613	0.2025	3.7996	1.8237	25	Male	cluster1	

Table B.8: Cluster assignments of drivers post-turns of 1 second with 2 clusters

instance_no	sub_no	avg_speed	std_speed	kurt_speed	skew_speed	avg_brake	std_brake	kurt_brake	skew_brake	avg_gas	std_gas	kurt_gas
0	1	0.6286	0.5951	0.0732	0.6478	0.0295	0.0563	0.114	0.5018	0.5204	0.2676	0.1423
2	3	0.502	0.3982	0.0926	0.6623	0.0616	0.0524	0.0052	0.4995	0.2866	0.125	0.1553
7	8	0.5194	0.3554	0.1001	0.6581	0.103	0.0864	0.0205	0.5147	0.2571	0.0629	0.1168
11	12	0.5719	0.4383	0.0909	0.6303	0.0885	0.0776	0.1159	0.506	0.2982	0.1062	0.1513
1	2	0.5339	0.4243	0.0807	0.6435	0.0117	0.0013	0.1272	0.5698	0.3349	0.0693	0.1011
3	4	0.5193	0.4041	0.0579	0.6657	0.0438	0.0345	0.1308	0.4896	0.3043	0.0732	0.1524
4	5	0.4652	0.2701	0.1166	0.6252	0.0116	0.0018	0.0932	0.5343	0.2277	0.0832	0.0723
5	6	0.6044	0.4209	0.085	0.6835	0.0117	0.0018	0.0932	0.4977	0.316	0.0844	0.1563
6	7	0.5434	0.3587	0.067	0.6678	0.0616	0.0045	0.0036	0.4969	0.2608	0.1492	0.0976
8	9	0.538	0.3527	0.0736	0.679	0.0195	0.0054	0.135	0.5097	0.2872	0.0314	0.0913
9	10	0.5241	0.3587	0.0792	0.6891	0.0115	0.0043	0.0829	0.5383	0.2801	0.0774	0.1094
10	11	0.5113	0.4466	0.0753	0.6708	0.0079	0.006	0.2977	0.4623	0.2875	0.0766	0.1233
12	13	0.5778	0.5904	0.0691	0.673	0.0116	0.0006	0.0311	0.5223	0.4169	0.1051	0.0722
13	14	0.5107	0.3603	0.0662	0.6701	0.0288	0.0553	0.1014	0.5026	0.2667	0.0684	0.1542
14	15	0.5507	0.4893	0.0561	0.6556	0.0479	0.064	0.1626	0.5263	0.3376	0.0533	0.0775
15	16	0.4685	0.3754	0.078	0.6756	0.0436	0.0272	0.0164	0.4873	0.2672	0.0869	0.0864
skew_gas	avg_wheel	std_wheel	kurt_wheel	skew_wheel	avg_acceleration	std_acceleration	kurt_acceleration	skew_acceleration	age	gender	cluster	
0.4464	0.4649	0.1785	0.0858	0.6702	0.3448	0.171	2.2176	1.4818	37	Male	cluster0	
0.509	0.4514	0.1614	0.0825	0.6722	0.2573	0.1517	9.3527	2.9536	41	Female	cluster0	
0.4681	0.5239	0.1572	0.1019	0.6216	0.2308	0.1148	2.8214	1.2754	21	Male	cluster0	
0.4947	0.5007	0.212	0.0931	0.6643	0.2295	0.0618	-1.1502	-0.1725	24	Female	cluster0	
0.4569	0.5097	0.1999	0.087	0.6036	0.294	0.1149	0.0207	0.7768	37	Male	cluster1	
0.3936	0.5426	0.2635	0.086	0.6061	0.2891	0.1978	6.4572	2.5086	41	Male	cluster1	
0.5412	0.4982	0.167	0.1008	0.6112	0.2028	0.0823	7.6521	2.8388	37	Female	cluster1	
0.4225	0.5181	0.1923	0.1094	0.6188	0.27	0.0789	-1.2218	0.4071	22	Female	cluster1	
0.4747	0.4812	0.2114	0.0768	0.6414	0.2563	0.1041	-1.1604	0.1134	31	Female	cluster1	
0.4706	0.4927	0.1937	0.0849	0.6484	0.2417	0.0962	4.9565	2.2015	21	Female	cluster1	
0.5382	0.4737	0.3177	0.0776	0.6342	0.2609	0.1111	1.2164	1.3378	20	Male	cluster1	
0.501	0.5127	0.1887	0.1205	0.6052	0.2717	0.1748	5.6881	2.5105	22	Female	cluster1	
0.4916	0.4366	0.2451	0.0788	0.6638	0.4053	0.1583	-0.398	0.924	23	Male	cluster1	
0.4521	0.5036	0.2766	0.0776	0.6247	0.245	0.092	0.7117	-0.9618	47	Female	cluster1	
0.4951	0.4624	0.2774	0.0757	0.6517	0.2694	0.1014	-0.1126	0.7876	44	Female	cluster1	
0.4499	0.5159	0.2245	0.098	0.6555	0.2621	0.1833	3.9029	1.9432	25	Male	cluster1	

Table B.9: Cluster assignments of drivers post-turns of 2 seconds with 2 clusters

instance_no	sub_no	avg_speed	std_speed	kurt_speed	skew_speed	avg_brake	std_brake	kurt_brake	skew_brake	avg_gas	std_gas	kurt_gas
7	8	0.5351	0.385	0.0472	0.5977	0.1202	0.0794	0.0646	0.4682	0.2828	0.0813	0.0421
11	12	0.5922	0.4402	0.0439	0.5782	0.1065	0.0808	0.1571	0.5214	0.3162	0.1154	0.1089
0	1	0.6577	0.6237	0.0454	0.5876	0.0435	0.0562	0.1685	0.5271	0.5538	0.3197	0.0547
1	2	0.557	0.4334	0.0577	0.5763	0.0117	0.001	0.1835	0.5427	0.3622	0.0902	0.0877
2	3	0.5235	0.4233	0.0527	0.6059	0.0712	0.0441	0.0045	0.4986	0.3153	0.1547	0.1058
3	4	0.5405	0.42	0.0458	0.6045	0.0486	0.0262	0.1193	0.4933	0.3278	0.1098	0.1347
4	5	0.4815	0.2749	0.1182	0.5755	0.0117	0.0015	0.1468	0.566	0.2529	0.1118	0.0723
5	6	0.6254	0.4241	0.0434	0.5902	0.0129	0.0103	0.2395	0.515	0.3304	0.1148	0.0625
6	7	0.5593	0.3605	0.0491	0.583	0.0623	0.0054	0.0069	0.5054	0.2813	0.15	0.0876
8	9	0.5572	0.3591	0.0455	0.6015	0.0197	0.004	0.1022	0.4976	0.3091	0.0388	0.0955
9	10	0.5442	0.3741	0.0478	0.6126	0.017	0.0215	0.0508	0.5171	0.3068	0.0809	0.0828
10	11	0.5344	0.4453	0.0462	0.5897	0.008	0.0048	0.3502	0.4608	0.3036	0.1003	0.0549
12	13	0.6099	0.6237	0.0429	0.6001	0.0118	0.001	0.1536	0.5845	0.4569	0.1279	0.0597
13	14	0.5311	0.3774	0.0718	0.6202	0.0234	0.0389	0.1778	0.5223	0.2863	0.0845	0.0639
14	15	0.5769	0.5025	0.0414	0.5992	0.0492	0.0492	0.1568	0.5326	0.3703	0.0766	0.0931
15	16	0.4897	0.397	0.0444	0.5971	0.0486	0.0245	0.0767	0.4715	0.294	0.0749	0.0811
skew_gas	avg_wheel	std_wheel	kurt_wheel	skew_wheel	avg_acceleration	std_acceleration	kurt_acceleration	skew_acceleration	age	gender	cluster	
0.4847	0.5377	0.17	0.152	0.5309	0.3038	0.1494	4.1139	1.7939	21	Male	cluster0	
0.5231	0.5133	0.227	0.1669	0.5661	0.2775	0.0699	-1.3556	0.0817	24	Female	cluster0	
0.4782	0.4735	0.2035	0.1192	0.5866	0.4159	0.188	1.8851	1.3312	37	Male	cluster1	
0.4948	0.5153	0.2478	0.1215	0.5291	0.3442	0.1043	-0.9225	0.3567	37	Male	cluster1	
0.4887	0.4548	0.1634	0.1408	0.5959	0.3097	0.1489	7.6437	2.5544	41	Female	cluster1	
0.3975	0.5511	0.2654	0.1155	0.5281	0.3458	0.1792	5.6334	2.2489	41	Male	cluster1	
0.539	0.5029	0.1989	0.1175	0.5543	0.269	0.0939	5.144	2.3704	37	Female	cluster1	
0.5059	0.5212	0.2259	0.1791	0.5399	0.3212	0.0807	-1.125	0.4062	22	Female	cluster1	
0.5084	0.4892	0.2164	0.1261	0.553	0.3293	0.1169	-0.7273	0.2603	31	Female	cluster1	
0.5192	0.501	0.2176	0.1075	0.5727	0.2978	0.0926	2.6874	1.7765	21	Female	cluster1	
0.5079	0.4834	0.3201	0.1276	0.5446	0.3192	0.1018	0.4353	1.1076	20	Male	cluster1	
0.4811	0.5228	0.1965	0.1218	0.5392	0.3242	0.1893	6.3888	2.6568	22	Female	cluster1	
0.4572	0.4443	0.2739	0.1278	0.57	0.4703	0.1623	-0.8368	0.7292	23	Male	cluster1	
0.4946	0.5071	0.305	0.0989	0.5305	0.2972	0.105	1.4725	-1.2079	47	Female	cluster1	
0.4963	0.4768	0.2714	0.115	0.5606	0.3273	0.0939	-0.1656	0.7205	44	Female	cluster1	
0.4472	0.5309	0.2756	0.0968	0.5588	0.3324	0.1935	4.3678	2.2221	25	Male	cluster1	

Table B.10: Cluster assignments of drivers post-turns of 3 seconds with 2 clusters



instance_no	sub_no	avg_speed	std_speed	kurt_speed	skew_speed	avg_brake	std_brake	kurt_brake	skew_brake	avg_gas	std_gas	kurt_gas
7	8	0.5491	0.3701	0.0548	0.4292	0.1335	0.086	0.0908	0.4969	0.2879	0.1032	0.0387
11	12	0.6099	0.4085	0.0557	0.3978	0.1209	0.084	0.1493	0.5233	0.3209	0.1044	0.0903
0	1	0.683	0.6058	0.0557	0.4001	0.0534	0.0563	0.2238	0.5535	0.5421	0.3001	0.0438
1	2	0.577	0.3992	0.0603	0.4185	0.0122	0.0009	0.184	0.543	0.3654	0.0995	0.0516
2	3	0.5425	0.4075	0.0564	0.4235	0.0775	0.0431	0.0541	0.5243	0.3231	0.1512	0.0394
3	4	0.5594	0.3991	0.0555	0.4306	0.053	0.0247	0.2289	0.5483	0.3311	0.1124	0.1068
4	5	0.4962	0.2517	0.081	0.4398	0.0121	0.0017	0.1713	0.5453	0.2617	0.1134	0.0507
5	6	0.644	0.3897	0.0524	0.4043	0.0189	0.023	0.278	0.5302	0.3264	0.1096	0.1062
6	7	0.5737	0.3319	0.057	0.4127	0.0636	0.0084	0.1219	0.4396	0.2883	0.1359	0.0664
8	9	0.5742	0.327	0.0496	0.4206	0.0205	0.0038	0.0888	0.4958	0.3133	0.0422	0.0643
9	10	0.5625	0.3554	0.06	0.4311	0.0266	0.0405	0.0453	0.515	0.3157	0.0784	0.07
10	11	0.5543	0.408	0.0555	0.4024	0.0081	0.0056	0.4443	0.5153	0.3001	0.0975	0.0678
12	13	0.6401	0.6185	0.0486	0.4235	0.0124	0.0033	0.2099	0.6135	0.4656	0.1269	0.0422
13	14	0.5485	0.3475	0.1111	0.4466	0.0217	0.0392	0.2579	0.5916	0.2897	0.0784	0.0365
14	15	0.6011	0.4904	0.0898	0.4119	0.0528	0.0477	0.1452	0.5401	0.377	0.0949	0.0411
15	16	0.5091	0.3816	0.0496	0.4232	0.0544	0.0327	0.081	0.4742	0.3031	0.0688	0.0867
skew_gas	avg_wheel	std_wheel	kurt_wheel	skew_wheel	avg_acceleration	std_acceleration	kurt_acceleration	skew_acceleration	age	gender	cluster	
0.4715	0.5475	0.1839	0.1864	0.3452	0.2835	0.1645	4.3075	1.8261	21	Male	cluster0	
0.5325	0.523	0.237	0.1676	0.4456	0.2513	0.0922	-0.7319	0.1823	24	Female	cluster0	
0.4863	0.4802	0.2183	0.1237	0.4453	0.3968	0.1925	0.2652	0.8077	37	Male	cluster1	
0.4503	0.5174	0.2958	0.1331	0.3918	0.3247	0.1066	-0.8958	0.4314	37	Male	cluster1	
0.501	0.4569	0.1727	0.1476	0.4659	0.2809	0.1524	4.6718	1.8254	41	Female	cluster1	
0.4226	0.5551	0.2887	0.1399	0.3689	0.3344	0.1863	4.9991	2.1208	41	Male	cluster1	
0.5139	0.5062	0.2347	0.1245	0.4257	0.2578	0.0981	3.613	2.038	37	Female	cluster1	
0.4764	0.5238	0.2502	0.1325	0.4388	0.2934	0.0794	-1.3342	0.224	22	Female	cluster1	
0.5184	0.4937	0.2597	0.1293	0.4394	0.3268	0.1383	-1.2803	0.09	31	Female	cluster1	
0.5006	0.5074	0.2162	0.1151	0.4296	0.2816	0.1126	3.7072	1.9887	21	Female	cluster1	
0.5292	0.4901	0.3162	0.1332	0.3998	0.3035	0.1102	-0.0643	0.9321	20	Male	cluster1	
0.5247	0.5287	0.209	0.142	0.3997	0.3001	0.2	5.8079	2.5502	22	Female	cluster1	
0.459	0.4509	0.2989	0.1433	0.4336	0.4633	0.165	-1.1789	0.4908	23	Male	cluster1	
0.5023	0.5092	0.3248	0.1124	0.3688	0.2781	0.1072	0.4121	-0.8853	47	Female	cluster1	
0.469	0.4872	0.2782	0.1361	0.4216	0.3093	0.1011	0.3289	0.9313	44	Female	cluster1	
0.4351	0.5412	0.2967	0.1038	0.3991	0.3203	0.2192	2.8481	1.9434	25	Male	cluster1	

Table B.11: Cluster assignments of drivers post-turns of 4 seconds with 2 clusters

instance_no	sub_no	avg_speed	std_speed	kurt_speed	skew_speed	avg_brake	std_brake	kurt_brake	skew_brake	avg_gas	std_gas	kurt_gas
0	1	0.7046	0.6004	0.0429	0.2016	0.0596	0.0563	0.1968	0.5804	0.5098	0.3388	0.093
1	2	0.5947	0.4023	0.0425	0.2236	0.0123	0.0008	0.1795	0.5408	0.3613	0.1141	0.1023
2	3	0.5588	0.4154	0.0439	0.2312	0.0803	0.0435	0.2283	0.5165	0.323	0.1669	0.0652
4	5	0.5091	0.2712	0.043	0.2519	0.0124	0.0031	0.1516	0.5591	0.2615	0.1221	0.0887
5	6	0.6595	0.3844	0.0408	0.2058	0.0249	0.033	0.2433	0.5171	0.3183	0.1217	0.1322
6	7	0.5865	0.3428	0.0468	0.2186	0.0633	0.0108	0.1789	0.4688	0.2874	0.163	0.1435
8	9	0.5886	0.3283	0.0373	0.2238	0.0209	0.0057	0.0686	0.5159	0.3084	0.0594	0.1502
9	10	0.578	0.3708	0.045	0.2253	0.0357	0.0538	0.1058	0.4749	0.3159	0.0832	0.1102
11	12	0.6253	0.4123	0.0452	0.2125	0.1221	0.0903	0.235	0.5391	0.3187	0.1113	0.1348
12	13	0.6673	0.6238	0.0381	0.2272	0.0218	0.0415	0.1523	0.5888	0.4573	0.156	0.082
13	14	0.5637	0.3477	0.1019	0.2614	0.0294	0.0737	0.2061	0.5855	0.2877	0.085	0.0854
14	15	0.6215	0.4891	0.0479	0.2196	0.0555	0.0489	0.1904	0.5744	0.3672	0.1375	0.07
3	4	0.5753	0.4006	0.0399	0.2287	0.0536	0.0234	0.2548	0.5856	0.3265	0.1262	0.0862
7	8	0.5613	0.3863	0.042	0.243	0.1367	0.1072	0.1494	0.5206	0.2851	0.137	0.0737
10	11	0.5716	0.4062	0.0416	0.2096	0.0221	0.0707	0.2958	0.5165	0.2935	0.1056	0.0943
15	16	0.5256	0.3918	0.04	0.2356	0.0633	0.053	0.0701	0.4692	0.301	0.0844	0.1013
skew_gas	avg_wheel	std_wheel	kurt_wheel	skew_wheel	avg_acceleration	std_acceleration	kurt_acceleration	skew_acceleration	age	gender	cluster	
0.4487	0.4975	0.1899	0.121	0.4732	0.3606	0.2006	-0.199	0.6418	37	Male	cluster0	
0.4252	0.5315	0.2817	0.1253	0.4429	0.2944	0.1156	-0.9763	0.4171	37	Male	cluster0	
0.4704	0.471	0.1731	0.1437	0.5022	0.2491	0.1544	3.4131	1.5203	41	Female	cluster0	
0.4854	0.5221	0.2185	0.117	0.4615	0.2354	0.1226	1.5752	1.5322	37	Female	cluster0	
0.4325	0.539	0.2139	0.125	0.4867	0.2539	0.0869	-1.2697	0.1732	22	Female	cluster0	
0.4992	0.5083	0.2534	0.1243	0.491	0.3014	0.1555	-1.3552	0.0881	31	Female	cluster0	
0.4431	0.5239	0.1782	0.1213	0.4696	0.2412	0.1143	3.813	1.9758	21	Female	cluster0	
0.489	0.5089	0.2645	0.1221	0.436	0.2707	0.1123	-0.4274	0.5973	20	Male	cluster0	
0.4825	0.5433	0.1983	0.161	0.4791	0.2198	0.1069	-0.3886	0.4996	24	Female	cluster0	
0.4122	0.468	0.2624	0.1412	0.4366	0.4412	0.1777	-1.1882	0.4013	23	Male	cluster0	
0.4658	0.5233	0.2713	0.1092	0.4146	0.2507	0.1057	-1.0879	-0.2124	47	Female	cluster0	
0.4222	0.5067	0.2321	0.1502	0.4478	0.2775	0.1031	-0.2517	0.6654	44	Female	cluster0	
0.4091	0.5701	0.2566	0.1301	0.4314	0.3057	0.2003	4.2334	1.9283	41	Male	cluster1	
0.4303	0.5668	0.1735	0.1726	0.3835	0.2557	0.1943	5.23	2.0654	21	Male	cluster1	
0.4804	0.5455	0.1838	0.1314	0.4504	0.2645	0.2103	5.7277	2.5126	22	Female	cluster1	
0.4203	0.5626	0.2583	0.0997	0.4216	0.2927	0.2339	2.1821	1.8153	25	Male	cluster1	

Table B.12: Cluster assignments of drivers post-turns of 5 seconds with 2 clusters

# Curriculum Vitae

**Name:** Jennifer Knull

**Post-Secondary Education and Degrees:** University of Western Ontario  
London, ON  
2011 - 2015 B.Sc.

**Honours and Awards:** Dean's Honor List  
2013 - 2014

**Related Work Experience:** Teaching Assistant  
The University of Western Ontario  
2014 - 2017

Research Assistant  
The University of Western Ontario  
2015 and 2017

## **Publications:**

J. Knull, C. Ardelean, S. Beauchemin, M. Bauer. *Automatic Identification of Turn Maneuvers from Vehicle Data*. 2017.